Cationic heats of transport in potassium chloride and sodium chloride single crystals.

Thesis

CATIONIC HEATS OF TRANSPORT IN POTASSIUM CHLORIDE AND SODIUM CHLORIDE SINGLE CRYSTALS.

A Thesis submitted for the degree of

Doctor of Philosophy of

The Open University

by

ANISUR RAHMAN, M.Sc.

Oxford Research Unit,

The Open University,

May 1976.

Date of submission 9.6.76

Date of award 28-10-1976

CONTENTS

LIST OF TABLES

LIST OF FIGURES

ACKNOWLEDGEMENTS

I wish to express my gratitude to Dr.D.A.Blackburn for his guidance, supervision and constant encouragement throughout the course of this work,

I am indebted to the Open University for offering me a research studentship without which this work would not have been done,

I wish to thank Prof.C.W.A.Newey for allowing me to use the laboratory facilities at the Oxford Research Unit,

I like to acknowledge the help of the Department of Metallurgy, University of Oxford for allowing me to use their workshop facilities and particularly of the members of the Electronics Workshop for helping me in designing a number of electronic circuits,

Lastly, I would like to thank the research and supporting staff of this unit for fruitful discussions and advice

ABSTRACT

Flows of heat through a hot solid entrain flows of material. These flow rates of matter and heat in a solid are related by a term called 'heat of transport'. In the experiments described, independent measurements of heats of transport and thermoelectric powers have been made in two strongly ionic solids - potassium chloride and sodium chloride single crystals in Pt|salt|Pt cells.

Measurements of electrical resistance in these materials have been made both at equilibrium and non-equilibrium conditions. The changes in resistance due to application of thermal and electric field forces have been used as indicators of deviations of equilibrium vacancy concentrations. The heat of transport which is related to the flow of vacancies can then be calculated from resistance change. The values of cationic heats of transport for pure potassium chloride and sodium chloride crystals are found to be $(0.37+4.74\times10^{-4}\times T)$ eV and $(0.52+2.87\times10^{-4}\times T)$ eV respectively.

The measurement of heat of transport from considerations of vacancy concentrations is quite distinct from the traditional approach which attempts to evaluate it from the thermoelectric power. Measured heat of transport can then be used to evaluate homogeneous thermoelectric power of the solid. Comparison of this component of thermoelectric power with the total thermoelectric power using Platinum electrodes offers a value of heterogeneous component.

In addition to these measurements, the present approach also gives values of vacancy life time and vacancy mean free path. An estimate of effectiveness of vacancy traps can be obtained from considerations of mean free path. These parameters together elucidate the actual process involved in vacancy migration under driving forces.

CHAPTER 1

INTRODUCTION

1.1. Aim of the experiment.

If a temperature gradient is maintained across a homogeneous material having more than one component, gradients in the concentration of components will slowly develop across it. The concentration gradients arise from deviations from randomness in atomic motion under a thermal driving force. This phenomenon, in which matter flow takes place in response to a thermal force, has been variously called thermodiffusion(30), thermal diffusion(3), thermal mass transport(42) or thermomigration(41). The term thermomigration is, in fact, a proper description of this phenomenon as it signifies a thermally activated process involving biased motion of atoms, vacancies or impurities.

The study of thermomigration and electromigration in solids provides valuable information about the fundamental properties of these materials(62). Of these properties, the heat of transport is the most important one. This quantity is defined as the amount of energy carried by a unit flux of material when the temperature gradient is effectively zero. The objective of the present work is the evaluation of heats of transport in two strongly ionic solids - potassium chloride and sodium chloride single crystals when they are subjected to thermo- and electromigration. The measured heat of transport provides means of testing the models produced in order to explain the processes of mass and energy transfer in a material.

1.2. Theoretical models of heat of transport.

There are two main approaches to the calculation of heat of transport in a material - one is based on isothermal method, that is, the heat of transport, Q^* is calculated from the equation $Q^* = \left(\frac{J_q}{J_1}\right)_{\nabla T=0}$ where J_q and J_1 are heat flux and matter flux respectively and the other is based on calculation of matter flux in a temperature gradient(57).

In the isothermal method, one attempts to evaluate energy flux accompanying matter flux and then calculate Q^*. A method for the calculation of matter flux in a material at thermal equilibrium was proposed by Wert(75) which can be called 'absolute rate-process description'. In this description he assumed that the average time of stay of an ion in a potential hole about an interstitial position was equal to the time spent at the saddle point when that ion was jumping from one interstitial site to another. This assumption was criticised by Rice(63) pointing out that the diffusing ion spends most of its time at one or other side of the potential barrier and actually crosses it very rapidly probably in a period of less than a few vibrations. The other fundamental drawback to this formulation is that an average potential energy was assigned to the jumping ion. This can only be done if the motions of the surrounding ions are completely unaffected by the transition.

Vineyard(74) tried to remove the assumption of average potential energy of the moving ion by considering the motion of an ion in N dimensional configuration. This formulation has thus the character of many-body problem. But this theory also could not break away from the transition-state character in the sense that it made use of the assumption that the state at the top of barrier was sufficiently long

enough to define thermodynamic functions.

Rice(63) developed a theory of self-diffusion in a crystal via vacancy mechanism from a dynamical model of ionic motion. He considered the frequency spectrum of vibrating ions at respective lattice positions from the harmonic approximation. The isothermal jump frequency ω_0 was taken as the product of $\omega_a \omega_b$. The term ω_a is the frequency with which the jumping ion attains a critical amplitude of vibration directed towards the adjacent vacancy. This is given by,

$$\omega_a = \nu' \exp(-U_a/KT) \quad \cdots\cdots\cdots\cdots\cdots\cdots \quad (1.1)$$

where ν' is the weighted mean frequency,

U_a is the energy required for the diffusing ion to reach critical vibration amplitude.

The other term ω_b is the frequency with which the shell ions adjacent to the vacancy attain out-of-phase configuration of vibration with respect to the diffusing ion such that the diffusing ion can be accommodated. ω_b is given by,

$$\omega_b = \Pi \exp(-U_j/KT) \prod_{k>1} g_{k1} \quad \cdots\cdots\cdots\cdots\cdots\cdots \quad (1.2)$$

where U_j is the energy to shift shell ions from equilibrium position such that the diffusing ion can pass,

and g_{k1} is the pair correlation function relating to the position of ions k and 1.

This dynamical model is also not free from criticism. Allnatt and Chadwick(1) mentioned that the introduction of the condition of irreversibility in the calculation of ω_a severely restricts its utility.

However the utility of the isothermal method of formulation of heat of transport in the successful interpretation of experimental evidence seems very limited as it predicts that the heat of transport is less than or at most equal to the energy of migration

of an ion. Experimental evidence that the heats of transport in TlCl(20), Ag_2S, Ag_2Se, Ag_2Te(37) and $SrCl_2$ in NaCl(3) are all greater than their respective energies of migration requires a more rigorous treatment of this problem.

The other approach to the calculation of Q^* is based on the kinetic motion of an ion under a thermal gradient. An important formulation in this approach is due to Wirtz(77). He assumed that the energy, E_m required for an ion to jump from an initial plane to a final plane through the saddle point configuration is comprised of three parts: (i) the energy, E_1 which must be given to the ion in the original plane, (ii) the energy, E_2 needed in the intermediate plane, that is, saddle point and (iii) the energy, E_3 required to prepare the final plane of the jumping ion. In a material under a temperature gradient, the original, intermediate and final planes may be supposed to be at temperatures T, $(T+\Delta T/2)$ and $(T+\Delta T)$ respectively. If this is so, the jump frequencies of the ions making jumps up the temperature gradient are given by,

$$\nu \exp\left(-\frac{E_1}{KT}\right) \exp\left(-\frac{E_2}{K(T+\frac{\Delta T}{2})}\right) \exp\left(-\frac{E_3}{K(T+\Delta T)}\right) \cdots\cdots\cdots (1.3)$$

where ν is the vibration frequency of an ion.

Similarly jumps in the reverese direction are given by,

$$\nu \exp\left(-\frac{E_1}{K(T+\Delta T)}\right) \exp\left(-\frac{E_2}{K(T+\frac{\Delta T}{2})}\right) \exp\left(-\frac{E_3}{KT}\right) \cdots\cdots\cdots (1.4)$$

Now for the condition of zero net flux of ions between the original and the final planes, one obtains,

$$Q^* = E_1 - E_3 \cdots\cdots\cdots (1.5)$$

As it is impossible to envisage any of these energies to be negative, so equation (1.5) leads to,

$$Q^* \leqslant E_1 \leqslant E_m \cdots\cdots\cdots (1.6)$$

Haga(37) made an attempt to calculate the energy flux carried by matter flux in an ionic solid subjected to a temperature gradient. His assumption that the energy of the moving ion through the potential barrier can be considered to be composed of its kinetic energy and the potential energy of interaction with the adjacent ions was very much similar to that of Wert(75). An expression for the heat of transport was given taking into account of variation of vibration frequency of lattice ions due to the presence of defects. This theory though successfully predicts the temperature dependence of heat of transport, it fails to account for the energy carried by the diffusing ion in excess of migration energy.

Allnatt and Rice(7) calculated heat of transport in a crystalline material from the flux of matter in a combined temperature and concentration gradient. They predicted that the heat of transport should be exactly equal to energy of migration which is experimentally unacceptable.

However Schottky(67) tried to incorporate all the essential elements of heat of transport with a model based on the dynamical theory of Rice(63). In this model a whole group of atoms contribute to the activation process in the sense that a jump of an ion is accomplished by the in-phase superposition of lattice modes. Thus the displacement of an ion adjacent to a vacancy is given by,

$$s_1 = \sum_k a_k \sqrt{\varepsilon_k} \cos(\omega_k t + \delta_k) \quad \cdots\cdots\cdots\cdots\cdots \quad (1.7)$$

where ε_k is the phonon energy of mode k

δ_k is the phase of mode k

ω_k is the angular frequency of vibration of mode k.

From this expression he evaluated the jump frequency of an ion. A calculation of jump frequencies of two ions adjacent to a vacancy up

and down the temperature gradient gave the expression,

$$\Delta\omega = \frac{U_a \tau W_1}{a K T^2} \quad \cdots\cdots\cdots\cdots\cdots\cdots\cdots\cdots \quad (1.8)$$

where τ is the phonon relaxation time,

a is the lattice constant,

W_1 is the mean phonon velocity,

and U_a ($=E_m$) is the energy of migration for a linear chain of atoms with harmonic forces.

Now substituting this expression in the equation for matter flux, he obtained the following expression for Q^*,

$$Q^* = U_a\left(1 - \frac{2\tau W_1}{a}\right) \quad \cdots\cdots\cdots\cdots\cdots\cdots \quad (1.9)$$

It should be noted that the term U_a was omitted by Schottky in his formulation of heat of transport. However the corrected expression for heat of transport, as given by equation (1.9), has some features which are worth considering. As $\tau \propto T^{-1}$ and W_1 is negative, the heat of transport decreases with increasing temperature. Experimental evidence that cationic heats of transport in AgCl and AgBr(18) increase with temperature contradicts with Schottky's above formulation. But the pleasing aspect of this model is that it offers a value of Q^* which could be greater than E_m.

Boswarva and Tan(14) in an attempt to explain simultaneously the magnitude and temperature dependence of heat of transport in silver halides considered a dynamical model similar to Schottky's and obtained an expression as follows,

$$Q^* = \left(2 + \frac{q}{T}\right) E_m \quad \cdots\cdots\cdots\cdots\cdots\cdots\cdots\cdots \quad (1.10)$$

where $q = -2\tau W_1 T/a$

and a and τ are lattice parameter and phonon relaxation time.

It is interesting to note that Boswarva and Tan did not calculate Q^* from equation (1.10). On the contrary they used this equation to evaluate q in systems where Q^* was known from thermoelectric power measurements. Their values of q for silver halides are reasonably constant and negative. They failed to apply their theory to alkali halides because of lack of knowledge of crystal-electrode interface effect. This theory does little to advance the calculation of heats of transport since it transfers interest from the unknown Q^* to the equally unknown q.

1.3. Experimental determination of heats of transport.

In the experiments to be described, an attempt was made to measure heats of transport in ionic solids. The phenomena covered by irreversible thermodynamics can very elegantly be described by a set of phenomenological equations relating fluxes of matter and heat to forces which cause their flow. The phenomenological description of ionic solids is considerably simplified if consideration is restricted to high purity materials where impurity considerations can be neglected. For the present work a further simplification was possible since alkali halide single crystals are known to diffuse almost completely by the motion of a single species of mobile defect - the vacancies of the cationic sublattice. Thus the measured heat of transport is effectively that of cations.

In ionic solids, biased vacancy motion due to the application of a thermal force produces a non-uniform distribution of the charged species. This is experimentally detectable as a thermoelectric potential difference between electrods attached to the faces of a specimen held in a temperature gradient. The potential difference due to a unit temperature difference between the faces under condition of zero current flow through the material is known as the thermoelectric power. Thermoelectric power is considered to be composed of (i) a homogeneous component which is attributed to the thermomigration of ions in the solid and is related to heat of transport, Q^* and (ii) a heterogeneous component which is attributed to temperature dependence of contact potentials and is related to entropies of formation of defects.

Thermoelectric power has been used as a basis for the calculation of heats of transport by a number of workers. One criticism inherent to this type of work is that the observed potential difference

arises only in part within the bulk of the solid, some fraction being always due to interfacial potentials between the salt and its contacting electrodes. Any measurement of a heat of transport based on total thermoelectric power is thus basically unreliable as there is no way of seperating the homogeneous component from the total effect.

For this reason, a central aim of this work is to derive estimates of heats of transport for cations from bulk properties of the solids. The approach depends on comparison of thermal and electric field forces and the effects they have on electric resistance. The interface effects and other uncertainties do not interfere with the measurements and thus they have the potential to provide uniquely precise estimates for heats of transport in ionic materials.

The evaluation of heats of transport in ionic solids using only bulk properties is also of extreme interest to the study of thermoelectric power. The homogeneous thermoelectric power can be precisely calculated if the heat of transport is uniquely known. By comparison with the experimentally observed total thermoelectric power it is therefore possible to determine the heterogeneous thermoelectric power. This is the pleasing aspect of this experimental work.

To promote confidence in the techniques and equipments to be used for the measurement of heats of transport, an initial experiment was done using crystals of potassium chloride so that estimates of the cationic heat of transport could be compared with the earlier work by Lowe(58). In the event these estimates gave the broad agreement required and through their internal consistency suggested that some improvements in techniques had been made.

An understanding of transport processes in ionic solids is critically dependent on the knowledge of their defect properties. Chapter 2 reviews these properties in both equilibrium and non-equilibrium

conditions. Here the vacancy flow is described in terms of motion between sources and sinks and the fundamental equations for ionic conductivity are deduced. Chapter 3 is used to develop equations from the phenomenological theory which allows the derivation of heats of transport in terms of experimentally accessible parameters. This chapter also deals with basic equations of homogeneous and heterogeneous thermoelectric powers deduced by different authors from kinetic as well as non-kinetic theories. Details of equipment and techniques of measurements are described in chapter 4. Chapter 5 analyses the experimental results and shows the calculated values of different parameters in tabular as well as graphical forms. A discussion on the theory of heat of transport is incorporated in chapter 6. Major conclusions drawn from the present work are also listed in this chapter.

CHAPTER 2

DEFECT PROPERTIES IN ALKALI HALIDES

2.1. Point defects.

Any crystalline solid will have an accurately stoichiometric composition only at absolute zero temperature since at that temperature its entropy is effectively zero. At all higher tempera-tures the solid must deviate to some extent from the perfect state due to the appearance of lattice defects. In ionic solids the two most important imperfections are vacant lattice sites and interstitials. These types of inherent thermodynamic defects are best described in terms of (a) Schottky defects(65,66) and (b) Frenkel defects(31).

A Schottky defect is an irregularity of crystal structure containing a single cation vacancy and a single anion vacancy without the existence of any interstitial ion. The structure of a Schottky defect in a crystal MX is shown in figure (2.1). It was

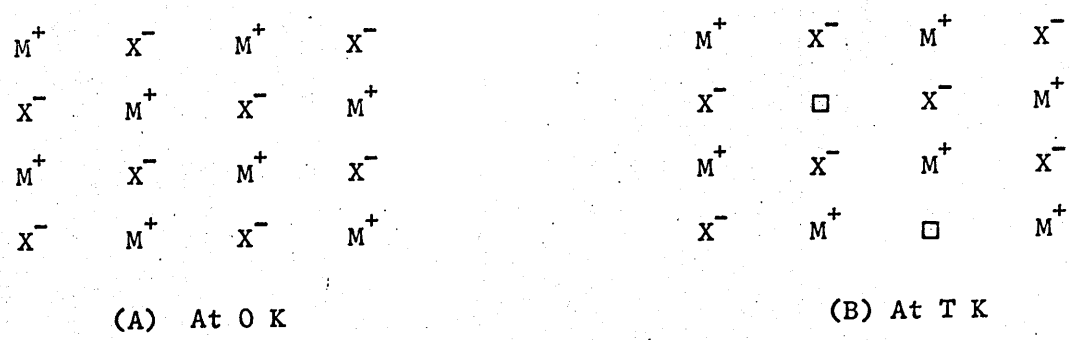

Figure 2.1. Formation of a Schottky defect. The crystal at absolute zero is perfectly regular, whereas at T K there are equal numbers of vacancies in anion and cation sublattices.

originally imagined that the vacancies originate in steps in the surface and then diffuse into the body of the crystal. But according to the recent ideas of dislocations, steps in dislocation lines provide a distribution of internal sources and sinks so that vacancies in the interior of a crystal have not necessarily come from the surface(56).

The number of Schottky defects in alkali halides at thermodynamic equilibrium is found by considering the fact that at thermal equilibrium the change in Helmholtz free energy, $\Delta F(=\Delta U - T\Delta S)$ with respect to change in the number of defects is zero(36). Thus putting expressions for change in internal energy ΔU and change in entropy ΔS due to introduction of C number of Schottky defects per unit volume at a temperature T K and then equating $\frac{\partial}{\partial C}(\Delta U - T\Delta S)$ to zero, the number of cationic or anionic defects per unit volume is found as,

$$C = N \exp(-\frac{E_f}{2KT}) \quad \ldots\ldots\ldots\ldots\ldots\ldots\ldots\ldots \quad (2.1)$$

where N is the number of sites of each type of ion per unit vol., and E_f is the measurable energy of formation of Schottky defect pair which is equal to enthalpy of formation.

In this expression the product $(\frac{C}{N})(\frac{C}{N}) = \exp(-\frac{E_f}{KT})$ is called the solubility product relation. In the derivation of equation (2.1) three important assumptions are made. These are: (a) that the concentration of defects is sufficiently small so that interactions between them can be neglected, (b) that the effect of change of volume on the number of Schottky defects can be ignored and (c) that the vibrational frequencies of the ions in the solid remain unaffected by the presence of vacant sites.

Another lattice defect common to ionic solids is the Frenkel defect. This can be seen as formed by the movement of an ion from a normal lattice site to an interstitial site, a vacancy being left behind. The combination of an interstitial ion and a vacancy is called the Frenkel defect. The formation of a Frenkel defect is shown in figure (2.2). The concentration of vacancies and interstitials must be equal to satisfy the condition of overall electrical neutrality. It should be noted that the vacancies and interstitials are so much apart

that there is no force of attraction between them.

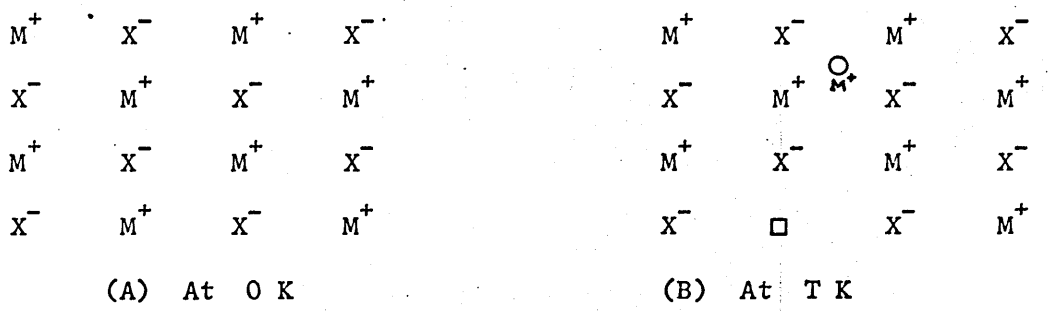

Figure 2.2. Formation of a Frenkel defect. The crystal at absolute zero is perfectly regular, whereas at T K there are equal number of interstitial ions and vacant lattice sites in one of the sublattices.

Early measurements to establish the dominant type of defect in different crystals demonstrated that alkali halides, silver halides, thallous and lead halides and alkaline earth halides have intrinsic ionic defects. Because of large forbidden gap in the energy band configuration of these solids, the electronic contribution to conductivity is totally negligible in comparison to the ionic

Table 2.1. Dominant types of defect in ionic solids.

Substance	Crystal structure	Intrinsic defect
Alkali halides	NaCl	Schottky
Alkaline earth halides	NaCl	Schottky
Alkali halides, TlCl, TlBr	CsCl	Schottky
Silver halides	NaCl	Cation Frenkel
Alkali earth flurides, CeO_2	CaF_2	Anion Frenkel

contribution. The cuprous halides show marked ionic and electronic conduction with ionic conduction predominant at high temperatures. The oxides, sulphides and selenides show predominantly electronic conduction with the exceptions of CeO_2, ThO_2 and ZrO_2. The dominant intrinsic defects in some common ionic solids are shown in Table(2.1)(10).

The formation of a Schottky defect or of a Frenkel defect in a solid is critically dependent on the energy of formation of these defects. Jost(48) applied classical Born-Mayer theory to the calculation of energy of formation of a defect. He assumed that the vacant lattice site may be considered as a spherical cavity of radius R_v in a non-vibrating lattice of dielectric constant and that the lattice is polarised by the formation of a defect. Faux and Lidiard(29) rejected this model pointing out that the Born-Mayer repulsive potential gives a static dielectric constant in the vicinity of the defect much larger than that of the substance. This anomaly can be resolved by considering the Shell model which has been so successful in describing lattice dynamics. But Boswarva (15) pointed out that Born-Mayer model is adequate for defect energy calculations if repulsive potential parameters are chosen as interionic distance of separation,r and static dielectric constant instead of r and the compressibility. In other words, he contends that the vacancy influences the crystal property through the electrical discontinuity rather than its elasticity. For the explicit calculations of energy of Schottky defects, it is necessary arbitrarily to divide the crystal into two regions - region 1 is the immediate vicinity of the defect and region 2 is the rest of the crystal. It is assumed that the harmonic approximation may be made in region 2. The calculated values of energy of formation of Schottky defect pairs using 6 and 32 ions in region 1 are listed in Table (2.2) (15).

Table 2.2. Calculated values of energy of formation of Schottky defect.

Substance	Energy of formation/ eV	
	6 ions	32 ions
NaCl	2.36	2.27
KCl	2.54	2.50
NaBr	2.33	2.33

Whatever the precision of these calculations point defects are responsible for conduction in ionic solids. In an attempt to establish the contributions of different species to conductivity in alkali and silver halides, Tubandt et al(72) had found that at low temperatures cations are wholly responsible for conduction whereas at high temperatures the contributions from anions become progressively higher. This contribution to conductivity is described in terms of the transport number of a species and is defined as the fraction of current carried by that species. The variation of transport numbers of cations and anions with temperature in two common alkali halides are shown in Table (2.3)(56).

Table 2.3. Dependence of transport numbers on temperature.

Salt	Temperature/K	Cation transport number, t_+	Anion transport number, t_-
NaCl	673	1.00	0.00
	773	0.98	0.02
	873	0.95	0.05
KCl	673	1.00	0.00
	773	0.94	0.06
	873	0.88	0.12

2.2. Ionic conductivity and diffusion.

Electrical conductivity in alkali halides is due to the movement of ions under a driving force. It has been established that the ions which are responsible for conductivity in solids like NaCl and KCl are mainly cations. Such cations normally execute to and fro motions about their respective lattice positions at all temperatures above absolute zero. Sometimes a particular ion may receive enough energy to jump from one lattice position to a neighbouring lattice position leaving behind a vacancy. Such jumps however occur only if there happens to be a vacant site at an adjacent position just at the time when the ion has sufficient energy to make the transition. A description of the situation may be made in terms of an energy barrier as shown in figure (2.3a). Here the height of the barrier E_m is the energy of migration for an ion. An important feature of the diagram is its symmetry. This has the consequence that ions at all times have an equal probability of moving to any of the sites which are adjacent and accessible to them. The pattern of movement that they make in this way through the sites of a lattice is known as random walk(59).

The application of an electric field perturbs the symmetry of the energy barrier. This is shown in figure (2.3b). Let a uniform electric field E act along the ⟨100⟩ crystallographic axis, which is taken as X axis. This electric field will reduce the energy barrier for ions jumping from plane 1 to plane 2 by (1/2)eaE and increase it by (1/2)eaE for ions jumping in the opposite direction(56).Let the number of ions per unit area that effectively take part in the jumping process in plane 1 and 2 be n_{p1} and n_{p2} respectively and their jump frequencies be ν_1 and ν_2. Now the jump frequency of an ion in the absence of an electric field can be described by $\nu = \nu_0 \exp(-E_m/KT)$

where ν_0 is the Debye frequency. Thus the jump frequencies of the ions from plane 1 to 2 and 2 to 1 in the presence of an electric field will be given by,

$$\nu_{12} = \nu_0 \exp\left(-\frac{1}{KT}\left(E_m - \frac{1}{2}eaE\right)\right) \quad \cdots\cdots\cdots\cdots\cdots \quad (2.2a)$$

$$\nu_{21} = \nu_0 \exp\left(-\frac{1}{KT}\left(E_m + \frac{1}{2}eaE\right)\right) \quad \cdots\cdots\cdots\cdots\cdots \quad (2.2b)$$

This asymmetry of jump rate produces a net flow of ions and hence of electric charge. The current density J of this charge flow in the

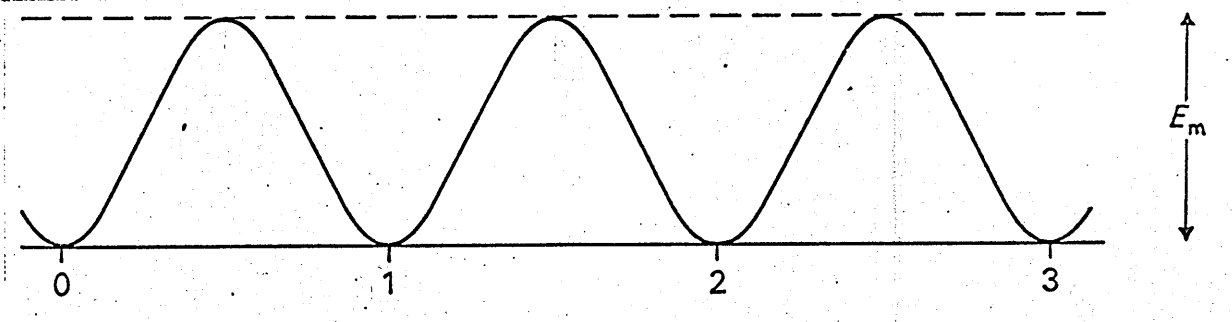

Figure 2.3.a. Energy barrier in the absence of any driving force.

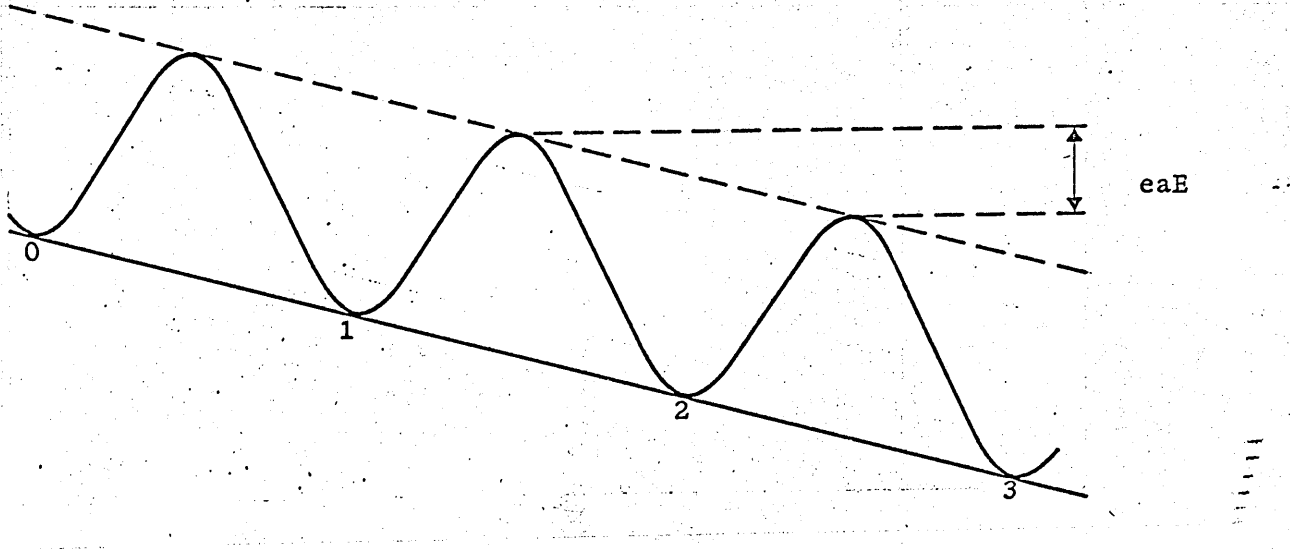

Figure 2.3.b. Energy barrier in the presence of electric driving force.

direction of the field is given by,

$$J = n_{p1}\, e\, \nu_{12} - n_{p2}\, e\, \nu_{21}$$

$$= n_{p1} e\, \nu_0 \exp(-\frac{1}{KT}(E_m - \frac{1}{2} eaE)) - n_{p2} e\, \nu_o \exp(-\frac{1}{KT}(E_m + \frac{1}{2} eaE))$$

Assming $eaE \ll KT$,

$$J = e\, \nu_0 \exp(-\frac{E_m}{KT})\, (n_{p1} - n_{p2}) + \frac{eaE}{2KT}\, (n_{p1} + n_{p2}) \cdots\cdots\cdots \quad (2.3)$$

Now $n_{p1} - n_{p2} = -a \frac{\partial n_p}{\partial x} = -a^2 \frac{\partial C}{\partial x}$

and $n_{p1} + n_{p2} = 2aC$, since $n_p = aC$

where C is the number of ions per unit volume that take part in conductivity process and is the concentration of Schottky defects and a is the lattice constant.

$$J = e\, \nu_0 \exp(-\frac{E_m}{KT})(- a^2 \frac{\partial C}{\partial x} + \frac{a^2 eCE}{KT}) \quad \cdots\cdots\cdots\cdots\cdots \quad (2.4)$$

Written in this form the first term in the parenthesis arises from normal diffusion movement while the second term has its origin in the driving force. The second term describes ionic flow in response to the applied field and since this is very much higher than the diffusion flow given by the first term, the equation for current density in a solid under an electric driving force is given by,

$$J = \frac{a^2 e^2\, C\, E}{KT}\, \nu_0 \exp(- \frac{E_m}{KT}) \cdots\cdots\cdots\cdots\cdots\cdots\cdots\cdots \quad (2.5)$$

As the conductivity of a material is defined as $\sigma = J/E$, this gives

$$\sigma = \frac{a^2 e^2\, C}{KT}\, \nu_0 \exp(- \frac{E_m}{KT}) \quad \cdots\cdots\cdots\cdots\cdots\cdots \quad (2.6)$$

An alternative way to describe ionic motion is in terms of the mobility μ. The defining equation for this is,

$$\sigma = C\, e\, \mu \quad \cdots\cdots\cdots\cdots\cdots\cdots\cdots\cdots\cdots\cdots \quad (2.7)$$

so $$\mu = \frac{a^2 e}{KT} \nu_0 \exp(-\frac{E_m}{KT}) \quad \cdots\cdots\cdots\cdots\cdots\cdots \quad (2.8)$$

If in equation (2.6) the concentration of Schottky defects C is substituted from equation (2.1), the conductivity is then given by,

$$\sigma = \frac{N a^2 e^2}{KT} \nu_0 \exp(-\frac{E_D}{KT}) \quad \cdots\cdots\cdots\cdots \quad (2.9)$$

where $E_D = (\frac{E_f}{2} + E_m)$ is the activation energy for diffusion.

In the derivation of equation (2.9) deviations from a biased motion due to interactions among defects or between defects and aliovalent impurities are ignored. Thus this equation describes the conductivity of a solid in a temperature region where contributions from sources other than equilibrium defect concentrations are negligible. For this reason it is called the intrinsic conductivity.

In ionic solids, point defects are responsible for both diffusion and conductivity. While diffusion represents a mixing up of the atoms in a crystal because of thermally induced random motion of the defects, the conduction represents biased motion due to application of an electric field. These two conceptually different processes are quantitatively related by the Nernst-Einstein equation which is, for the present purposes, given by,

$$\frac{\sigma}{D} = \frac{C e^2}{KT} \quad \cdots\cdots\cdots\cdots\cdots\cdots\cdots \quad (2.10)$$

With this equation it is in principle possible to derive diffusion coefficient D from conductivity σ and vice versa. However this sort of calculation will generally be inaccurate as the diffusion coefficient obtained from measurements of total conductivity represents a total diffusion coefficient which may or may not equal

to the diffusion coefficient of one particular species. On the contrary neutral defect complexes such as impurity-vacancy associations or vacancy pair complexes contribute to diffusion but not to conductivity. Despite these limitations, diffusion coefficients derived from the above equation may offer a reasonable approximation to the true value under suitable conditions of measurement. In an alkali halide at temperatures well below the melting point, the transport number for cations is almost equal to unity and the factor D obtained from equation (2.10) and the self-diffusion coefficient for cations are almost equal.

The experimentally measured diffusion coefficient in the intrinsic temperature range normally fits Arrhenius equation,

$$D = D_0 \exp(-\frac{Q}{KT}) \quad \cdots\cdots\cdots\cdots\cdots\cdots \quad (2.11)$$

where D_0 is the pre-exponential factor,

and Q is the experimental activation energy for diffusion.

For self-diffusion in alkali halides, Q has been found to be equal to the activation energy E_D to a high degree of accuracy. But for impurity diffusion Q may differ considerably from E_D (59).

Downing and Friauf (26) measured diffusion of Na^+ in NaCl from 863 K to 963 K by the sectioning method. Their results, when fitted to the Arrhenius equation for diffusion, give the following values,

$$D_0 = (3.2 \pm 1.1) \text{ cm}^2/\text{sec} \quad \cdots\cdots\cdots \quad (2.12a)$$

$$Q = (1.78 \pm .03) \text{ eV} \quad \cdots\cdots\cdots\cdots\cdots \quad (2.12b)$$

They also measured ionic conductivity and calculated the total diffusion coefficient using the Nernst-Einstein relation. Comparison of the two values of D shows an excess diffusion of (10 % - 20 %). They attribute this excess diffusion to vacancy pairs.

Beniere et al (13) employed radio tracer and

conductivity measurements to study movement of cation vacancies, anion vacancies and vacancy pairs in pure as well as Sr^{++} doped single crystals of KCl. For intrinsic diffusion, they obtained,

$$D_0 = 33.16 \text{ cm}^2/\text{sec} \quad \cdots\cdots\cdots\cdots\cdots\cdots \quad (2.13a)$$

$$Q = 1.975 \text{ eV} \quad \cdots\cdots\cdots\cdots\cdots\cdots \quad (2.13b)$$

In this section an equation for the electrical conductivity of an ionic solid held at a uniform temperature has been obtained. This equation will be used in section (3.2) for the evaluation of total resistance of a specimen when subjected to a gradient of temperature. Also the values of D_0 and Q from equations (2.12) and (2.13) will be used in chapter 5 when attempts will be made to calculate mean free paths of cation vacancies in NaCl and KCl respectively.

2.3. Principal features of ionic conductivity.

Interest in the detailed study of ionic conductivity in solids like alkali and silver halides arises mainly because it provides a unique opportunity for the measurement of parameters that describe defect structures. The parameters obtainable from such studies are enthalpies and entropies of formation, migration and interaction of defects. These parameters not only describe thermally generated defects but also aliovalent impurities which are dissolved substitutionally or interstitially in the solvent.

Ionic conductivity, in its essentials, can be described according to Kock and Wagner(53), by considering two distinct regions in a conductivity plot as shown in figure (2.4) where the variables are σT - the product of conductivity and absolute temperature and the

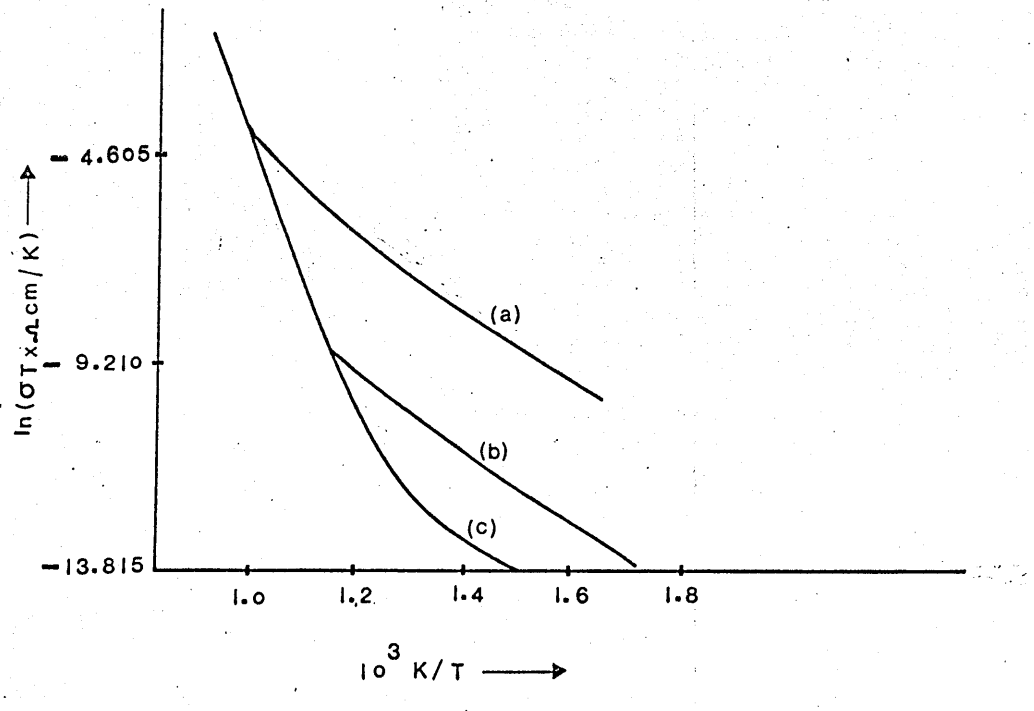

Figure 2.4. Ionic conductivity as a function of temperature in KCl; (a) KCl+200 ppm $CaCl_2$, (b) KCl analytically pure and (c) recrystallized KCl.

reciprocal of absolute temperature. Following their analysis the conductivity plot is a superposition of two roughly linear curves; (a) $A_1 \exp(-\frac{E_1}{KT})$ for low temperature part and (b) $A_2 \exp(-\frac{E_2}{KT})$ for high temperature part.

The low temperature part of the conductivity curve displays a smaller slope and is mainly due to non-stoichiometry of the solid substance. Since in this region aliovalent metallic impurities associate with cationic vacancies, it is called the association range(27). In this low temperature range surface and grain boundary conduction as well as impurity content and thermal history contribute significantly to the conduction and it is unique to each specimen. The exponent E_1, the slope of the conductivity plot in this extrinsic range, is the energy of migration of a defect while the pre-exponential factor A_1 depends inversely on the purity of the specimen. The transition region or 'knee' of the plot may be taken as that temperature at which structural defects are equal to the thermally activated defects (56).

Conductivity above the knee is an intrinsic property of the crystal. In this region the number of thermally produced defects outweighs the structural defects to such an extent that the contribution of structural imperfections to the conductivity can be considered negligibly small in relation to that of thermal defects. Assuming a single diffusion mechanism, the exponent E_2 of this region is the activation energy which equals the sum of energies of migration and formation for the diffusing species. This activation energy for diffusion can be obtained from the slope of the plot in the intrinsic range.

Systematic variations of conductivity with purity are well documented. Figure(2.4) shows the positions of the knee

regions in recrystallized and analytically pure KCl specimens together with a KCl specimen having deliberate and controlled impurity content of 200 ppm of $CaCl_2$. It may be seen that the temperature of the knee point increases with the impurity content. Shapiro and Kalthoff(69) had shown that the conductivity of ionic solids like AgBr may have a dip at the knee region if the specimen is thermally aged and that the conductivity is significantly smaller in thermally aged specimens than in fresh ones.

Analyses of the above type based on an assumed linearity of the conductivity plot are now considered inadequate. First, the linearity of the intrinsic and extrinsic regions is an experimental oversimplification. Second, it is naive to think that extrinsic conductivity is dependent only on the free energy of migration of defects. In fact, conductivity at low temperatures show a concave pattern towards the T^{-1} axis which is due to association of divalent cation impurities and cation vacancies. The intrinsic range of conductivity shows on the other hand a convex pattern towards the $\ln(\sigma T)$ axis. This is so because at high temperatures the intrinsic is enhanced by the increased mobility of cation and anion vacancies.

The modern approach to conductivity analysis is to use a non linear least squares programme to calculate the best fit values of defect parameters into the experimentally observed points. Beaumont and Jacobs(11) analysed the conductivity curve between 643 K and 963 K for KCl using a simple nearest-neighbour association approximation based on the Teltow model. They used eight parameters namely; enthalpy and entropy of formation of defect pairs, enthalpy and entropy of cation vacancy migration, enthalpy and entropy of anion vacancy migration, Gibbs free energy of impurity-vacancy association and total fraction of impurity ions. Their procedure was to fit these

parameters to their experimental values using a subroutine which minimised the function

$$F = 100((N-1)^{-1} ((\ln\sigma T)_{calc} - (\ln\sigma T)_{expt})^2)^{\frac{1}{2}} \quad \cdots\cdots \quad (2.14)$$

where N is the number of data points,

and suffixes denote calculated and experimental values.

The method is quite successful in calculating cation as well as anion migration and formation energies and results are in reasonable agreement with Fuller(33). But in spite of this success, there are some inherent deficiencies in their analyses: (i) that only the nearest neighbour interactions of defects were considered, the long range Debye-Huckel interactions being ignored and (ii) that the analysis was restricted to conductivity data between 643 K and 963 K, that is, to about 90 K below the melting point.

Fuller et al(34) analysed the complete intrinsic region (833 K - 1048 K) of the conductivity plot of KCl using what is known as 'Intrinsic-only' computer fitting. In this method only four intrinsic parameters were considered. The concentration of divalent impurities was ignored. Fuller et al found that their calculated parameters did not agree well with those of Beaumont and Jacobs(11). However they demonstrated a striking inadequacy of the Beaumont and Jacobs method by extrapolating the conductivity curve to high temperatures (>1023 K) using Beaumont and Jacobs parameters and showed that the projected points lie well below their experimental points above 963 K.

Further information on this matter comes from Allnatt and Pantelis(6) who found an abnormal increase in conductance in alkali halides at high temperatures. Fuller and Reilly(35) attempted to explain this increase in conductance at high temperatures by assuming that this was due to trivacancy mechanism. But this

explanation had been criticised by Jacobs and Pantelis(46) on the ground that the difference between calculated best fit points and experimental points cannot be accepted as due to a trivacancy contribution alone.

Recognising all these inadequacies, Jacobs and Pantelis(46) felt the necessity for critical analysis of existing theories and careful reevaluation of parameters which could describe adequately the conductivity of alkali halides over the whole range of temperatures. They started with the analysis of Beaumont and Jacobs(11) and modified it to include the Debye-Huckel interactions. They then took up the suggestion put forward by Allnatt and Pantelis(6) that NaCl might contain Frenkel defects at high temperatures and attempted to analyse the conductivity on the basis of a cationic Frenkel defect model. Having shown that none of the above mentioned models was completely satisfactory, they then examined what they term an 'excess conductance model' by introducing an extra term $(B/T)\exp(-E/KT)$ into the conductivity equation. Though they failed to produce any physical basis for this extra term, they assumed in line with Barr and Dawson(9) that it might be due to a dislocation contribution. The unknown parameter B was taken proportional to $eC_d\mu_d$ where C_d and μ_d are respectively the dislocation density and dislocation mobility. But due to lack of knowledge about the values of C_d and μ_d, they did not pursue this dislocation model any further. The question of the role of dislocations in the diffusion process is of some consequence to the present study. However this subject will be taken up in section (2.5) for detailed discussion.

While there is still some discussion on the values of the parameters describing defect motion in sodium and potassium chlorides, the present work depends only to a lesser degree on their precise evaluation. Some general confirmatory data - intended

mainly as a check on experimental method - will be presented in chapter 5, but for purposes of calculation it will be assumed that defect parameters are adequately described by data of other workers as shown in Table 2.4.

Table 2.4. Characteristic enthalpies of Schottky defects.

Authors	KCl			
	Enthalpy of formation of defect pair/eV	Enthalpy of migration of cation vacancy /eV	Enthalpy of migration of anion vacancy /eV	Enthalpy of association divalent-impurity vacancy /eV
Beaumont and Jacobs(11)	2.26	0.71	1.04	0.43
Jacobs and Pantelis(Debye Huckel model) (46)	2.30	0.68	1.39	0.58
Chandra and Rolfe(18)	2.59	0.73	0.99	0.58
	NaCl			
Allnatt and Pantelis(6)	2.17	0.66	1.17	-
Kirk and Pratt(51)	2.30	0.69	1.83	0.29(Mn^{++})
Brown and Hoodless(17)	2.30	0.76	-	0.46(Sr^{++})

2.4. Specimen-electrode interface phenomena.

The phenomena occuring at the interface between a specimen and its electrodes are important factors in the study of a.c. ionic conductance in alkali halides at temperatures within 300 K of the melting point. These interface effects are responsible for the variation of conductance and capacitance with frequency. When an a.c. field is applied to a sodium chloride or potassium chloride specimen, the mobile charge carriers move back and forth in phase with the applied voltage. Their movement constitutes ionic conductance. Ideally each carrier would discharge as it arrives at the crystal-electrode interface, but in fact this may not quite happen as carriers discharge at a rate which differs from the rate of arrival at the interface. When this happens a charged layer is built up which retards the approach of further charge carriers. This may be detected experimentally as an increase in resistance and capacitance(32). This increase in resistance and capacitance is normally described in terms of polarization conductance and polarization capacitance.

These effects are however frequency dependent, high frequency conductance showing little interface effects. In this way it is possible to define polarization conductance as the measured conductance minus the high frequency conductance. Similarly the polarization capacitance is taken as measured capacitance minus geometric capacitance per unit area measured at low temperatures when polarization is negligible.

Recently there have been both theoretical and experimental investigations into the effect of interfacial polarization on conductance and capacitance. The theoretical approach has been to assume a constant rate of carrier discharge at electrodes which is characterised by a dimensionless discharge parameter, ρ. For a

completely blocked electrode ρ is zero and for a completely free electrode ρ is infinite. Beaumont and Jacobs(12) developed a theory, referred to as a 'linearised electrode blocking theory'. It is based on the assumption of small applied a.c. voltage in order to linearise the constituent non-linear differential equations. Here the criterion of small voltage is that it should be far less than KT/e. The deficiency of the linearised electrode blocking theory is its neglect of the space charge layer occuring at the interface at thermodynamic equilibrium. The thoery does however predict a correct order of magnitude for both polarization capacitance and polarization conductance in KCl over a limited temperature range. Beaumont and Jacobs(12) recognise the approximate nature of their theory and hold the view that its usefulness may be extended into the high temperature region by assuming a distribution of ρ over the crystal-electrode surface instead of fixed discreet values of ρ .

Miliotis and Yoon(60), on the other hand, contend that the observed dependence of ionic conductance on frequency is not due to interfacial polarization but due to the existence of actual gaps between the specimen and its electrodes. They assume that the gaps act as capacitors in series with the parallel combination of specimen conductance and capacitance and maintain that high frequency ($>$1MHz) dielectric relaxation is caused by large air-gaps which can be eliminated by improving crystal-electrode contacts. Though this theory successfully accounts for the high frequency effects, it fails to explain low frequency phenomena.

Allnatt and Sime(8) maintain that polarization conductance and capacitance at low frequencies can be explained in term another air-gap model. Their model assumes that a fraction α of the interface is in perfect contact, the polarization effect there being negligible, and that the rest $(1-\alpha)$ is in series with

air-gaps having complete electrode blocking. They have measured the polarization impedence of pure and $SrCl_2$ doped NaCl in the frequency range of 100Hz to 2KHz to establish the validity of their theory. Unfortunately their theory fails to offer a complete account of the experimental evidence.

In fact the experimental evidence for the existence of interface effects is much too detailed to be described by existing theories. Sastry and Srinivasan(64) have observed dispersions in dielectric constant of KCl and NaCl crystals at temperatures between 873 K and 973 K in the frequency range of 1 and 10MHz which they attribute to relaxation of cation-anion vacancy pairs. Dielectric losses due to relaxation of divalent impurity-vacancy complexes at a temperature of about 773 K in the frequency range of 1 to 10KHz are also reported by Wimmer and Tallan(76).

For present purposes the phenomena noted above are important mainly in fixing the frequency range at which a.c. conductivity may reliably be measured over the temperature range of 700 K and 1000 K. At high frequencies (>1MHz), even small air-gaps contribute substantially to the dispersion of dielectric constant and this alters the true ionic conductivity. As it is very difficult to eliminate small air-gaps even by thermal cycling, it was decided that the working frequency should be considerably smaller than 1MHz. Again the lower limit of the frequency range set by the appearance of interfacial polarization is about 2KHz. Considering these limiting factors, a signal frequency of 5KHz was used for this work, but some initial testswere made at 3KHz to ensure that the resistance data were not frequency dependent. Additional confirmation that this frequency of 5KHz is reasonable lies in the fact that the experimental data proved reproducible to about 2 % .

2.5 Dislocations

Point defects are not the only disorders found in the lattice structure of alkali halide crystals. Dislocations are lattice defects which can extend beyond the volume of one or two atoms and like point defects they have some influence on diffusion and electrical conduction in these solids.

For present purposes the main points of interest are that the core of an edge dislocation is a place at which impurities will tend to accumulate and that it is also a place which can act as a source or sink for vacancies. The density of dislocations thus determines the rate at which a salt will rid itself of an excess concentration of vacancies above the thermal equilibrium number and the rate at which it will produce vacancies to make up a deficit.

Eshelby et al(28) proposed a theory, called charged dislocation theory, which in essence says that dislocations even at thermal equilibrium may be charged if cationic and anionic defect formation energies are unequal and this charged dislocation core is surrounded by Debye-Huckel cloud of vacancies. Consequently a minimum amount of stress is required for slip to occur since the dislocation and its vacancy cloud will experience electrostatic attraction. By studying stress-strain curves, they found that a finite force is required to separate the dislocation from the cloud in ionic solids like sodium chlorides.

This charged dislocation theory was elaborated by Kanzaki et al(49) who studied the effects of dislocation density upon ionic conductivity in both pure and doped potassium chloride crystals. They performed both a.c. and d.c. measurements and produced evidence that ionic conductivity in pure crystals is strongly influenced by the dislocation concentration, whereas in impure crystals aliovalent

impurity concentration effect is much more prominent. By counting etch pits, they found that at room temperature the mean dislocation density in pure unstrained potassium chloride crystal was about $3x10^6$ cm^{-2} but rose to $1x10^7$ cm^{-2} in deformed and annealed specimens.

Vacancies can be created in a crystal both by mechanical and thermal means. Davidge et al(23) have reported the generation of vacancies in alkali halides through the intersection of dislocation arrays during straining of these materials. In these circumstances the vacancies tend to form small but stable clusters. Vaughan et al(73) have produced evidence for dislocation generation of point defects by showing density changes in crystals.

Thermal production of vacancies at edge dislocations is due to movement of atoms onto the extra half-plane of atoms above the dislocation line from the regular lattice sites. This movement leaves behind vacancies which are free to perform normal thermally activated motion through the crystal. In thermal equilibrium vacancy production in this way must be accompanied by an equal rate of vacancy loss by reverse movement of atoms off the extra half-plane. This pattern of vacancy motion makes it appropriate to describe dislocations as sources and sinks for vacancies.

Both impurity atoms and dislocations may be expected to accept vacancies. In the first case however the vacancies are merely trapped, while in the second case they are annihilated. In carefully purified crystals such as used in this present work the effect of divalent impurity concentration is much smaller than that of the dislocation density. This can be seen from the following considerations. According to the manufacturer's quotation the total divalent impurity concentration in these crystals is about 10 ppm. Expressed in terms of area this is about $3x10^4$ cm^{-2} for divalent

impurity concentration, a number which is to be compared with the mean dislocation density of 2×10^6 cm^{-2} of Harshaw potassium chloride crystal(49). Thus dislocations are almost totally responsible for the creation and annihilation of vacancies in these crystals. The average distance by which a vacancy can migrate before being annihilated is termed as the mean free path, λ. A quantitative relation can be found connecting mean free path, λ and the dislocation density, ρ.

Let it be assumed that at a particular plane, a dislocation has a certain area of influence given by d^2. So,

$$d^2 = \frac{1}{\rho}$$

In ionic solid, the number of atoms, N_A of each species in this area of atomic monolayer is,

$$N_A = \frac{d^2}{a^2} = \frac{1}{a^2 \rho}$$

where a is the lattice spacing.

The effective concentration of dislocations, C_D is thus

$$C_D = 3 N_A = \frac{3}{\rho a^2}$$

Assuming then that vacancies follow a true random motion which terminates on arrival at a dislocation site, the mean number, $\bar{n}$ of vacancy jumps between source and sink is,

$$\bar{n} = \frac{3}{\rho a^2}$$

This number may be related to the mean free path of the vacancy by,

$$\lambda = a\sqrt{\bar{n}}$$

$$= a\sqrt{\frac{3}{\rho a^2}}$$

so $$\rho = \frac{3}{\lambda^2} \quad \ldots\ldots\ldots\ldots\ldots\ldots\ldots\ldots\ldots\ldots\ldots\ldots\ldots\ldots\ldots\ldots (2.15)$$

If dislocations are indeed the dominant sources and sinks for vacancies, this equation should allow the vacancy mean free path or alternatively the vacancy life time to be tied to the dislocation density. This equation will be used in chapter 5 to

calculate the mean dislocation density from a knowledge of mean free path of vacancies. An estimate of relative efficiency of dislocations can be made from the calculated values of dislocation density.

The concept of vacancy source and sink will be utilised in next chapter in the mathematical formulation of excess vacancy concentration in potassium and sodium chloride crystals. But it should be emphasised that the basic mechanism of atomic migration remains unaffected even in the presence of vacancy sources and sinks. Under thermal and electric field gradients, the vacancies execute non-random motion and are influenced by these sources and sinks.

CHAPTER 3

THEORIES OF TRANSPORT

3.1 Phenomenological description of thermomigration.

Phenomenological equations are used for the description of solid materials in non equilibrium conditions. Such equations relate fluxes of matter and heat flowing in a material to thermodynamic forces that cause the flow(25). The advantage of using this description is that one can describe the physical processes occuring inside a solid material quite adequately without knowing the precise nature of atomic migration. The assumption that is made in this description is the existence of local thermodynamic equilibrium. This implies that the local concentration and distribution of lattice defects can be calculated from the knowledge of local values of state variables such as temperatures and pressures. Thus the knowledge of isothermal systems forms the basis for the study of systems under non equilibrium conditions(57).

Regular crystalline solids subjected to a gradient of temperature will develop a gradient in the concentration of defects, simply because at the hot end there are more defects than at the cold end. Thus the chemical potential, which is defined as the change in Gibbs free energy due to change of one mole of defects, will have different values at hot and cold ends. These gradients of temperature and chemical potentials are the thermodynamic forces which are related by the phenomenological equations to the fluxes of matter and heat. The generalised phenomenological equations allowing for interactions of the two gradients are(1),

$$J_i = \sum_{k=1}^{n} L_{ik} X_k + L_{iu} X_u \quad \cdots\cdots\cdots\cdots\cdots\cdots \quad (3.1)$$

$$J_q = \sum_{k=1}^{n} L_{uk} X_k + L_{uu} X_u \quad \cdots\cdots\cdots\cdots\cdots\cdots \quad (3.2)$$

The subscripts i and k (= 1 to n) denote different species which can be atoms, molecules, ions or even vacancies of different kinds. The

quantity J_i denotes the flux of species i, that is, the number of species i crossing unit area in unit time; it is thus the matter flux. J_q is the reduced heat flux. The reduced heat flux is the heat flux in excess of average enthalpy transported by the matter flux. The thermodynamic forces are defined as,

$$X_k = -(\nabla \mu_k)_T - e_k \nabla \Phi \quad \cdots\cdots\cdots\cdots\cdots\cdots \quad (3.3)$$

$$\text{and} \quad X_u = -\frac{\nabla T}{T} \quad \cdots\cdots\cdots\cdots\cdots\cdots\cdots\cdots \quad (3.4)$$

where μ_k is the chemical potential of species k

e_k is the charge of species k

Φ is the electric potential .

The chemical potential of a species can be written as,

$$\mu_k = \mu_{ok} + KT\ln(c_k) \quad \cdots\cdots\cdots\cdots\cdots\cdots \quad (3.5)$$

where μ_{ok} is the change in Gibbs free energy on introducing one atom of k at a particular site keeping concentrations of other species constant,

and c_k is the fractional concentration of species k.

Since at thermodynamic equilibrium the vacancy chemical potential is zero, equation (3.5) gives the fractional vacancy concentration at thermal equilibrium.

If these ideas are applied to a specific system like NaCl or KCl where the intrinsic defects are vacancies in the cationic sublattice, equation (3.1) for matter flux is given by,

$$J_1 = L_{11}(X_1 - X_v) + L_{1u}X_u \quad \cdots\cdots\cdots\cdots\cdots \quad (3.6)$$

where J_1 is the flux of cations in X direction

$$X_1 \cong -(\nabla \mu_1)_T \quad \cdots\cdots\cdots\cdots\cdots\cdots\cdots\cdots \quad (3.7)$$

$$\text{and} \quad X_u = -\frac{\nabla T}{T} \quad \cdots\cdots\cdots\cdots\cdots\cdots\cdots\cdots \quad (3.8)$$

The Onsager reciprocal relation gives that

$$L_{1u} = L_{u1} \quad \cdots\cdots\cdots\cdots\cdots\cdots\cdots\cdots \quad (3.9)$$

The thermodynamic heat of transport q^* for cations is defined by,

$$L_{1u} = L_{11}\, q^* \qquad \cdots\cdots (3.10)$$

so putting equation(3.10) in equation (3.6),

$$J_1 = L_{11}(X_1 - X_v + q^* X_u) \qquad \cdots\cdots (3.11)$$

From equation (3.5),

$$\mu_1 = \mu_{01}(p,T) + KT\ \ln(c_1) \qquad \cdots\cdots (3.12)$$

Using equations (3.7) and (3.12),

$$X_1 \cong -(\nabla\mu_1)_T = -\nabla\,(\mu_{01}(p,T) + KT\ \ln(c_1))_T$$

$$= -\,KT\,\left(\frac{d\ln c_1}{dc_1}\nabla c_1\right)$$

$$= -\,KT\,\frac{\nabla c_1}{c_1} \qquad \cdots\cdots (3.13)$$

Now $X_v = -\,(\nabla\mu_v)_T$

$$= -\,\left(\frac{d\mu_v}{d\,\bar{c}_v}\right)\nabla\bar{c}_v \qquad \cdots\cdots (3.14)$$

where $\bar{c}_v$ is the equilibrium fractional concentration of vacancies. It can now be assumed that the vacancies are locally in thermal equilibrium, so that,

$$\mu_v = \mu_v(\bar{c}_v, T) = 0$$

$$\left(\frac{d\mu_v}{d\bar{c}_v}\right)\delta\bar{c}_v = -\left(\frac{d\mu_v}{d\,T}\right)_{\bar{c}_v}\delta T \qquad \cdots\cdots (3.15)$$

Substituting equation (3.15) in (3.14),

$$X_v = \left(\frac{d\mu_v}{dT}\right)\nabla T \qquad \cdots\cdots (3.16)$$

Now using equation (3.5) along with (3.16), X_v becomes,

$$X_v = \left(\left(\frac{d\mu_{0v}}{dT}\right) + KT\,\frac{d}{dT}(\ln c_v)\right)\nabla\ T$$

For equilibrium, it can be written as,

$$X_v = -\left(\frac{d\ (\mu_{ov}/\ KT)}{d(1/\ KT)} + \frac{d\ln c_v}{d(1/\ KT)}\right)\frac{\nabla T}{T}$$

$$= -\left(h_{ov} + \frac{d\ln c_v}{d(1/\ KT)}\right)\frac{\nabla T}{T} = -\,h_{fv}\,\frac{\nabla T}{T} \qquad \cdots\cdots (3.17)$$

where $\frac{d(\mu_{ov}/KT)}{d(1/KT)} = h_{ov}$ is the enthalpy of formation of a vacancy in the pure solvent

and $(h_{ov} + \frac{d\ln c_v}{d(1/KT)}) = h_{fv}$ is the effective enthalpy of formation of a vacancy.

Now substituting equations (3.13) and (3.17) in (3.11),

$$J_1 = L_{11}(-KT\frac{\nabla c_1}{c_1} - h_{fv}\frac{\nabla T}{T} - q^*\frac{\nabla T}{T} \quad \cdots\cdots\cdots\cdots\cdots \quad (3.18)$$

Since $D_1 = \frac{K\,T}{N}\frac{L_{11}}{c_1}$, so

$$J_1 = -D_1 N \nabla c_1 - D_1 N c_1 (q^* + h_{fv})\frac{\nabla T}{KT^2} \quad \cdots\cdots\cdots\cdots\cdots \quad (3.19)$$

For alkali halide single crystals having diffusion by vacancy mechanism in cationic sublattice, the equation (3.19) can be written as,

$$J_v = -D_v \nabla C_v + D_v C_v Q^* \frac{\nabla T}{KT^2} \quad \cdots\cdots\cdots\cdots\cdots \quad (3.20)$$

where C_v is the vacancy concentration

and $Q^*(= q^* + h_{fv})$ is the cationic heat of transport.

The conductivity in an alkali halide crystal is due to vacancy flux which is given quantitatively by equation(3.20). Any variation of conductivity due to application of thermal and electric field forces will ultimately depend on the variation of this vacancy flux and this in turn will depend on variation of vacancy concentration. But whether this variation of equilibrium vacancy concentrations from one lattice plane to another at a thermal gradient is the only mechanism for conductivity change or whether non-equilibrium concentrations have contributions to make, is a matter which will be considered in the next section.

3.2. Resistance in a temperature gradient. (Local equilibrium condition)

The assumption of local thermodynamic equilibrium in the defect concentration can be tested experimentally by measuring the electrical resistance of an alkali halide crystal in a temperature gradient. If equilibrium holds, the a.c. conductance should be derivable simply by integration of known isothermal values of conductivity from one side of the specimen to the other. Any deviations from this estimate is presumably due to corresponding deviation of the defect concentration from its equilibrium value.

The total resistance of a crystal of width 2m can be found by integration of the reciprocal of isothermal conductivity.

$$R = \int_{-m}^{m} \frac{1}{\sigma(x)A}\, dx \qquad \cdots\cdots\cdots\cdots\cdots\cdots \quad (3.21)$$

Substituting the value of isothermal conductivity from eqn(2.9) ,

$$R = \int_{-m}^{m} \frac{K\,T(x)}{Na^2\, e^2\, \nu_0\, A} \exp\left(\frac{E_D}{K\,T(x)}\right) dx$$

$$= \frac{B}{A} \int_{-m}^{m} T(x) \exp\left(\frac{E_D}{KT(x)}\right) dx \qquad \cdots\cdots\cdots\cdots \quad (3.22)$$

Let the specimen be subjected to a temperature gradient which is assumed to be uniform over the crystal width. Let the central temperature be T(0) and the face temperatures be T(m) and T(-m). The temperature gradient a_1 is then given by,

$$a_1 = \frac{T(m) - T(-m)}{2m} \qquad \cdots\cdots\cdots\cdots\cdots\cdots \quad (3.23)$$

The temperature T(x) can be written as,

$$T(x) = T(0) + a_1 x \qquad \cdots\cdots\cdots\cdots\cdots\cdots \quad (3.24)$$

Substituting equation (3.24) in equation (3.22),

$$R = \frac{B}{A} \int_{-m}^{m} (T(0)+a_1 x) \exp\left(\frac{E_D}{KT(0)(1+ a_1 x/\, T(0))}\right) dx$$

$$= \frac{BT(0)}{A}\int_{-m}^{m} \exp\left(\frac{E_D}{KT(0)}\left(1-\frac{a_1 x}{T(0)}\right)\right)dx + \frac{a_1 B}{A}\int_{-m}^{m} x\exp\left(\frac{E_D}{KT(0)}\left(1-\frac{a_1 x}{T(0)}\right)\right)dx$$

$$= \frac{BT(0)}{A}\exp\left(\frac{E_D}{KT(0)}\right)\int_{-m}^{m}\exp\left(-\frac{E_D a_1 x}{KT^2(0)}\right)dx$$

$$+ \frac{a_1 B}{A}\exp\left(\frac{E_D}{KT(0)}\right)\int_{-m}^{m} x\exp\left(-\frac{E_D a_1 x}{KT^2(0)}\right)dx$$

Let $\beta = \frac{E_D a_1}{KT^2(0)}$, then

$$R = \frac{BT(0)}{A}\exp\left(\frac{E_D}{KT(0)}\right)\int_{-m}^{m}\exp(-\beta x)\,dx$$

$$+ \frac{a_1 B}{A}\exp\left(\frac{E_D}{KT(0)}\right)\int_{-m}^{m} x\exp(-\beta x)\,dx$$

$$= \frac{BT(0)}{A}\exp\left(\frac{E_D}{KT(0)}\right)\left(-\frac{1}{\beta}\exp(-\beta x)\right)_{-m}^{m}$$

$$+ \frac{a_1 B}{A}\exp\left(\frac{E_D}{KT(0)}\right)\left(-\frac{x}{\beta}\exp(-\beta x) - \frac{1}{\beta}\exp(-\beta x)\right)_{-m}^{m}$$

Now if the temperature gradient a_1 is small enough to make $\beta \ll 1$, then

$$R = \frac{BT(0)}{A}\exp\left(\frac{E_D}{KT(0)}\right)\cdot 2m\left(1+\frac{m^2\beta^2}{6}\right)$$

$$+ \frac{a_1 B}{A}\exp\left(\frac{E_D}{KT(0)}\right)\left(-\frac{2m}{\beta}\left(1+\frac{\beta^2 m^2}{2}\right)+\frac{2m}{\beta}\left(1+\frac{\beta^2 m^2}{6}\right)\right)$$

$$\cong R(0)\left(1+\frac{m^2\beta^2}{6}\right)$$

$$\frac{R(T)-R(0)}{R(0)} = \frac{m^2\beta^2}{6} = \frac{m^2 E_D^2 a_1^2}{6K^2T^4(0)}$$

$$\frac{\Delta R_{\Delta T}}{R(0)} = \frac{1}{24}\left(\frac{E_D}{KT(0)}\right)^2\left(\frac{\Delta T}{T(0)}\right)^2 \qquad \text{(3.25)}$$

where ΔT is the total temperature difference.

This equation relates the resistance change, $\Delta R_{\Delta T}$ due to the imposition of a temperature difference ΔT across the crystal to its isothermal resistance R(0) and the activation energy for diffusion, E_D. The equation is correct only if the defect concen-tration in each isothermal plane of the specimen is equal to the

equilibrium value appropriate to its temperature.

It has been found that there is a definite but small difference between experimental observations of $\Delta R_{\Delta T}$ and evaluations of $\Delta R_{\Delta T}$ based on the use of equation (3.25). This is shown in figure (5.3) for potassium chloride crystal. This goes to prove that the assumption of local thermodynamic equilibrium is not rigorously true. Thus a model is required which may explain physical phenomena occurring in a material under non-equilibrium conditions.

3.3 Resistance in a temperature gradient. (Non-equilibrium condition)

In a material at equilibrium, vacancies are produced and annihilated at a rate such that there is no net change of vacancy concentration. Now if a uniform driving force is maintained across the material, there would be sustained deviation of the vacancy concentration from its equilibrium value. On the other hand an alternating driving force will cause the equilibrium vacancy concentration to move to a new value with a relaxation time given by the life time of the vacancies.

At equilibrium the production and loss rates for vacancies are equal and hence

$$P = L = \frac{C_e}{\tau}$$

where C_e is the equilibrium vacancy concentration
and τ is the vacancy lifetime.

It will be assumed that this production rate is maintained even when conditions are not those of equilibrium, but that the loss rate changes to $L = \frac{C}{\tau}$ where C is the instantaneous and generally non-equilibrium value of the vacancy concentration.

At non-equilibrium condition, the vacancy concentration varies both with position and time. The variation with position can arise through the variation of the thermodynamic force, $\frac{\nabla T}{T}$ which causes a non-zero divergence of the vacancy flow, J_v. In such conditions the loss rate is given by $\frac{C}{\tau} + \text{div } J_v$. Since the production rate is still $\frac{C_e}{\tau}$, this gives rise to a change in the vacancy concentration described by,

$$\frac{dq}{dt} = P - L = \frac{C_e}{\tau} - \frac{C}{\tau} - \text{div } J_v$$

$$= -\frac{q}{\tau} - \text{div } J_v \qquad \cdots\cdots\cdots\cdots\cdots\cdots \qquad (3.26)$$

where $q\ (= C - C_e)$ is the excess vacancy concentration.

The above equation is in fact a modification of Fick's second law to include effects due to vacancy sources and sinks in non-equilibrium conditions. The expression for J_v as given in equation (3.20) can be extended to include effect of electric driving force. This is given by,

$$J_v = - D_v \nabla C_v + D_v C_v Q_1^* \frac{\nabla T}{KT^2} + \frac{Z_v e E C_v D_v}{KT} \quad \cdots\cdots\cdots \quad (3.27)$$

where J_v is the flow of cationic vacancies crossing unit area in unit time in the direction of thermal and electric forces,
$Z_v e$ is the charge carried by a cationic vacancy,
E is the applied electric field intensity,
Q_1^* is the cationic heat of transport,
C_v is the vacancy concentration,
and D_v is self-diffusion coefficient for vacancies.

For one dimension, the above equation can be written as,

$$(J_v)_x = - D_v \frac{dC_v}{dx} + \frac{D_v C_v Q_1^*}{KT^2} \frac{dT}{dx} + \frac{Z_v e E C_v D_v}{KT}$$

So the divergence of the vacancy flux, J_v is given by,

$$(\mathrm{div} J_v)_x = - \frac{d}{dx}\left(D_v \frac{dC_v}{dx}\right) + \frac{d}{dx}\left(\frac{D_v C_v Q_1^*}{KT^2} \frac{dT}{dx}\right) + \frac{d}{dx}\left(\frac{Z_v e E C_v D_v}{KT}\right) \quad \cdots\cdots \quad (3.28)$$

The first term on the right hand side can be written as,

$$- \frac{d}{dx}\left(D_v \frac{dC_v}{dx}\right) \cong - \frac{N D E_f E_D}{2K^2 T^4} \left(\frac{dT}{dx}\right)^2 \quad \cdots\cdots\cdots\cdots \quad (3.29)$$

Here it has been assumed that the temperature is a linear function of distance when thermal gradient is imposed and so $\frac{d^2T}{d^2x} = 0$.

The second term becomes,

$$\frac{d}{dx}\left(\frac{D_v C_v Q_1^*}{KT^2} \frac{dT}{dx}\right) \cong \frac{Q_1^* N D E_D}{K^2 T^4} \left(\frac{dT}{dx}\right)^2 \quad \cdots\cdots\cdots\cdots \quad (3.30)$$

Similarly the third term of equation (3.28) is,

$$\frac{d}{dx}\left(\frac{Z_v e C_v D_v}{KT}\right) \cong \frac{Z_v e E N D E_D}{K^2 T^3}\left(\frac{dT}{dx}\right) \quad \cdots\cdots\cdots\cdots \quad (3.31)$$

So substituting equations (3.29),(3.30),(3.31) in (3.28), it becomes,

$$(\mathrm{div}J_v)_x = -\frac{NDE_f E_D}{2K^2T^4}\left(\frac{dT}{dx}\right)^2 + \frac{Q_1^* NDE_D}{K^2 T^4}\left(\frac{dT}{dx}\right)^2 + \frac{Z_v eENDE_D}{K^2 T^3}\left(\frac{dT}{dx}\right) \cdots \quad (3.32)$$

So equation (3.26) becomes,

$$\frac{dq}{dt} = -\frac{q}{\tau} - \frac{ND}{K^2T^4}\left(\left(Q_1^* - \frac{E_f}{2}\right) E_D\left(\frac{dT}{dx}\right)^2 + Z_v eEE_D T\left(\frac{dT}{dx}\right) \cdots\cdots\right. \quad (3.33)$$

Now a solution of the above equation is required giving q as an explicit function of time which can then be used to evaluate the excess resistance due to application of thermal and electric fields. Such a solution can only be found for specific values of driving fields E and gradT. In the present work the conditions set were a fixed value for the temperature gradient, $\frac{dT}{dx}$ and a sinusoidal variation of the applied electric field, $E = E_0 \mathrm{Sin}\omega t$.

So equation (3.33) becomes,

$$\frac{dq}{dt} = -\frac{q}{\tau} - \frac{ND}{K^2T^4}\left(\left(Q_1^* - \frac{E_f}{2}\right) E_D\left(\frac{dT}{dx}\right)^2 + Z_v eE_D TE_0 \mathrm{Sin}\omega t\left(\frac{dT}{dx}\right)\right) \cdots\cdots \quad (3.34)$$

A steady state solution is attained when q becomes independent of t i.e. $\frac{dq}{dt} = 0$. This is possible when the applied electric field is zero, so

$$q = -\frac{ND\tau E_D}{K^2T^4}\left(Q_1^* - \frac{E_f}{2}\right)\left(\frac{dT}{dx}\right)^2 = q_{\Delta T} \quad \cdots\cdots\cdots\cdots \quad (3.35)$$

Here $q_{\Delta T}$ is the excess vacancy concentration in the steady state due only to thermal gradient. So equation (3.34) is,

$$\frac{dq}{dt} = -\left(\frac{q}{\tau} - \frac{q_{\Delta T}}{\tau}\right) - \frac{Z_v eE_D ND}{K^2T^3}\left(\frac{dT}{dx}\right) E_0 \mathrm{Sin}\omega t \quad \cdots\cdots\cdots\cdots \quad (3.36)$$

Using the substitutions,

$$g = q - q_{\Delta T} \qquad \cdots\cdots\cdots\cdots\cdots\cdots\cdots\cdots \quad (3.37)$$

$$\text{and} \quad \beta = \frac{Z_v e E_D N D}{K^2 T^3} \left(\frac{dT}{dx} \right) E_0 \qquad \cdots\cdots\cdots\cdots\cdots\cdots \quad (3.38)$$

The equation (3.36) takes the form,

$$\frac{dg}{dt} = - \frac{g}{\tau} - \beta \, \mathrm{Sin}\omega t \qquad \cdots\cdots\cdots\cdots\cdots\cdots\cdots \quad (3.39)$$

The solution of this equation is given by,

$$g(t) = \frac{g(0)\left(\frac{1}{\tau^2} + \omega^2 \right) - \omega\beta) \exp\left(- \frac{t}{\tau} \right) + \omega\beta \mathrm{Cos}\omega t - \frac{\beta}{\tau} \mathrm{Sin}\omega t}{\frac{1}{\tau^2} + \omega^2} \qquad \cdots (3.40)$$

where $g(0)$ is the value of $g(t)$ at $t = 0$

For the present work the condition of interest is a sustained application of the sinusoidal driving field for periods well in excess of the vacancy lifetime τ . The transient term may therefore be neglected and hence

$$g(t) = \frac{\omega\beta \mathrm{Cos}\omega t - \frac{\beta}{\tau} \mathrm{Sin}\omega t}{\frac{1}{\tau^2} + \omega^2} \qquad \cdots\cdots\cdots\cdots\cdots\cdots \quad (3.41)$$

Now substituting the expression for $g(t)$ from equation (3.41) and from eqn (3.38), the expression for $q(t)$ becomes,

$$q(t) = \frac{N D E_D \tau}{K^2 T^4} \frac{dT}{dx} \left(\frac{Z_v e T E_0}{(1+\omega^2 \tau^2)} \left(- \mathrm{Sin}\omega t + \omega\tau \mathrm{Cos}\omega t \right) - \left(Q_1^* - \frac{E_f}{2} \right) \left(\frac{dT}{dx} \right) \right) \cdots (3.42)$$

This equation of the excess vacancy concentration as a function of time is the basis of the present work. This demonstrates the possibility of deriving a value for the heat of transport by comparing the material flow in a temperature gradient with the flow in combined electric and thermal fields. Within the main parenthesis, the two terms in the bracket show that the applied electric field will produce components

in the vacancy concentration which are respectively in-phase and $\frac{}{2}$ out of phase with the driving field. If the relative magnitudes of the in-phase and quadrature components could be measured at a particular frequency, it would then be possible to estimate the vacancy lifetime, . Knowing and the temperature gradient, $\frac{dT}{dx}$ it should then be possible to derive a value for $(Q_1^* - \frac{E_f}{2})$.

It should be noted that q(t) in the above equation is not directly accessible to experiment. Actual measurements are related to the a.c. resistance of the specimen which is the only available measurable quantity. To put the equation in a form which can be used, it is noted that the conductivity is proportional to vacancy concentration and mobility and so,

$$\sigma = a'' C \mu = a'(C_e + q(t)) \exp(- \frac{E_m}{KT})$$

$$= a' C_e (1 + \frac{q(t)}{C_e}) \exp (- \frac{E_m}{KT})$$

where C_e is the equilibrium vacancy concentration given by $N \exp (- \frac{E_f}{2KT})$

μ is the mobility

and a'', a' are constants of proportionality.

$$\sigma = a \exp(- \frac{E_D}{KT}) (1 + \frac{q(t)}{C_e}) \quad \cdots\cdots\cdots\cdots\cdots\cdots \quad (3.43)$$

This expression can be used to find out total resistance R by integrating over the thickness 2m of the crystal.

$$R = \int_{-m}^{m} \frac{dx}{\sigma A}$$

$$= \int_{-m}^{m} \frac{dx}{a A \exp(- \frac{E_D}{KT})(1 + \frac{NDE_D\tau}{K^2T^4} \frac{dT}{dx} (\frac{Z_v e T E_0}{(1+\omega^2\tau^2)}(-\sin\omega t + \omega\tau\cos\omega t)}{N \exp (- \frac{E_f}{2KT})}$$

$$- (Q_1^* - \frac{E_f}{2}) \frac{dT}{dx})$$

$$R = \int_{-m}^{m} \frac{dx}{a\,A\,\exp(-\frac{E_D}{KT})}\left(1 - \frac{NDE_D\tau}{K^2T^4 N\exp(-\frac{E_f}{2KT})}\right)\frac{dT}{dx} X$$

$$\left(\frac{Z_v eTE_0}{1+\omega^2\tau^2}\left(-\sin\omega t + \omega\tau\cos\omega t\right) - (Q_1^* - \frac{E_f}{2})\frac{dT}{dx}\right) \quad \cdots (3.44)$$

In this equation, the integration of the first term in the main parenthesis gives the isothermal resistance. The integration of the second term gives a change in resistance due to a.c. electric field in presence of thermal field. The integration of the third term offers a change in resistance due only to thermal driving force. Thus the change in resistance due to thermal field is,

$$\Delta R_{\Delta T} = \int_{-m}^{m} \frac{dx}{a\,A\,\exp(-\frac{E_D}{KT})} \cdot \frac{NDTE_D}{K^2T^4} \frac{(Q_1^* - \frac{E_f}{2})}{N\exp(-\frac{E_f}{2KT})}\left(\frac{dT}{dx}\right)^2 \quad \cdots\cdots\cdots (3.45)$$

The change in resistance as evidenced in the quadrature component is,

$$\Delta R_{E,\Delta T} = \int_{-m}^{m} \frac{dx}{a\,A\exp(-\frac{E_D}{KT})}\left(-\frac{NDE_D\tau^2\omega Z_v eTE_0\cos\omega t}{K^2T^4(1+\omega^2\tau^2)N\exp(-\frac{E_f}{2KT})}\right) \quad \cdots\cdots (3.46)$$

Taking equation (3.45),

$$\Delta R_{\Delta T} = \int_{-m}^{m} \frac{\exp(\frac{E_D}{KT})\,D_0\tau E_D \exp(-\frac{E_m}{KT})(Q_1^* - \frac{E_f}{2})\left(\frac{dT}{dx}\right)^2}{a\,A\,K^2T^4} dx \quad \cdots\cdots\cdots (3.47)$$

Let $T = T(0) + a_1 x$ ..... (3.48)

whence $a_1 = \frac{T(m) - T(-m)}{2m}$ ..... (3.49)

where T(m) is the temperature in Kelvin at face A of the crystal and 2m is the thickness of the crystal.

$$\Delta R_{\Delta T} = \int_{-m}^{m} \frac{\tau E_D D_0 (Q_1^* - \frac{E_f}{2})a_1^2}{a\,A\,K^2} \frac{\exp(\frac{E_f}{2KT(0)(1+a_1 x/T(0))})}{T^4(0)(1+\frac{a_1 x}{T(0)})^4} dx$$

$$= \frac{\tau E_D D_0 (Q_1^* - \frac{E_f}{2})\, a_1^2}{a A K^2} \int_{-m}^{m} \frac{\exp(\frac{E_f}{2KT(0)})}{T^4(0)} \exp(-\frac{E_f a_1 x}{2KT^2(0)})(1-\frac{4a_1 x}{T(0)})\, dx$$

$$= \frac{\tau E_D D_0 (Q_1^* - \frac{E_f}{2})\, a_1^2}{a A K^2} \frac{\exp(\frac{E_f}{2KT(0)})}{T^4(0)} \left(\int_{-m}^{m} \exp(-\frac{E_f a_1 x}{2KT^2(0)} \cdot dx - \right.$$

$$\left. \int_{-m}^{m} \exp(-\frac{E_f a_1 x}{2KT^2(0)}) \frac{4 a_1 x}{T(0)} \cdot dx \right)$$

$$= \frac{\tau E_D D_0 (Q_1^* - \frac{E_f}{2})\, a_1^2}{a A K^2 T^4(0)} \exp(\frac{E_f}{2KT(0)}) (2m(1+\frac{E_f^2 a_1^2 m^2}{24 K^2 T^4(0)})$$

$$- \frac{4 a_1}{T(0)} 2m^2 (1+\frac{E_f^2 a_1^2 m^2}{24 K^2 T^4(0)}))$$

$$\cong R(0) \cdot \frac{\tau E_D D_0 \exp(-\frac{E_m}{KT(0)})}{K^2 T^4(0)} (Q_1^* - \frac{E_f}{2}) \cdot a_1^2 (1+\frac{E_f^2 a_1^2 m^2}{24 K^2 T^4(0)})$$

$$\frac{\Delta R_{\Delta T}}{R(0)} = \frac{\tau E_D D_0 \exp(-\frac{E_m}{KT(0)}) (\Delta T)^2 (Q_1^* - \frac{E_f}{2})}{K^2 T^4(0)\, l^2} \quad \cdots\cdots\cdots \quad (3.50)$$

Similarly taking equation (3.46),

$$\frac{\Delta R_{E,\Delta T}}{R(0)} = \frac{\omega \tau^2}{1+\omega^2 \tau^2} \frac{E_D D_0 \exp(-\frac{E_m}{KT(0)})}{K^2 T^3(0)} E_0 \frac{|\Delta T|}{l} \quad \cdots\cdots\cdots\cdots \quad (3.51)$$

Using equations (3.50) and (3.51),

$$\frac{\Delta R_{\Delta T}}{\Delta R_{E,\Delta T}} = \frac{(Q_1^* - \frac{E_f}{2})(1+\omega^2 \tau^2)|\Delta T|}{\omega \tau E_0 l T(0)}$$

$$Q_1^* = \frac{E_f}{2} - \frac{\Delta R_{\Delta T}}{\Delta R_{E,\Delta T}} \frac{V \tau \omega T(0)}{(1 + \omega^2 \tau^2) |\Delta T|} \quad \cdots\cdots\cdots\cdots\cdots\cdots\cdots\cdots \quad (3.52)$$

The above equation thus offers an expression for the heat of transport for cations in terms of quantities which can be measured. This equation will be used for the calculation of Q^* in chapter 5. The techniques for the measurement of $\Delta R_{\Delta T}$ and $\Delta R_{E,\Delta T}$ will be described in next chapter.

3.4. Thermoelectric power.

When an ionic solid is placed between two metallic electrodes at different temperatures, a thermoelectric potential difference develops. The difference of temperatures produces a thermal driving force which causes cations and anions to migrate across the specimen at rates dependent on their mobilities. In the absence of an external circuit between the electrodes, no current flow can be sustained and consequently a potential difference develops across the material as migration takes place. This potential acts in opposition to the drifting motion reaching a steady state level at which there is zero net flow of cations and anions(39). This diffusion potential is called the homogeneous potential difference and its magnitude per unit temperature difference is called the homogeneous thermoelectric

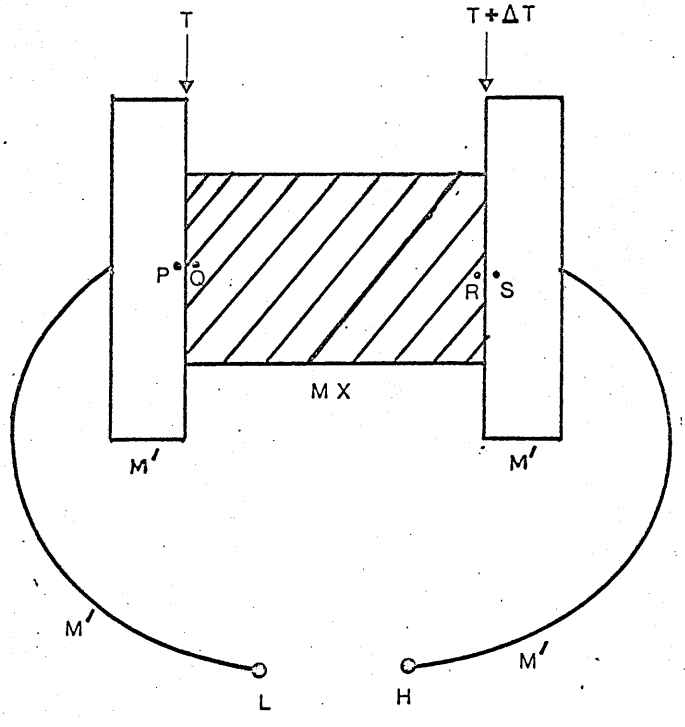

Figure 3.1. Measurement of total thermoelectric potential in an ionic solid

power. This thermoelectric power is a quantity which is not directly accessible to measurement since any electrodes attached to the specimen to measure it will themselves generate potential differences. So experimentally total thermoelectric potential between the leads attached to the electrodes is measured. This is shown in figure (3.1). The total potential difference, $(V_H - V_L)$ measured at zero current flow is composed of three parts(5) ;

(i) homogeneous thermoelectric potential, $(V_R - V_Q)$ generated due to thermomigration of charged species in the ionic solid,

(ii) heterogeneous thermoelectric potential,$((V_S - V_R) - (V_P - V_Q))$ which is due to variation with temperature of contact potential differences at the crystal-electrode interfaces,

(iii) homogeneous potential differences in the metal leads, $((V_H - V_S) - (V_L - V_P))$.

The third component is very small in comparison with the first two and hence it can be neglected. The total thermopower is thus,

$$\theta = \frac{V_R - V_Q}{\Delta T} + \frac{(V_S - V_R) - (V_P - V_Q)}{\Delta T} \quad \cdots\cdots\cdots \quad (3.53)$$

$$= \theta_{hom} + \theta_{het} \quad \cdots\cdots\cdots\cdots\cdots\cdots\cdots\cdots \quad (3.54)$$

The sign convention used here is that the potential of the hot electrode is taken as positive relative to that of the cold electrode.

3.4.1. Homogeneous thermoelectric power.

A theory of homogeneous thermoelectric power for ionic crystals was developed by Holtan et al(38) using the formalism of the thermodynamics of irreversible processes. They took as their starting point the expression for rate of entropy production per unit volume in a continuous medium.

$$T\sigma = \sum_{K=1}^{n} J_K \cdot X_K + J_u \cdot X_u \quad \cdots\cdots\cdots\cdots\cdots\cdots\cdots\cdots \quad (3.55)$$

where J_K and J_u are matter flux and reduced heat flux respectively,

X_K and X_u are the corresponding thermodynamic forces.

For uni-univalent ionic solid MX, their equation for homogeneous thermoelectric power is,

$$\theta_{hom} = -\left(\frac{t_+ (\nabla\mu_+)_T}{e\ T} - \frac{t_- (\nabla\mu_-)_T}{e\ T}\right) - \frac{Q^*}{eT} \quad \cdots\cdots\cdots \quad (3.56)$$

where e is the charge of the proton

μ_+ and μ_- are chemical potentials for cations and anions respectively

t_+ and t_- are transport numbers for cations and anions

Q^* is the cationic heat of transport.

They assume that the condition of electroneutrality ($n_+ = n_-$) implies that the gradients of chemical potentials for both cations and anions are zero and hence it becomes,

$$\theta_{hom} = -\frac{Q^*}{eT} \quad \cdots\cdots\cdots\cdots\cdots\cdots\cdots\cdots\cdots\cdots \quad (3.57)$$

The serious objection to this derivation is that only the material constituents of the solid were considered, the defect concentrations were altogether neglected. For this reason the final expression, though usefully simple, at best offers a rough estimate of homogeneous thermoelectric power.

Allnatt and Jacobs(5) formulated an expression for

homogeneous thermoelectric power again using irreversible thermodynamics but with vacancies treated as a seperate thermodynamic species. Their equation for the rate of entropy production is modified to take account of the defect structure of the ionic solid and new expressions for the chemical potentials being substituted in that equation. The final expression is given by,

$$\theta_{hom} = ((-Q_+^* + \frac{1}{2} E_f)\, t_+ - (-Q_-^* + \frac{1}{2} E_f)\, t_-)/\, eT \cdots\cdots (3.58)$$

where Q_+^* and Q_-^* are reduced heats of transport for cations and anions

t_+ and t_- are cations and anions transport numbers

E_f is the energy of formation of a Schottky defect pair.

In a later paper Allnatt and Jacobs(4) question the validity of the argument based on irreversible thermodynamics which leads to the conclusion that the heats of transport for cations and anions will add to zero. The heat of transport is in fact kinetically related to jump frequencies and hence the above conclusion implies that the motions of cations and anions in an ionic solid are correlated. As any mathematical deduction of homogeneous thermoelectric power from irreversible thermodynamics is based on Onsager's reciprocal relation i.e. $L_{1u} = L_{u1}$, so any wrong conclusion leads to doubt about the validity of this relation.

Howard and Lidiard(40), on the other hand, developed a theory for the homogeneous thermoelectric power from kinetic arguments. The argument is based on the following assumptions : (i) the impurities and defects are electrically charged species migrating in an electrically neutral medium, (ii) the interactions between defects are negligible, (iii) the defects are in local thermodynamic equilibrium and (iV) the current densities of defects are independent of each other. On applying the condition of zero current, the expression for homogeneous thermoelectric power in an alkali halide

material is,

$$\theta_{hom} = \frac{t_1}{e}\left(\frac{q_1^*}{T} + \frac{KT\nabla C_1}{C_1\nabla T}\right) - \frac{t_2}{e}\left(\frac{q_2^*}{T} + \frac{KT\nabla C_2}{C_2\nabla T}\right) - \frac{t_3}{e}\left(\frac{q_3^*}{T} + \frac{KT\nabla C_3}{C_3\nabla T}\right) \quad \cdots(3.59$$

where subscripts 1,2 and 3 denote cation vacancies, anion vacancies and impurity cations

C_r is the concentration of species r

t_r is the transport number of r

q_r^* is heat of transport of species r

and e is charge of a proton

For a pure crystal,

$$C_1 = C_2, \qquad C_3 = 0$$

and $$\frac{\nabla C_1}{C_1} = \frac{\nabla C_2}{C_2} = \frac{E_f \nabla T}{2KT^2}$$

So equation (3.59) becomes,

$$\theta_{hom} = \frac{1}{eT}\left(t_1\left(q_1^* + \frac{1}{2}E_f\right) - t_2\left(q_2^* + \frac{1}{2}E_f\right)\right) \quad \cdots\cdots\cdots\cdots \quad (3.60)$$

It should be noted that the equations (3.58) and (3.60) are virtually same if only the following substitutions are made; $Q_+^* = -q_1^*$ and $Q_-^* = -q_2^*$. The justification for this substitution is that ions and their vacancies move in opposite directions and hence the heat of transport of an ion will be equal and opposite to that of a vacancy.

Shimoji and Hoshino(71) discuss the homogeneous thermoelectric power from the point of view of non equilubrium statistical mechanics. Their final equation is,

$$\theta_{hom} = -\frac{t_+ Q_+^*}{e_+ T} - \frac{t_- Q_-^*}{e_- T} \quad \cdots\cdots\cdots\cdots\cdots\cdots\cdots\cdots \quad (3.61)$$

where + indicates cations

and - indicates anions.

In a recent paper Jacobs and Knight(44) described a

technique of studying thermoelectric power in ionic solid using what are called 'reversible electrodes'. They measured θ for KCl in a $Pt|C,H_2+HCl|KCl|H_2+HCl,C|Pt$ cell. This is in fact a measurement of thermoelectric power of KCl with Pt. electrodes in a controlled atmosphere of (H_2 + HCl) gas when the specimen surfaces are rubbed with graphite. The reversibility of the chlorine ion in the electrode reaction is shown as,

$$Cl^-(S) + \frac{1}{2} H_2(g) \rightleftharpoons HCl(g) + e(Pt)$$

where $Cl^-(S)$ denotes chlorine ion in the surface of KCl. However they admit that it is very difficult to maintain a constant pressure of HCl gas over the period of an experiment and thus much of their accuracy is lost.

3.4.2. Heterogeneous thermoelectric Power.

Heterogeneous thermoelectric power arises from the temperature dependence of contact potentials between metal electrodes and the ionic solid. The electrodes used to measure thermoelectric potential across the ionic material may have ions which are present also in the material or may have entirely different kinds of ions. For this reason two parallel streams of theories have been developed to describe heterogeneous thermoelectric power.

Howard and Lidiard(40) derived an expression for heterogeneous thermoelectric power from kinetic approach for the case when a common ionic species is present in the salt and its contacting electrodes. They equated the electrochemical potential, $\bar{\mu}$ ($=\mu + Ze\phi$, where μ is chemical potential and ϕ is electrical potential) of an ion M^+ in salt MX to the electrochemical potential $\bar{\mu}$ of M^+ in metal M to find the contact potential. The heterogeneous thermoelectric power is then easily found by dividing the difference of contact potentials at $(T+\Delta T)$ and T by the temperature difference, ΔT. For present purposes it must be noted that in this project Platinum electrodes were used to measure thermoelectric potentials in NaCl and KCl. Thus in this case no ion was common to both the salt and the electrodes and so the formulation of Howard and Lidiard is of little relevance here.

Allnatt and Jacobs(5) derived an expression for the heterogeneous thermoelectric power of an alkali halide crystal, MX in contact with metal electrodes, M' containing no cation in common with the salt. They assumed that equilibrium is established at interfaces between the electrons in the salt and in the metal, as these are the only species common to two phases. On equating electrochemical potentials, they obtained,

$$\bar{\mu}_e^{M'} = \mu_e^{M'} + e\phi^{M'} = \bar{\mu}_e^{MX} + e\phi^{MX}$$

$$e\,(\phi^{M'} - \phi^{MX}) = e\Phi = \mu_e^{MX} - \mu_e^{M'}$$

$$\theta_{het} = (\Phi(T + \Delta T) - \Phi(T))/\Delta T$$

$$\theta_{het} = -(s_e^{MX} - s_e^{M'})/e \quad \cdots\cdots\cdots\cdots\cdots\cdots\cdots\cdots \quad (3.62)$$

where s is the partial entropy

and e is the electronic charge.

In this treatment it was shown that the concentration of electrons in the conduction band of the salt due to thermal excitation from the valence band is exceedingly small as the forbidden gap of an alkali halide crystal like KCl is 9.4 eV. It was suggested therefore that the dominant source of electrons arose from non-stoichiometry of the crystal. These electrons are trapped at anion vacancies most of the time forming F-centres and the majority of electrons in the conduction band are excited from these trapped sites. The expression for heterogeneous power obtained by them is,

$$\theta_{het} = \frac{1}{e}\left(\left(H_f - \frac{1}{2}E_f\right)/T + k \ln n_B\right) \quad \cdots\cdots\cdots \quad (3.63)$$

where H_f is the change in enthalpy on taking an electron from an F-centre to the conduction band

E_f is enthalpy of formation of a Schottky defect pair

n_B is the number of electrons per unit volume in the conduction band

k is the Boltzmann constant.

$$\text{Now} \quad n_B = \frac{n_f}{n_-}\left(\frac{2\pi m k T}{h^2}\right)^{\frac{3}{2}} \exp\left(-\frac{G_f}{KT}\right) \quad \cdots\cdots\cdots\cdots \quad (3.64)$$

where n_f is the number per unit volume of electrons residing

in F- centres

and n_- is the anionic concentration.

In the derivation of equation (3.63), Allnatt and Jacobs assumed the existence of uniformly distributed excess anionic vacancies to trap electrons in the bulk of the material, but presented no physical basis for the assumption. Kroger(54) argues that if Allnatt and Jacobs' assumption were true, then this uniform distribution of F- centres throughout the volume would demonstrate its effect in the homogeneous thermoelectric power. However Jacobs and Maycock(45) in a subsequent publication argue that equilibrium is established not between conduction electrons and F-centres but between conduction electrons and surface charges in the alkali halide crystals. But again they fail to produce reasons for the existence and origin of the surface charges.

Shimoji and Hoshino(71) also assumed that an equilibrium is established between metallic electrons and electrons in the salt as there are no other species common to them. But the basis of their argument is the existence of charge on the surface of the salt and a prevalence of space charge of opposite sign adjacent to the surface. Their final equation for heterogeneous thermoelectric power is very much similar to that of Allnatt and Jacobs(5).

CHAPTER 4

DESIGN OF EQUIPMENT

4.1. The structure of the vacuum chamber.

Thermomigration takes place only in materials subjected to a gradient of temperature. One way of producing this condition was to construct two small and identical furnaces so that each one of them could maintain a desired temperature irrespective of the condition of the other. Since alkali halide crystals readily absorb moisture, it was necessary to perform the experiment in a dry atmosphere. This was done by designing a chamber large enough to enclose two furnaces which could then be evacuated and kept dry. The crystal in its mount was placed between the furnaces which is shown in figure(4.1)

A circular base plate of stainless steel having a diameter of 33 cm and a thickness of 2.3 cm was used. One 1 cm diameter hole and seven 3 cm diameter holes were drilled in the base plate. Two stainless steel tubes, one of 12 cm long and 1 cm outer diameter and the other of 24 cm long and 3 cm outer diameter were pushed through the holes and welded to the base plate. The 12 cm long tube which protruded downwards was connected to a T junction, so that one end could be connected to a gas inlet system and the other end to a bourdon gauge. The 24 cm long tube protruding upwards from the base plate was used for water cooling the system. The other six holes were used for connections to the vacuum system, to a Pirani gauge and for electrical lead-throughs. The furnaces were then mounted on rails. Two tungsten springs attached to two furnaces could be clamped at convenient positions in the rail so that the furnace heads could exert light pressures to the electrodes of the crystal. This pressure helped to embed the electrodes firmly into the crystal when baked at 950K. A semicircular stainless steel sheet was placed above the furnaces as a radiation

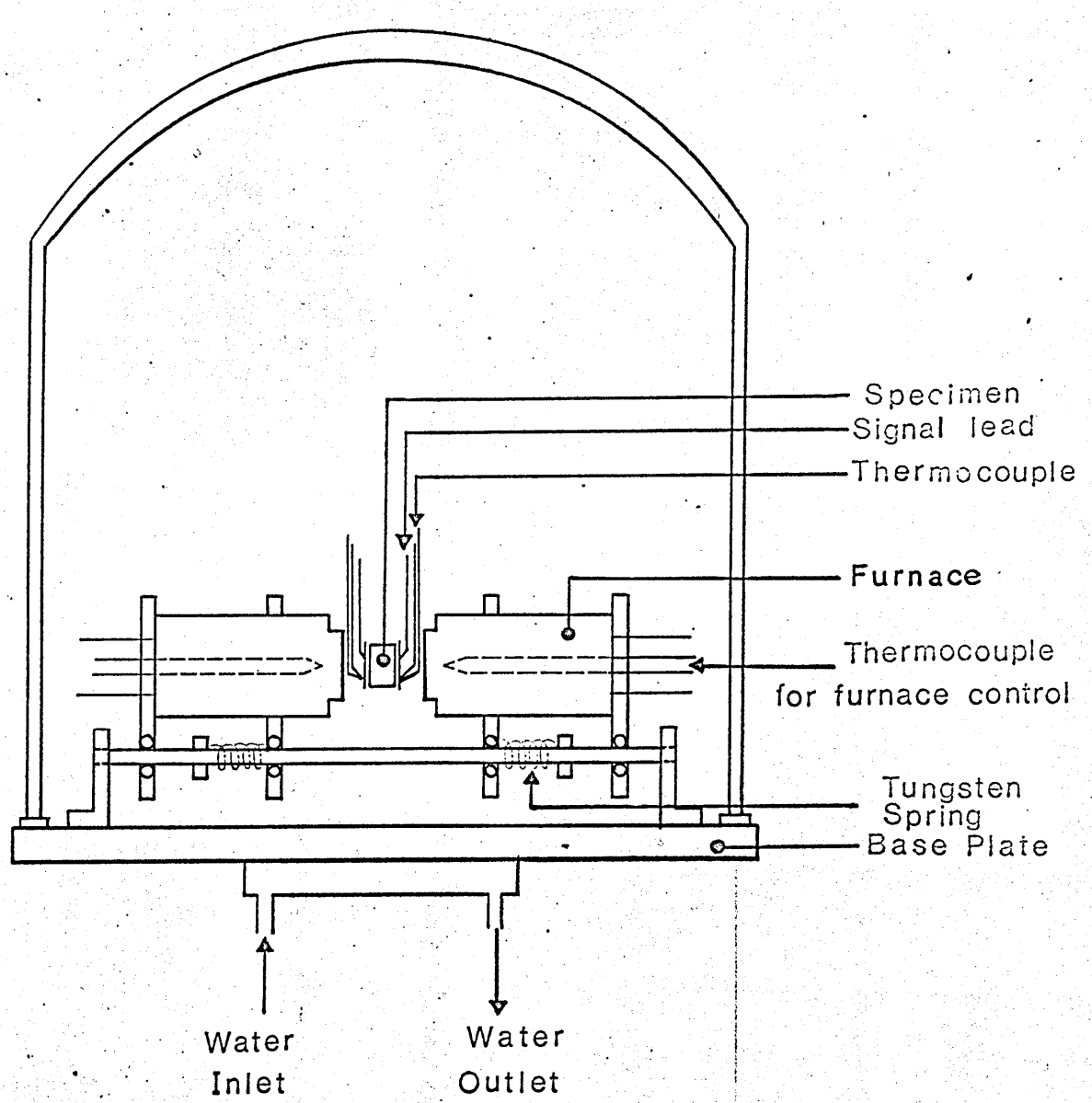

Figure 4-1. The position of the specimen between the furnaces in the bell-jar

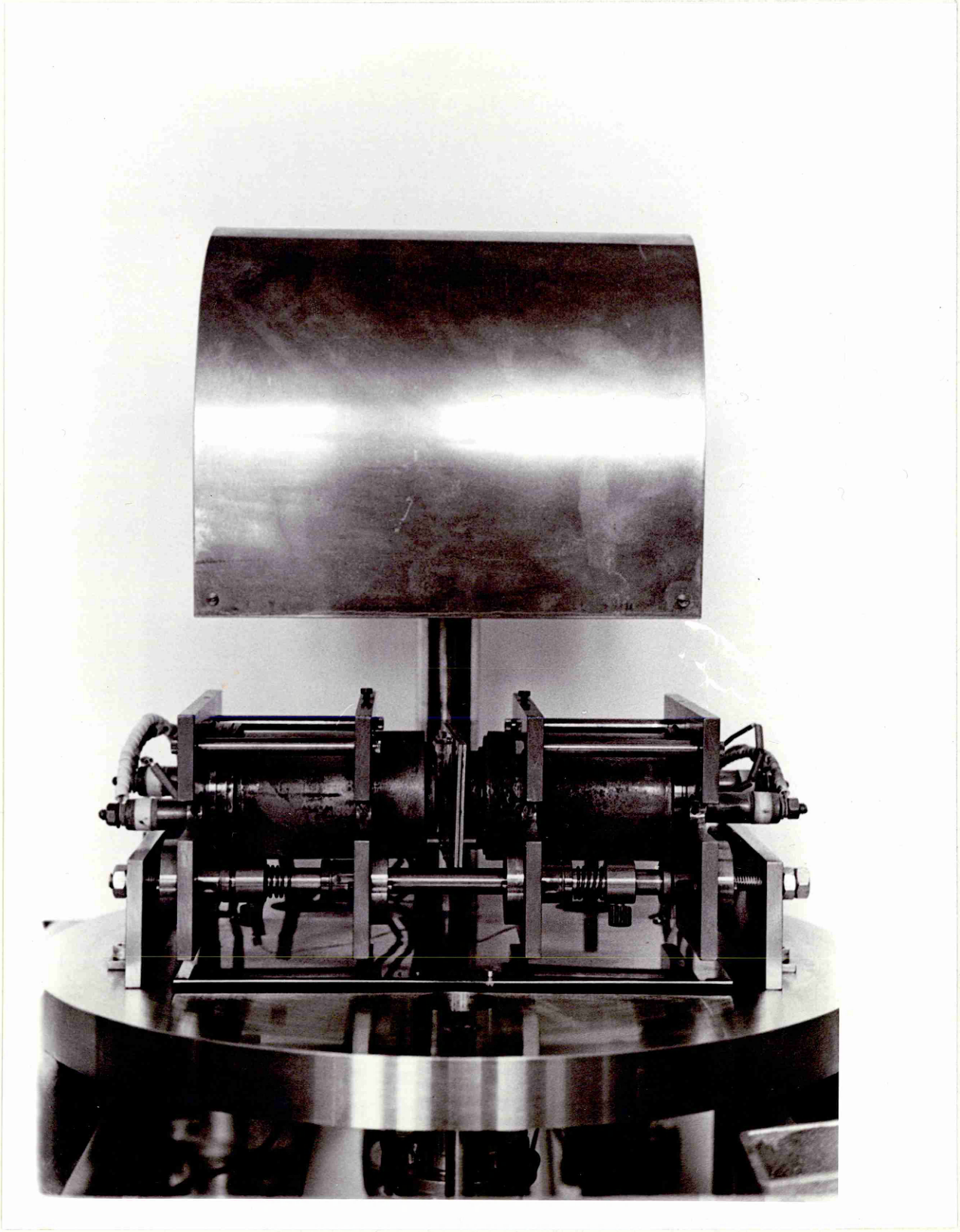

Plate 4.1. The structure of the vacuum chamber.

shield. A photograph of the vacuum chamber is shown in plate (4.1). The chamber was sealed by a 32 cm diameter bell jar.

4.2. Crystal preparation and mounting.

The crystals used in this work were grown and purified by Harshaw Chemical Company. According to their specification the total impurity content was less than 10 p.p.m. The specimens were microtomed to rectangular parallelopipeds of 1 cm X 1 cm X .35 cm by the manufacturer and were delivered packed in vacuum sealed polythene bags for protection against moisture.

To mount the specimen it proved necessary to develop a form of crystal package which would maintain the positions of the electrodes, the thermocouples for the measurement of face temperatures and the signal injecting leads. This package took the form of two stainless steel plates, one for each electrode. Figure (4.2) shows one of these plates. A slot of 2 cm X 2 cm was cut at the centre of each plate for placing electrode. A thin Pt. foil of 1 cm X 1 cm was used as an electrode. A pair of Pt.- Pt. 13/ Rh. thermocouple wire as well as a single Pt. wire, all of .01 cm diameter, were spot welded using an Emihus Spot Welder, model VTW - 30C - MC to the electrode. A thin mica sheet was pushed between the wires and the Pt. electrode to ensure that a single contact was made at the point of welding. The wires were led out through ceramic tubes which fitted into the radial grooves of a stainless steel block. After preparing the two sides of the package, the crystal was positioned in the middle of the square hole. A silica glass encircling the specimen prevented microcrystals formed at

high temperatures from shorting the signal to the metallic mount. Two thin mica sheets, one on each plate, screwed by 10 BA screws held the whole assembly in place and at the same time isolated the furnace faces

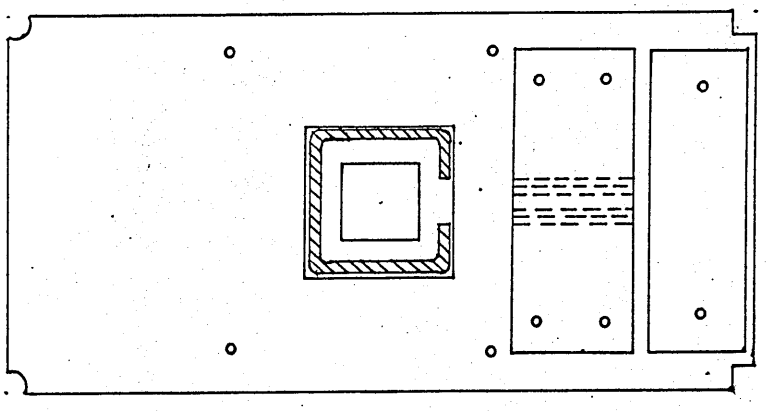

Figure 4.2. One of the plates of the crystal package.

electrically from the electrodes. The completed package was placed on the rails between the furnaces. The furnaces were then brought forward and clamped by tungsten springs so that the package sat tightly in place. Great care was taken to ensure that the furnace faces, the electrodes and the crystal faces were all accurately parallel. The thermocouple wires and signal leads were then connected to respective leads.

4.3. Furnace design.

The basic requirements on the furnaces used in this experiment were that they should maintain a uniform temperature across their faces over a wide range of experimental temperature. They should also be capable of attaining temperatures in the range of 1000K. These

requirements were met by designing a furnace as shown in plate (4.2). The cylindrical copper core of diameter 3cm and length 5cm helped to maintain a uniform temperature at its face when heated by nicrome heating wire, type SWG 22, wound over a refrasil layer. The total resistance of the furnace that could be made without risking any cross path for current was about 12 ohms. A concentric hole was drilled in the copper core to accommodate a temperature controlling thermocouple close to the furnace

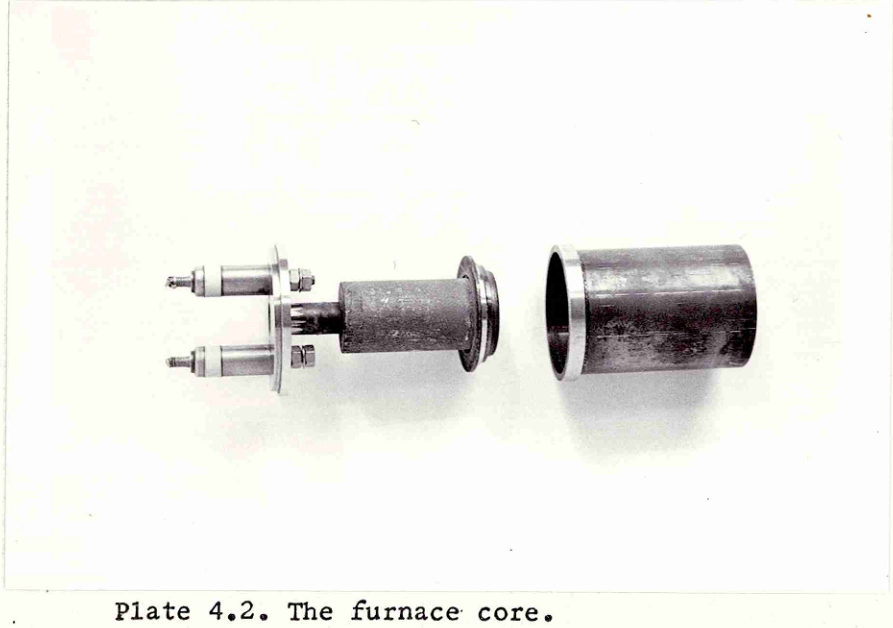

Plate 4.2. The furnace core.

head. Finally the outer stainless steel case was welded to the body of the furnace so that any out-gassing at high temperatures could not contaminate the vacuum system. The highest temperature which could reliably be attained with this furnace was about 1000K. Most of the attempts to raise temperatures beyond this range were unsuccessful as one or the other furnaces were burned. This was the compelling reason for limiting investigations to about 980K. The furnace body was carefully earthed before the start of the experiment in order to prevent magnetic field interfering with the signal in the specimen.

4.4. The vacuum system.

To avoid oil contamination in the vacuum system, two sorption pumps of type A.R.E.L., SP 600 were used. Each of the pumps contained about 600 gms of molecular sieve and produced a vacuum of about 10^{-3} torr in 30 minutes when cooled by liquid nitrogen. The pressure was monitored bu an Edwards Pirani Gauge, model 9A. After attaining a pressure of 10^{-3} torr, the system was flushed with a high purity argon gas and brought to a pressure of about 250 torr. The entire vacuum system is shown in figure (4.3).

4.5. Temperature Controlling Circuit.

The temperature of each furnace was controlled by a three term WHME Centinel Temperature Controller designed to operate with a Pt.-Pt. 13/ Rh. thermocouple. The proportional band, the integration and differentiation times of the controllers were carefully matched to the furnaces so that the temperature could be held constant to about $\pm$0.1 K over an hour. The temperature controlling circuit is shown in figure (4.4). The supplementary circuit using a rheostat, a rectifier and a 24V relay was used to protect the furnace from accidental burning.

During the experiments it was necessary to produce a series of temperature differences between the specimen faces while holding the mean temperature of the faces precisely constant. This was done by a modification of the controllers which allowed them to accept external voltages to cause a change in the set points. With this

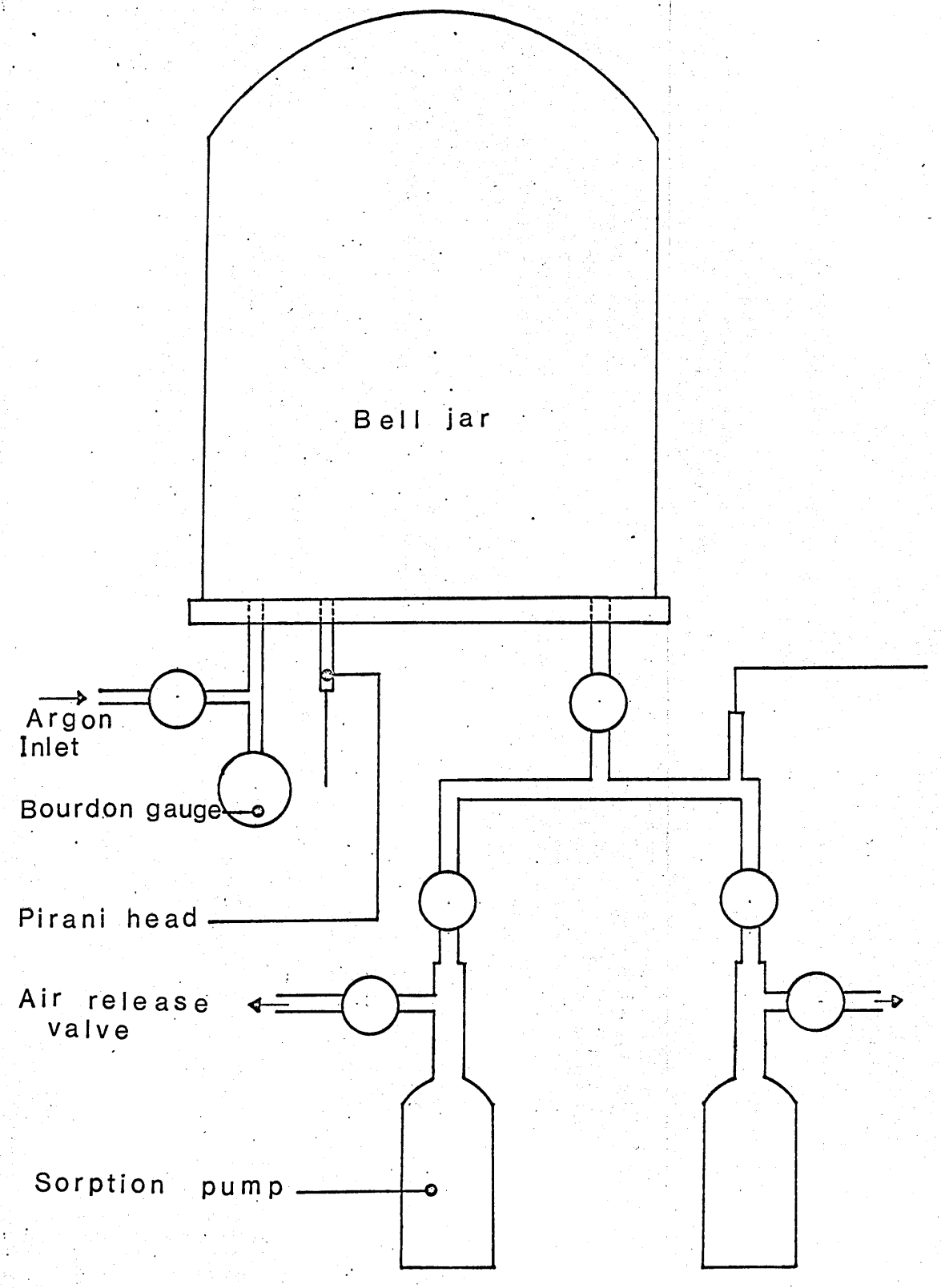

Figure 4.3. The vacuum system

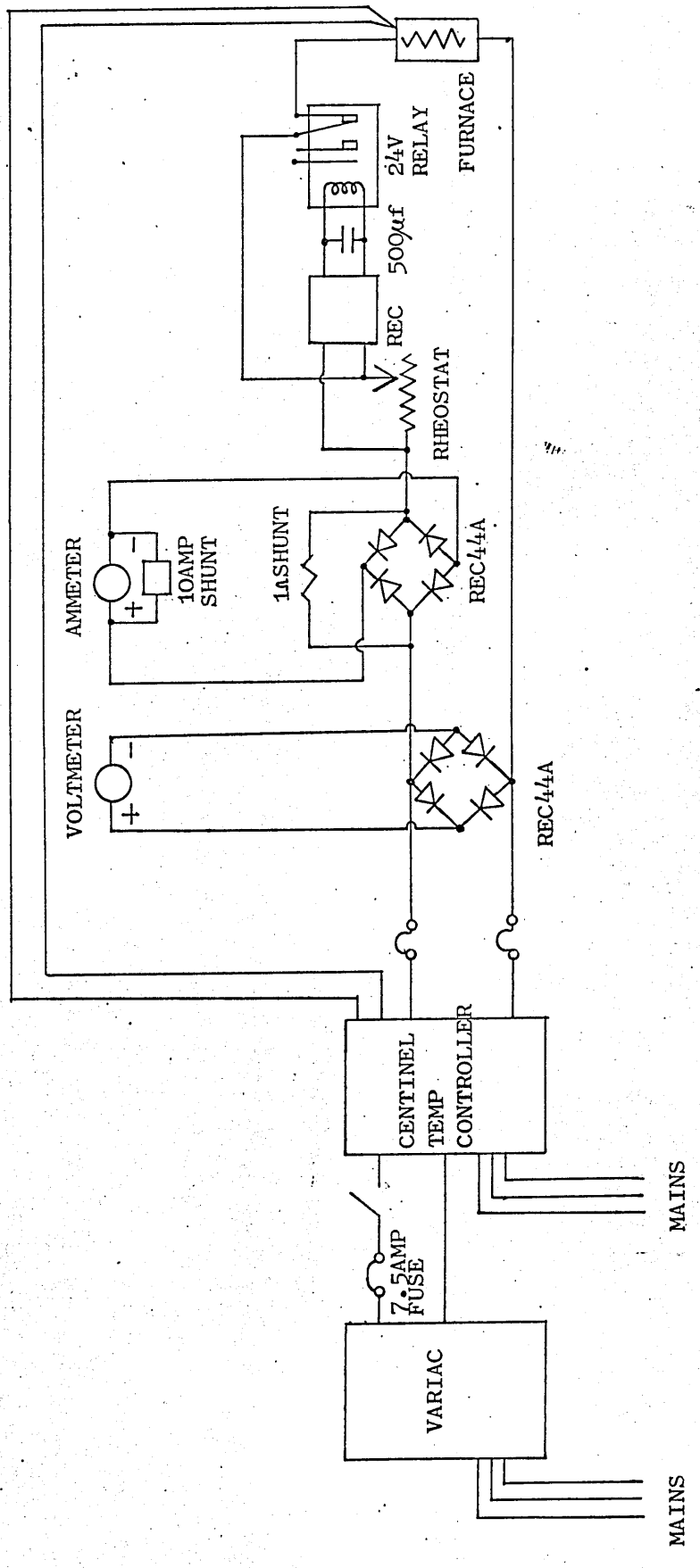

Figure 4.4. Temperature controlling circuit.

modification the specimen faces could be set at a precise temperature with zero injection voltage and then equal and opposite injection voltages could be used to produce surface temperatures which deviated from the initial isothermal condition by equal and opposite amounts. Since the specimen resistance changed quite rapidly with mean temperatures, this modification was necessary in obtaining precise temperature settings required by the experiment.

4.6. Measurement of thermoelctric potentials.

Before commencing measurements of ionic resistance, the thermoelectric potential difference between the faces of the specimen ($V_S - V_P$) under each temperature gradient was measured. For this the specimen was connected to a Keithley Microvolt Ammeter, type 150B whose input impedence was greater than 10^{10} ohms. Thus the current flow through the specimen was held to less than $10^{-3} / 10^{10} = 10^{-13}$ amp for a thermoelectric potential of 1mV. The effect of this small current on the measured potential was disregarded in comparison with other uncertainties inherent to this type of measurement. The face temperatures as well as the thermoelectric potentials were read by a Solartron data logger, printed by IBM typewriter and paper taped by Addo paper tape punch. Thus knowing the thermoelectric potential difference and the temperature gradient, the total thermoelectric power, θ could be evaluated.

4.7. Electric Signal Processor.

The requirement of this experiment was the ability to measure a.c. resistance of a specimen in the presence of thermal and electric driving fields. For this purpose an electric signal processor was made which supplied a summed output of two signals e.g. a high frequency low amplitude signal for the measurement of ionic resistance and a low frequency high amplitude signal for the detection of electro--migration effect. The high frequency measuring signal was generated by a Farnell Instrument Sine/Square Oscillator, type LMF 2 whereas low frequency drive signal was taken from a Feedback Test Wave Generator, type TWG 300. An additional requirement of this signal processor, set by the subsequent detection system, was that its output should be fully floating. This was done by using a miniature mains transformer. The circuit diagram of this signal processor is shown in figure (4.5).

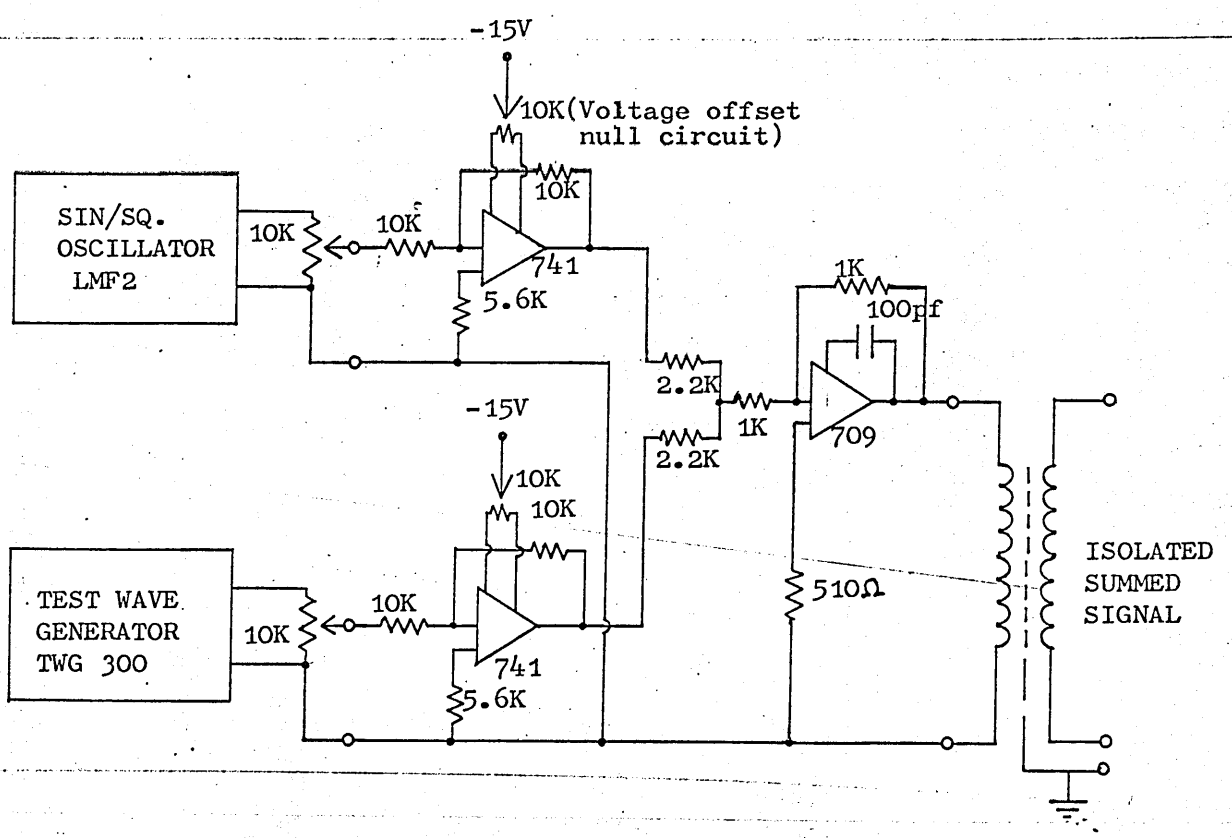

Figure 4.5. Electric signal processor.

The choice of frequency for the measuring signal was dictated by the consideration that the measurement should be free from effects such as dielectric polarization and interface phenomena. Following the discussion on Section (2.4) a 5KHz signal frequency was chosen to estimate a.c. resistance of the specimen. The drive frequency was chosen after considering the effect of frequency change from about 15 Hz to 1000 Hz on the specimen resistance which is shown in figure (5.4). It became evident that reliable and relatively noise free measurements could be done at 40 Hz drive signal. The amplitude of 40 Hz signal was chosen such that electric field causing migration became comparable with the thermal drive field. A temperature difference of 10K would give a thermal force of $Q^* \frac{\nabla T}{T} \cong 2\ eVm^{-1}$, if Q^* is assumed to be 0.8eV and hence the electric field strength should be about 2 eVm^{-1}. This was done by an electric drive signal of 4 mV across the specimen which was equivalent to a field strength of 1.14 eVm^{-1}. The amplitude of the measuring signal of 5 KHz was kept at a level of about $\frac{1}{20}$ th of that of drive signal i.e. 0.057 Vm^{-1}.

4.8. Measurement of specimen resistance.

The principal measurement problem in the present work was that of detecting the small changes of a.c. resistance produced in the specimen by thermomigration or electromigration while under the requirement to use small bridge input voltage so that it makes no significant perturbation of the vacancy concentration. The measuring

field strength was set to 0.06 Vm^{-1} = 0.2 mV across the specimen and so a measurement of 10/ precision in a 1/ resistance change demanded a 0.2 V sensitivity in the bridge detection circuit.

Phase sensitive detection readily provided a technique of adequate sensitivity for the thermomigration experiments. A suitable combination of amplifier gain and time constant brought the detection sensitivity well below the required 200 nV. For the electro--migration work, phase sensitive detection also provided the answer but in this case a system of measurement using phase sensitive detectors on two frequencies had to be developed. Plate (4.3) is a photograph of equipments used in this work.

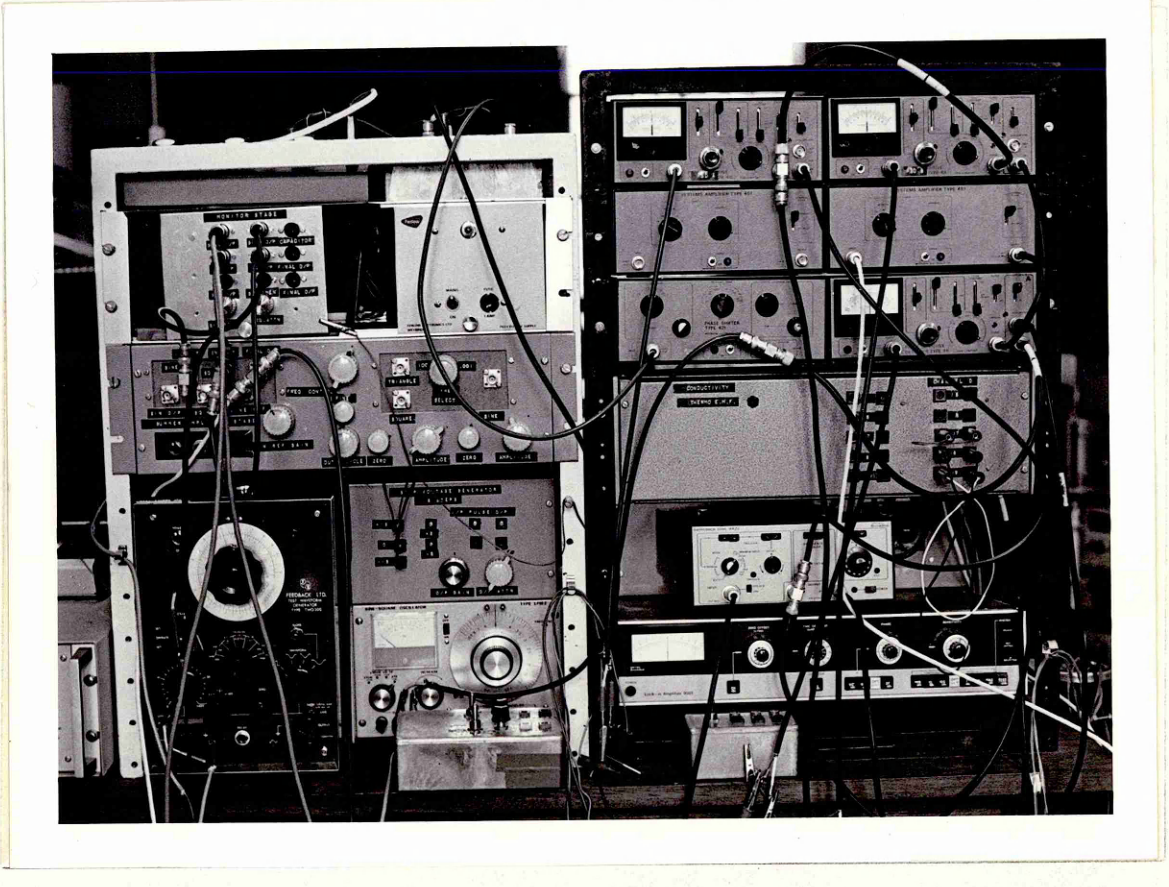

Plate 4.3. Experimental set-up for the detection system.

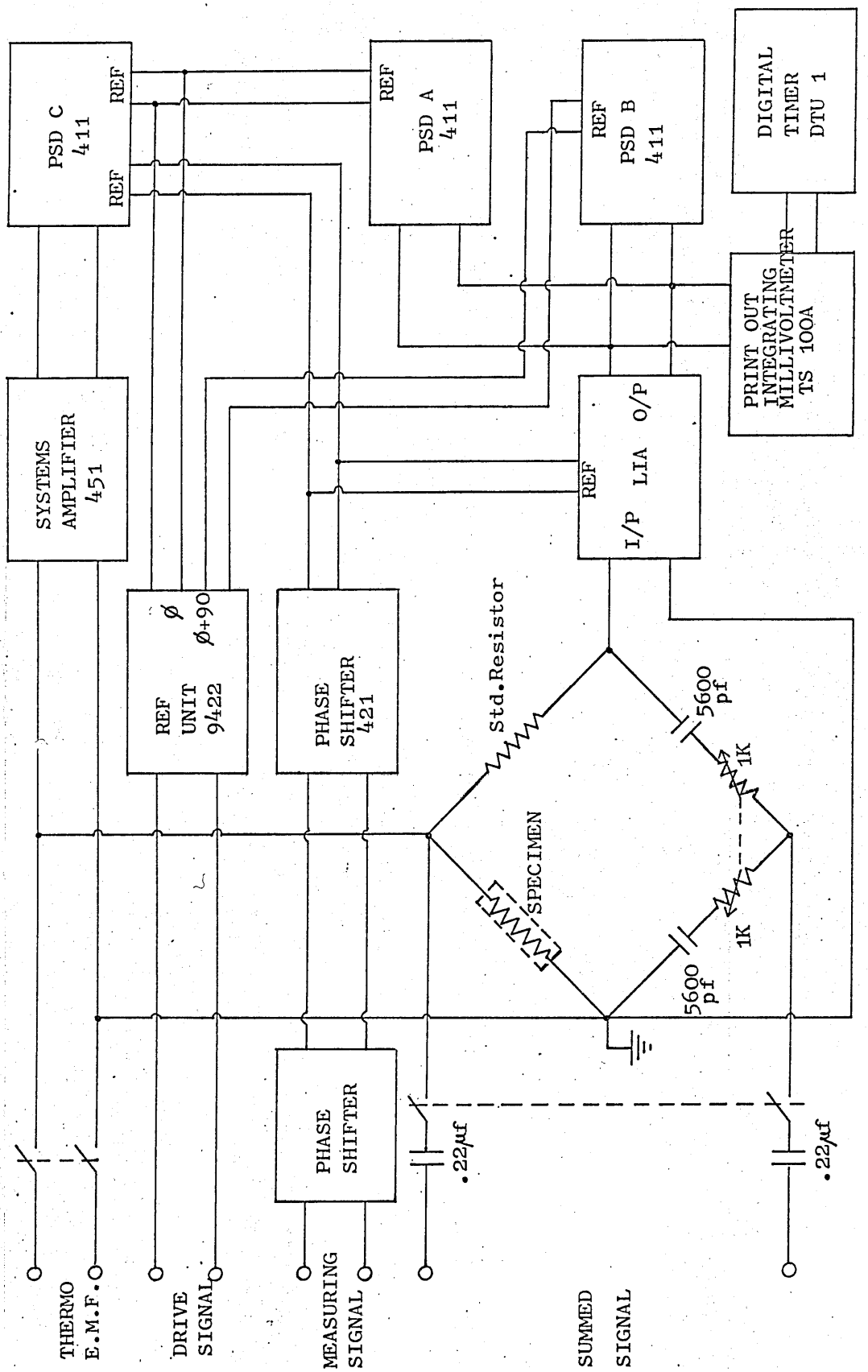

Figure 4.6. Block diagram of the detection system.

The signal processor output was fed to a bridge through two .22 μF coupling capacitors. The block diagram of the detection system is shown in figure (4.6). The resistance of the specimen was balanced by the standard resistor keeping other two arms symmetrical. The capacitors of 5600 pF were used to block d.c. path since the specimen would act as a voltage source under thermal gradients. The Brookdeal's Lock-in-amplifier, type 9501, was used to detect bridge imbalance with reference to 5KHz signal.

At the start of the experiment, the Lock-in-amplifier (LIA) was connected across the specimen. Using the phase shifters, the reference signal was shifted so as to align its phase exactly with the input signal to the LIA. This alignment was done using in-phase and quadrature component read out facility of the LIA. When they were in phase, the in-phase component would be maximum and the quadrature component would be zero. The LIA was then connected to the bridge to receive a signal v_i while keeping the conditions of the phase shifters unaltered.

A phase sensitive detector, marked PSD C in the diagram, was connected across the specimen through a system amplifier. The reference signal to PSD C was the same as that of the LIA. The total gain in the PSD C channel was 10^3. The amplitude of the 5KHz signal was varied so that the PSD C output, V_c read by the data logger was exactly .2V. In this condition the voltage drop across the specimen was $0.2V - 10^3 = 0.2$ mV r.m.s.

For the detection of the effect of thermal gradient on resistance, the LIA output, v_o was connected to a Print-out integrating millivoltmeter, model TS 100A, in association with a digital timer, type DTU 1, in order to increase the integration time beyond the limit of 10 sec offered by LIA. This increased integration time helped to smooth

out the transient variations in v_o. The LIA was set to a maximum sensitivity of 10 μV signifying a gain of 10^5. Its time constant was set at 3sec. The integrating millivoltmeter had been offset by 0.5V in the 1V range so that it could have equal excursion in both directions and the rate was set at 3/sec f.s. The digital timer was set to activate the millivoltmeter every 100sec. So for $v_o = 0$, the millivoltmeter should print 0.5X3X100 = 150 . Now to balance the bridge, the standard resistor was varied until the millivoltmeter printed out 150. The specimen resistance in this isothermal condition was exactly equal to that of the standard resistor. This isothermal resistance as well as face temperatures of the specimen were noted.

At each isothermal measurement of the specimen, a calibration line for the integrating millivoltmeter was drawn. The calibration line was important in the sense that it showed directly any change in isothermal resistance, $\Delta R_{\Delta T}$ due to imposition of a temperature gradient. Initially the specimen resistance was accurately determined at a fixed temperature. The specimen was then replaced by a standard reistor box and set to a value exactly equal to the isothermal value. By changing the values of this standard resistor, a set of print out values was obtained. These values were computerised and a gradient for the calibration line was obtained. The calibration line for the specific case when KCl crystal was at 835K could be drawn from the following values:

Mean temperature/K	Resistance/Ω	Print out value
835	45986	150
	46586	165
	45386	135

By injecting a small d.c. voltage to two controllers in reverse polarity, a temperature gradient was established. The gradient changed the equilibrium resistance of the specimen and this was detected by the millivoltmeter. By reading the millivoltmeter print out and using the computerised gradient of the calibration line, the resistance change for a given temperature gradient could be calculated.

For the measurement of the effects of combined electric and thermal fields on specimen resistance , $\Delta R_{E,\Delta T}$ the drive signal was set to a measured value and the integrating millivoltmeter was disconnected. The drive reference signal was fed to a Brookdeal's Reference Unit, model 9422, which had the facility of generating two reference signalsgiven by ϕ and (ϕ + 90) where ϕ was the controlled phase shift. The ϕ component was delivered to PSD C and PSD A whereas (ϕ + 90), the quadrature component, was delivered to PSD B. The signal v_o was delivered to PSD A and PSD B. The PSD C was still hooked across the specimen. The input signal and the refernce signal to PSD C were aligned by changing ϕ so that it could read the voltage drop across the specimen at 40Hz signal. The purpose was to look at the variation of specimen resistance due to simultaneous application of electric and thermal fields and this could only be done by keeping the time constant in the LIA considerably shorter than the period of the 40Hz signal so that subsequent detectors could detect any variation of v_o. So the time constant was set to 1msec in the LIA and sensitivity to 1mV so as to limit noise level. The outputs of PSD A, PSD B and PSD C denoted respectively by V_A, V_B and V_C were read by the Solartron data logger.

The significance of the in-phase component, V_A and the quadrature component, V_B was very important. When the electric drive field was applied to the bridge, the resistance of the specimen was perturbed. This perturbation in resistance was due to migration of

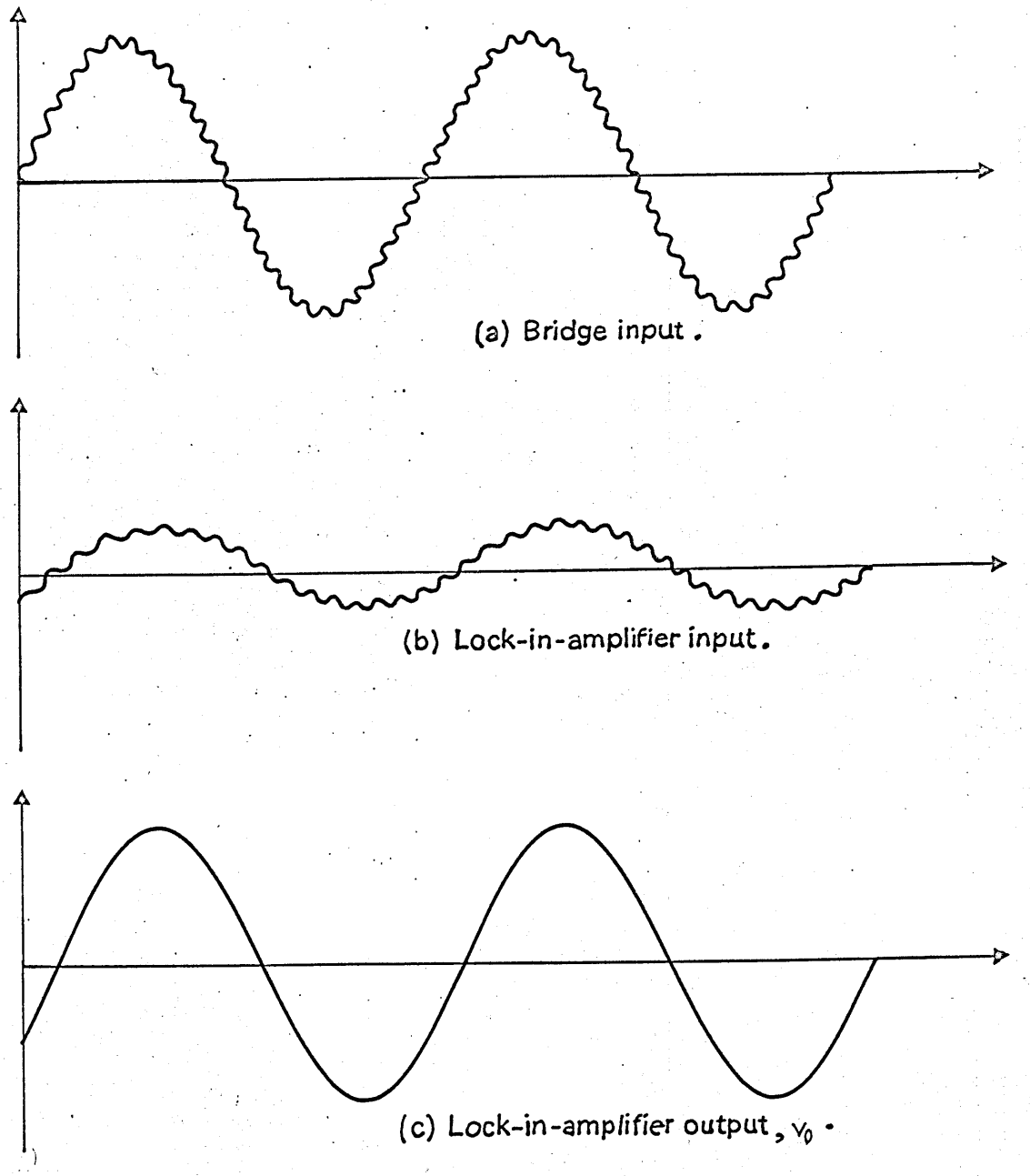

Figure 4.7. Detection of perturbation by the Lock-in-amplifier.

vacancies in response to the driving force. The LIA was set to detect signals referenced to 5 KHz signal and so any variation of v_i due to the drive signal would also be present at v_0. This is shown in figure (4.7). The change in v_0 took the form of phase and amplitude

variations which were then detected by the in-phase and quadrature components of phase sensitive detectors. So V_A and V_B gave an estimate of specimen resistance perturbation due to application of an electric driving field. This aspect of the electric field will be dealt with in section(5.1.3) when in-phase and quadrature components will be plotted at different thermal and electric field conditions.

CHAPTER 5

EXPERIMENTAL RESULTS

5.1.1. Thermoelectric power in a potassium chloride crystal.

Measurements of thermoelectric potentials were made at each experimental setting before beginning experiment on electrical resistance. During the course of these measurements it was found that there existed a certain amount of potential difference between the faces of the crystal even in the absence of a temperature gradient. The existence of anomalous potentials had also been reported by Allnatt and Jacobs(4) for potassium chloride crystals. They pointed out that this potential could be eliminated almost entirely by annealing the specimen overnight at 950 K. Accordingly the specimen was annealed for about 12 hours at 950 K at the start of the experiment. It should be mentioned that even after annealing, this spurious potential reappeared when the experimental temperature was decreased substantially from the melting point. As an example, a potential difference of 29 mV was found at zero temperature gradient at a temperature of 600 K. However maintaining this temperature of 600 K for about 12 hours, it became possible to reduce the potential to about 7.5 mV and after that it remained almost steady. So this anomalous potential imposed a lower limit on temperature at which thermoelectric power can reliably be made.

It had been the practice in this work to lower the temperature of the specimen from 950 K in steps of about 5 K to a desired temperature and maintain that temperature for about an hour in order to establish an equilibrium condition. After imposing a temperature difference between 5 K and 22 K across the specimen, the readings of thermoelectric potentials and face temperatures were taken only when it became certain that the potential difference was time independent. Initially, for each central temperature, thermo-electric potentials were measured for six temperature differences. But it was found that ΔV-ΔT points formed a good straight line

which passed right through the origin. So subsequently only two temperature differences were taken and the mean thermoelectric power calculated. The sign convention used here was that the potential at the hot end was taken positive. Table (5.1) shows the dependence of thermoelectric power on temperature.

Table 5.1. Thermoelectric power of pure KCl with Pt. electrodes.

Central temperature, T/K	Temperature difference, ΔT/K	Potential difference, ΔV/K	Mean thermoelectric power, θ K/mV
806.5	-20.5 +12.6	+19.02 -13.05	-0.98±.05
825.0	-19.0 +16.0	+19.38 -14.89	-0.97±.04
847.0	-17.0 +18.5	+18.70 -19.57	-1.08±.02
869.5	-18.5 +18.0	+20.65 -19.57	-1.10±.01
892.5	-20.0 +18.5	+23.48 -21.13	-1.16±.02
917.0	-16.0 +14.0	+18.11 -15.50	-1.12±.01
939.0	-18.0 +20.0	+22.69 -24.80	-1.25±.01

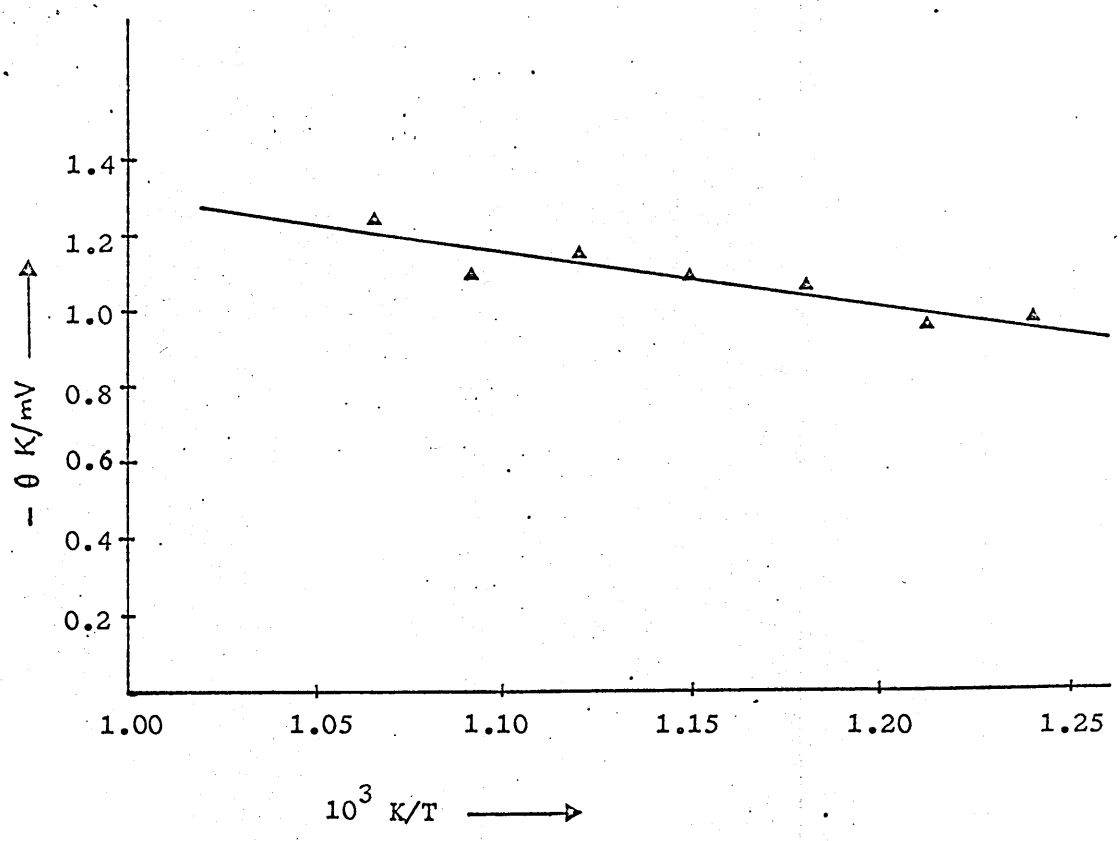

Figure 5.1. Temperature dependence of thermoelectric power of pure potassium chloride.

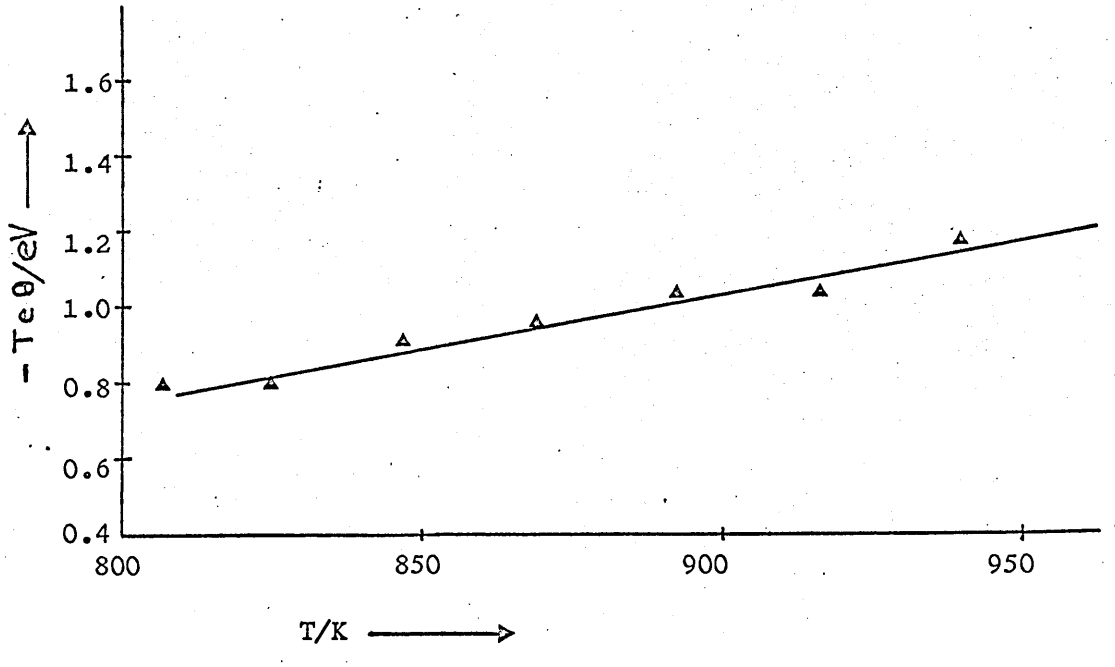

Figure 5.2. Temperature dependence of Teθ in potassium chloride.

Thermoelectric power θ mVK^{-1} is plotted in figure (5.1) as a function of $10^3/T$ K . A linear least squares fit of θ against $10^3/T$ gives the following equation,

$$\theta = (-(2.75 \pm 0.28) + (1.14 \pm 0.19) \times \frac{10^3}{T}) \text{ mVK}^{-1} \cdots\cdots (5.1)$$

It is apparent from this graph that there is a systematic variation of θ with T in pure potassium chloride specimen. Jacobs and Knight(44) plotted $Te\theta$ against T in order to assess dependence of Q^* on T. For purposes of comparison, the present data are also plotted in the form of $Te\theta$ eV against T K in figure(5.2). A linear least square fit in this plot gives,

$$Te\theta = (1.44 \pm 0.24) - (28.0 \pm 2.8) \times 10^{-4} \times T \cdots\cdots\cdots (5.2)$$

5.1.2. Comparison of observed and evaluated variations of resistance under thermal gradient in potassium chloride specimen.

As shown in section(3.2), neglect of thermomigration effects leads to the prediction that the resistance of a specimen with surface temperatures differing by ΔT will deviate from that of isothermal specimen at the same mean temperature by an amount proportional to $(\Delta T)^2$, the constant of proportionality being fixed by the activation energy for diffusion, the mean temperature and the isothermal resistance. Comparison of the values of $(\Delta R)_{\Delta T}$ obtained from equation(3.25) with experimental observations then gives an indication of the extent to which matter had been transported due to biased motion of vacancies under the thermal gradient. This aspect of the problem was examined using a potassium chloride single crystal at a central temperature of 895 K .

It is evident from equation (3.25) that $(\Delta R)_{\Delta T}$ can be evaluated if the activation energy for diffusion E_D is known. The value of E_D can be obtained from Jacobs and Pantelis(46) evaluation of E_f= 2.30 eV and E_m= 0.68 eV. So E_D comes to 1.83 eV. The isothermal resistance of the specimen at 895 K was 45986 Ω . The variations of evaluated and observed $(\Delta R)_{\Delta T}$ as a function of ΔT are shown in figure (5.3).

This plot is very important in the context of the present work. It shows that the experimentally observed values of $(\Delta R)_{\Delta T}$ deviate more and more from the evaluated values of $(\Delta R)_{\Delta T}$ as the temperature difference between the faces increases. In alkali halides the charged carriers are vacancies and hence it is reasonable to assume that vacancy concentration is perturbed by the imposition of the temperature gradient. There is of course an underlying

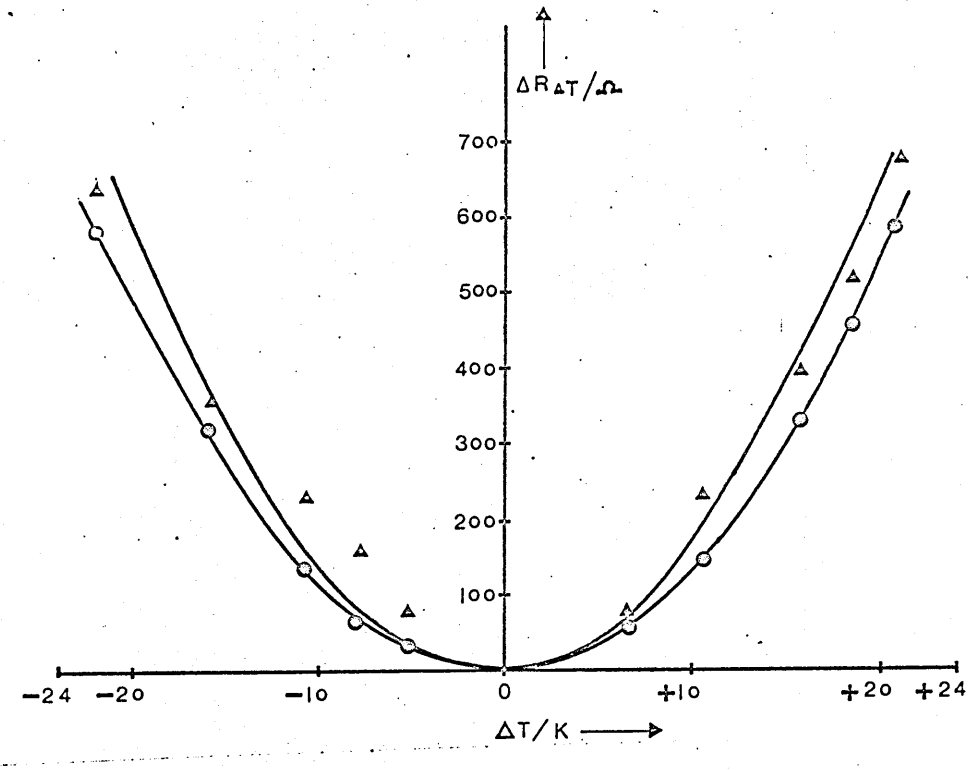

Figure 5.3. Comparison of observed and evaluated values of $(\Delta R)_{\Delta T}$ with ΔT; Observed points - ▲, Evaluated points - O .

assumption that the vacancy mobility is unperturbed by this non-equilibrium situation. This variation of vacancy concentration is precisely the reason for the consideration of section(3.3) where non-equilibrium situation is explicitely considered.

5.1.3. Modulation of specimen resistance by the electric driving field.

As shown in section(4.8), the effect of an a.c. driving field on the specimen resistance can be described in terms of its modulation. This may be detected by phase sensitive detectors locked to in-phase and quadrature components of the driving signal. The technique used to measure the change in resistance of a specimen due to the electric field in the presence of a thermal field will be described in the next section. This section is devoted to an estimation of the effect of the driving field frequency on specimen resistance.

To do this, a.c. driving fields in the range of 20 Hz to 850 Hz were used, their amplitudes being fixed at 4 mV across the specimen. The changes in the outputs of the phase and quadrature detectors then showed the extent to which specimen resistance was perturbed by the driving field. A plot showing the phase and quadrature outputs for two temperature gradients at the central temperature of 895 K over the full range of frequencies is shown in figure(5.4).

The plot has two important features. First, there is a strong dependence of detected outputs on frequency even when the temperatures gradient is zero. Second, there is the expected difference of the temperature gradient output from the isothermal output. Although presented for a single specimen at a fixed central temperature, the plot is characteristic of that found under all operating conditions.

No quatitative explanation has been found for the zero gradient output. It does not appear to be instrumental, but neither should it arise from displacements of vacancy population of the type under present consideration, except of course when there is a non-zero temperature gradient. A likely source of the effect could be the specimen-electrode interface but the theory of this phenomenon

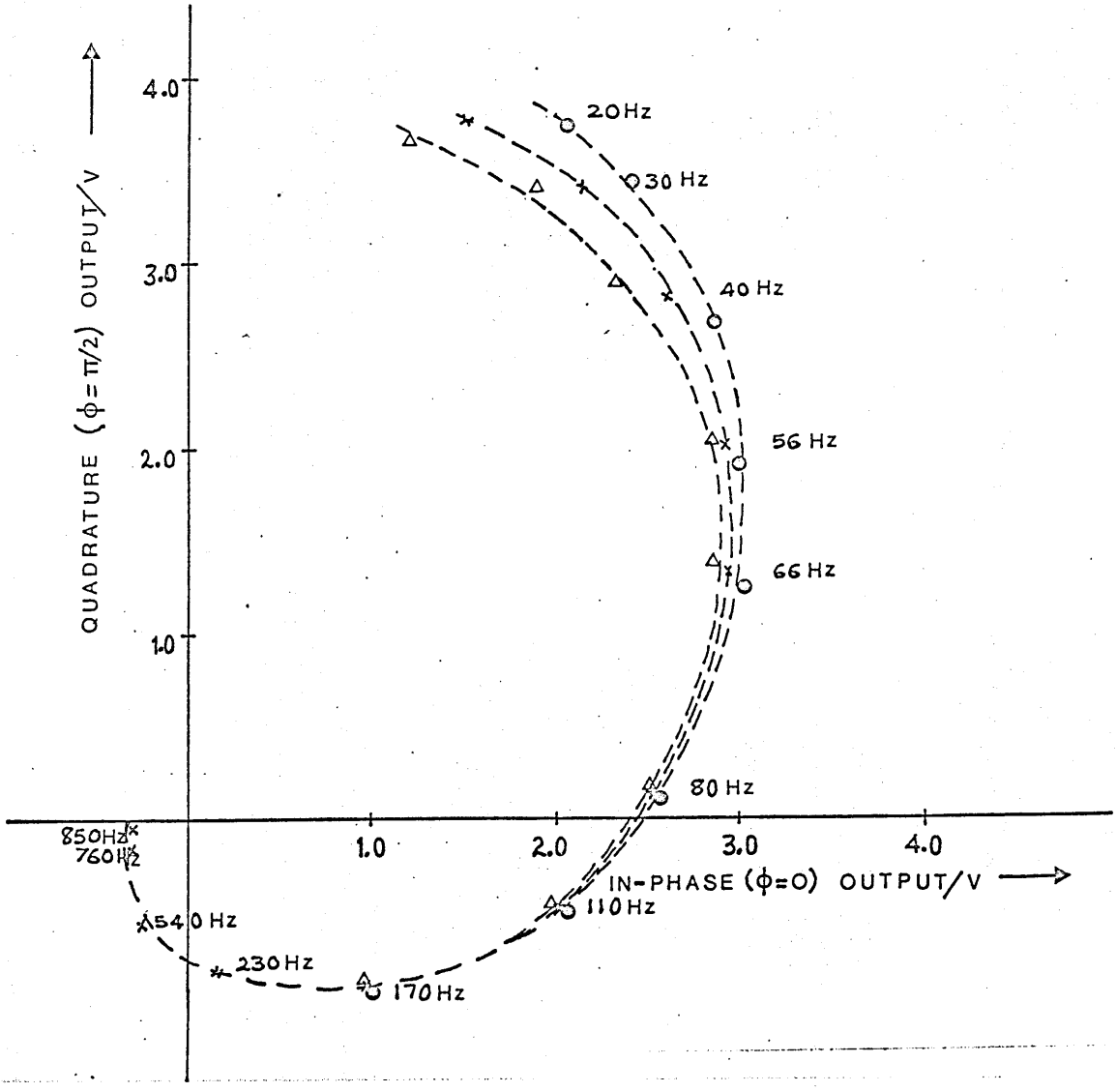

Figure 5.4. Frequency effect on detected outputs at 895 K.

Isothermal points - ×

ΔT =+20 K points - Δ

ΔT =-20 K points - o

is not very well developed at the moment. Though explanation of this zero gradient effect might have required a major investigation in its own right, attention here is restricted to the vector difference between the isothermal and temperature gradient points.

The difference between the isothermal and temperature gradient points is of the general form expected on the basis of vacancy kinetics. An increase in frequency resulted in a reduced amplitude for the difference vector. Also the expected reversal of phase with reversal of the temperature gradient was observed. On the basis of these observations it seemed reasonable to interpret the resistance modulation phenomena following equations(3.42) and (5.3).

From this analysis it is clear that a frequency of 40 Hz as driving signal would give good estimate of the perturbation. It leaves a good margin of frequency from the lower limit of the instrument's working frequency which is 3 Hz. At the same time it is not high enough to have outputs so small as to limit reliable estimates of the effect.

5.1.4. Calculation of heat of transport in potassium chloride crystal.

The cationic heat of transport Q^* can be calculated if the vacancy life time τ is evaluated beforehand. As is evident from equation(3.42) that if the phase and quadrature components of the electric field effect in association with thermal field are known, then the parameter τ can easily be evaluated by taking ratio of the two components. In terms of experimental quantities, the vacancy life time, τ is given by,

$$\tau = - \frac{1}{\omega} \frac{V_B}{V_A} \quad \ldots\ldots\ldots\ldots\ldots\ldots\ldots\ldots \quad (5.3)$$

where V_B and V_A are the quadrature and in-phase detectors outputs.

It is evident from figure(5.4) that the modulation of the specimen resistance depends not only on applied field frequency but also to some extent on the thermal condition existing at the specimen. Thus to find out the resultant effect on specimen resistance due to simultaneous application of thermal and electric fields, the effect at zero thermal gradient condition must be taken away from the total effect. In other words it can be written as,

$$\tau = - \frac{1}{\omega} \frac{V_B(E, \Delta T) - V_B(E, 0)}{V_A(E, \Delta T) - V_A(E, 0)} \quad \ldots\ldots\ldots \quad (5.4)$$

where $V_B(E,\Delta T)$ is the quadrature detector output when both E and Δ T are present

and $V_B(E,0)$ is the output of the same detector when E is on and ΔT is zero

Similar definition applies for V_A.

Experimentally it was found that V_A and V_B were straight lines passing almost through the origin. So each line of V_B or V_A can then be represented by an equation of the form $V_B = M_B X$

where X is proportional to the strength of the applied field. The applied field strength was detected by a phase sensitive detector hooked right across the specimen. So equation(5.4) becomes,

$$\tau = -\frac{1}{\omega}\frac{M_B(E,\Delta T) - M_B(E,0)}{M_A(E,\Delta T) - M_A(E,0)} \quad \ldots\ldots\ldots\ldots\ldots\ldots\ldots\ldots \quad (5.5)$$

The advantage of using equation(5.5) having slopes as variables instead of equation (5.4) having outputs as variables is that transient variations in the outputs due to noise will be smoothed out in the evaluation of the slopes from a large number of such points.

The calculation of vacancy life time, τ offers the possibility of evaluating the mean free path, λ of a vacancy. The relationship between τ and λ is given by,

$$\lambda = (D_v \tau)^{\frac{1}{2}} \quad \ldots\ldots\ldots\ldots\ldots\ldots\ldots\ldots \quad (5.6)$$

where D_v is the self-diffusion coefficient for vacancy.

Now $D_v C_v = D N$

and so, $D_v = \dfrac{D_0 \exp(-E_D/KT) \times N}{N \exp(-E_f/2KT)}$

$$= D_0 \exp(-E_m/KT)$$

So λ is given by,

$$\lambda = (D_0 \exp(-E_m/KT) \times \tau)^{\frac{1}{2}} \quad \ldots\ldots\ldots\ldots\ldots\ldots \quad (5.7)$$

This equation can then be used for the calculation of λ if D_0 and E_m are known. Taking these values from Beniere et al (13), and E_f = 2.30eV from Jacobs and Pantelis (46), the value of E_m becomes 0.82 eV.

$$\lambda = (33.16 \exp(-.82/KT) \times \tau)^{\frac{1}{2}} \quad \ldots\ldots\ldots\ldots\ldots\ldots \quad (5.8)$$

The calculation of resistance change due to thermal field was quite straight forward. The integrating millivoltmeter readings were taken at regular intervals and a mean value was found. When this mean value was transposed by the calibration line of the millivoltmeter, it gave $(\Delta R)_{\Delta T}$ straight away. But the evaluation of isothermal resistance change due to simultaneous electric and thermal fields was not that straight forward. The technique was to convert the voltage $(V_B(E,\Delta T) - V_B(E,0))$ into the input signal by dividing it with the gain in channel B. This input signal would then correspond to v_0 which could be used to determine $(\Delta R)_{E,\Delta T}$ if the gain in the integrating millivoltmeter was known and the calibration line was drawn. Thus knowing $(\Delta R)_{\Delta T}$ and $(\Delta R)_{E,\Delta T}$ as well as τ, the heat of transport could be calculated for each central temperature. The equation for the calculation of Q^* is,

$$Q^* = \frac{2.30}{2} - \frac{(\Delta R)_{\Delta T}}{(\Delta R)_{E,\Delta T}} \cdot \frac{4\times10^{-3} \times \tau \times 251 \times T}{(1 + (251 \times \tau)^2)\,|\Delta T|} \quad \cdots\cdots \quad (5.9)$$

Table (5.2) shows the values of different parameters necessary for the calculation of Q^* along with vacancy mean free path, λ.

Table 5.2. Calculation of cationic heat of transport in potassium chloride crystal.

T/K	$(\Delta T)/K$	$(\Delta R)_{\Delta T}/\Omega$	$(\Delta R)_{E,\Delta T}/\Omega$	$(M_A(E,\Delta T) - M_A(E,0)) \times 10^2$	$(M_B(E,\Delta T) - M_B(E,0)) \times 10^2$	$\tau \times 10^3$/sec	Mean $\tau \times 10^3$/sec	Mean $\lambda/\mu M$	Mean Q^*/eV
806.5	-20.5	1849	352	+2.10	-2.60	4.93	4.81±.12	10.6±1.6	.752±.006
	+12.6	786	253	-1.10	+1.30	4.70			
825.0	-19.0	1145	249	+2.20	-2.40	4.39	4.38±.01	11.5±.55	.750±.002
	+16.0	708	181	-1.80	+2.00	4.37			
847.0	-17.0	510	132	+2.50	-2.10	3.34	3.39±.05	11.8±.1.4	.765±.006
	+18.5	595	138	-2.10	+1.81	3.43			
869.5	-18.5	358	89	+3.40	-2.60	3.04	3.07±.03	13.0±1.3	.789±.003
	+18.0	346	90	-3.40	+2.60	3.10			

Table 5.2. - contd -

T/K	(ΔT)/K	$(\Delta R)_{\Delta T}/\Omega$	$(\Delta R)_{E,\Delta T}/\Omega$	$(M_A(E,\Delta T) - M_A(E,0)) \times 10^2$	$(M_B(E,\Delta T) - M_B(E,0)) \times 10^2$	$\tau \times 10^3$/sec	Mean $\tau \times 10^3$/sec	Mean $\lambda/\mu M$	Mean Q^*/eV
892.5	-20.0	365	84	+3.48	-2.10	2.40	2.35±.05	13.1±1.9	.796±.009
	+18.5	314	72	-3.80	+2.20	2.30			
917.0	-16.0	188	51	+3.20	-1.70	2.11	1.99±.12	13.9± 3.4	.808±.008
	+14.0	162	49	-3.40	+1.60	1.87			
939.0	-18.0	98	19	+4.50	-1.70	1.50	1.53±.02	13.8±1.5	.802±.008
	+20.0	112	21	-4.90	+1.90	1.55			

5.1.5. Temperature dependence of heat of transport in potassium chloride.

To investigate possible systematic variation of heat of transport, Q^* with temperature, T a graph of Q^* versus T was drawn. This is shown in figure (5.5). While data show some scatter, it does seem that there is an increase of Q^* with temperature. To check that this is statistically significant, a linear least-squares fit was calculated which gave the following equation,

$$Q^* = ((36.7 \pm 6.2)\times10^{-2} + (4.74 \pm .71)\times10^{-4} \times T) \text{ eV} \quad \cdots\cdots \quad (5.10)$$

The gradient of this line clearly deviates from zero and so the tendency of Q^* to increase with temperature is confirmed. It should be noted however that the change of Q^* over the accessible diffusion range of $(3/4)T_m$ to $(9/10)T_m$ (790 K to 945 K) is .074 eV or about 10 % of the mean value of $Q^* = (.78 \pm .007)$ eV over this range.

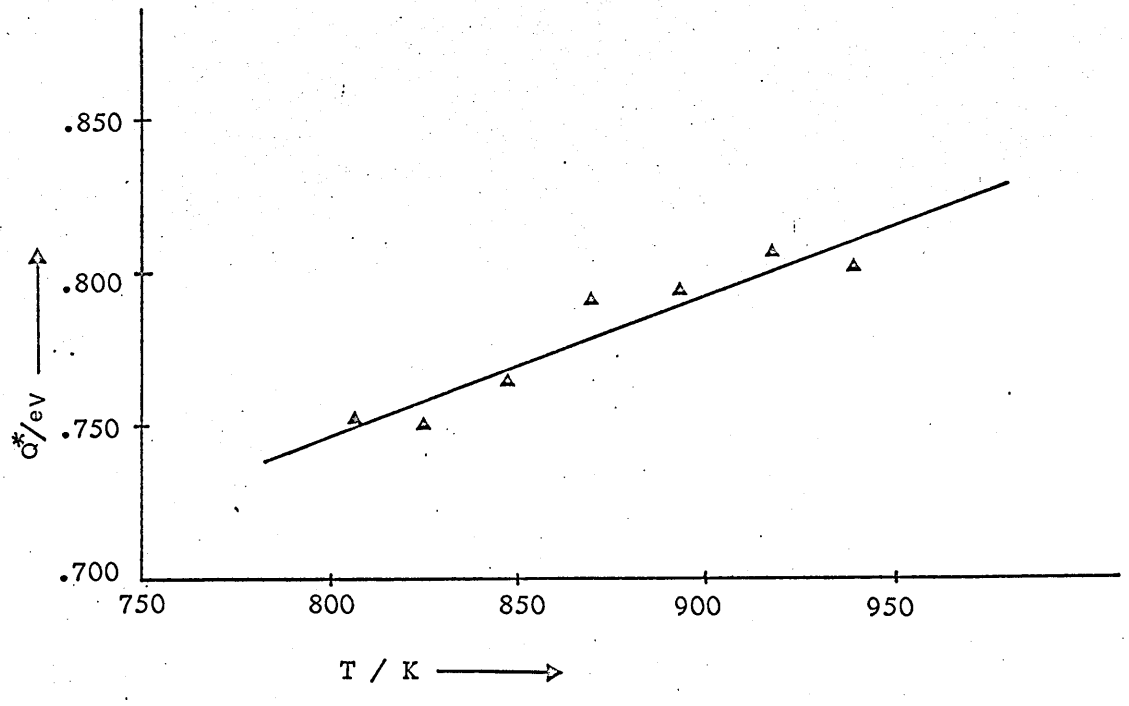

Figure 5.5. Variation of heat of transport with temperature.

5.1.6. Variation of vacancy life time in potassium chloride with temperature.

A parameter which is of importance in this study is the vacancy life time, τ. From table (5.2) it is evident that there is some temperature dependence of τ. To evaluate this temperature variation, it is appropriate first to consider an idealised model of vacancy motion. The vacancy life time is taken as the time for which a vacancy follow a random motion due to thermal activation between a source and a sink. Now assuming for the purpose of this calculation that the sources and sinks are fixed in number and are randomly distributed throughout the crystal, then the vacancy lifetime is expected to depend on basic parameters characterising vacancy motion, that is, the energy of migration, E_m. In other words, it can approximately be written as,

$$\tau = a \exp(E_m/KT) \quad \cdots\cdots\cdots\cdots\cdots\cdots\cdots \quad (5.11)$$

where a is a constant of proportionality.

Thus the above model predicts that a plot of $\ln \tau$ against $1/T$ would be a straight line. Figure(5.6) shows the variation of $\ln \tau$ against $10^3/T$. A least squares line fit gives the following equation,

$$\tau = 1.67 \times 10^{-6} \exp(.56/KT) \quad \cdots\cdots\cdots\cdots \quad (5.12)$$

It should be noted that the value of E_m based on above model is not a very accurate one. The above model only gives a rough estimate of E_m. However, E_m obtained here is comparable with the precisely estimated value of 0.68 eV by Jacobs and Pantelis(46).

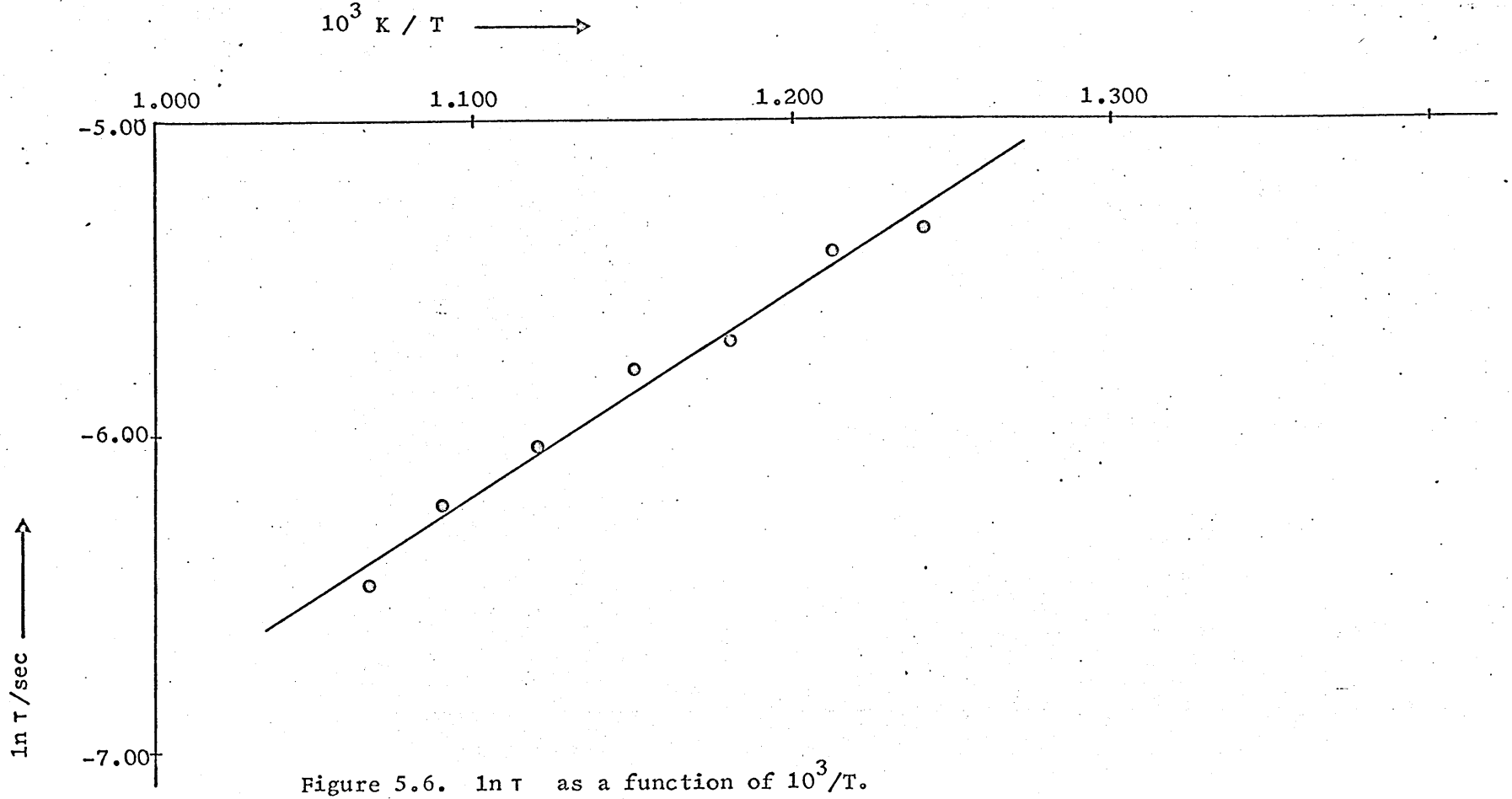

Figure 5.6. ln τ as a function of $10^3/T$.

5.1.7. Calculation of homogeneous and heterogeneous thermoelectric powers in potassium chloride specimen.

A special feature of this work is that it allows evaluation of homogeneous and heterogeneous thermoelectric powers in the specimen. This separation becomes possible because a knowledge of heat of transport permits evaluation of homogeneous thermoelectric power, θ_{hom}. Given experimental data for the total thermoelectric power, θ, it is therefore possible to estimate the heterogeneous thermo power, θ_{het} by subtracting θ_{hom} from θ.

For the evaluation of θ_{hom} from Q^*, equation (3.57) was used. The values of θ and Q^* were taken from Table (5.1) and (5.2) respectively. Table (5.3) shows the variation of θ_{hom} and θ_{het} against temperature and figure (5.7) shows it diagrammatically.

Table 5.3. Evaluation of homogeneous and heterogeneous thermoelectric powers in potassium chloride.

T/K	θ K/mV	Q^*/eV	θ_{hom} K/mV	θ_{het} K/mV
806.5	-0.98	0.752	-0.93	-0.05
825.0	-0.97	0.750	-0.91	-0.06
847.0	-1.08	0.765	-0.90	-0.18
869.5	-1.10	0.789	-0.91	-0.19
892.5	-1.16	0.796	-0.89	-0.27
917.0	-1.12	0.808	-0.88	-0.24
939.0	-1.25	0.802	-0.85	-0.40

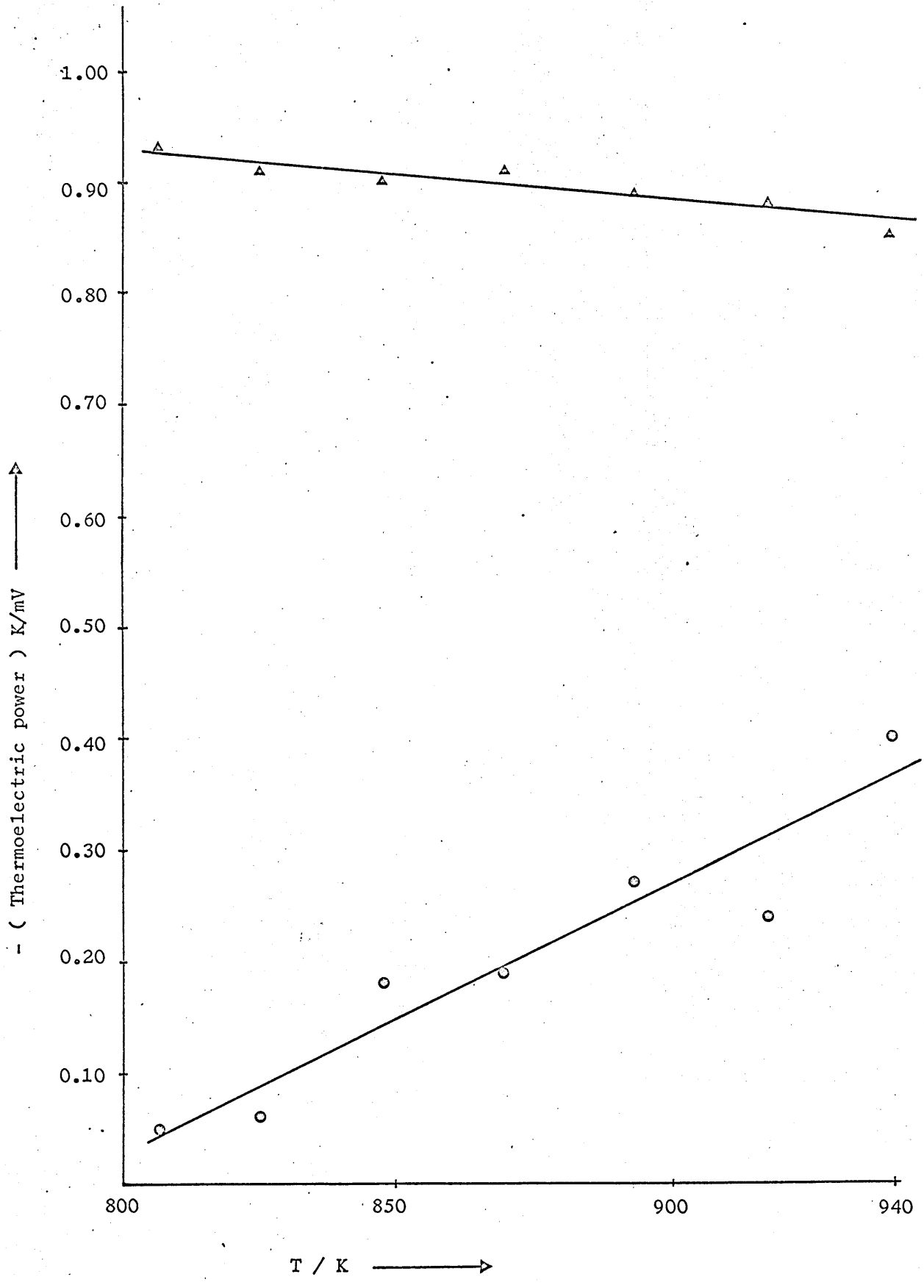

Figure 5.7. Thermoelectric powers in potassium chloride
Homogeneous component - △.
Heterogeneous component - ○.

5.1.8. Efficiency of dislocations in potassium chloride.

It has been mentioned in section(2.5) that the dislocations are primarily responsible for the variation of vacancy concentration at non-equilibrium conditions. The vacancy concentration is related to life-time and consequently to mean free path of a vacancy. Now if dislocations are assumed to be static and fixed in number over the range of experimental temperature, a change of dislocation density with temperature as calculated from equation(2.15), can only be explained by a change of efficiency of dislocations as vacancy traps. But it should be mentioned that efficiency of a dislocation cannot be measured in absolute quantity as there is no way of finding precisely the number of dislocations at a non-equilibrium condition. So only relative efficiency of dislocations can be found. This has been done here assuming dislocations at 806.5 K to have efficiency of 1. The dislocation density, ρ and relative efficiency, ε as a fuction of temperature are shown in Table(5.4).

Table 5.4. Relative efficiency of a dislocation as a function of temperature in potassium chloride.

T/K	λ /cm	ρ cm^2	ε
806.5	10.6×10^{-4}	2.67×10^{6}	1.00
825.0	11.5×10^{-4}	2.26×10^{6}	0.85
847.0	11.8×10^{-4}	2.15×10^{6}	0.81
869.5	13.0×10^{-4}	1.78×10^{6}	0.67
892.5	13.1×10^{-4}	1.75×10^{6}	0.66
917.0	13.9×10^{-4}	1.55×10^{6}	0.58
939.0	13.8×10^{-4}	1.58×10^{6}	0.59

5.2.1. Thermoelectric power in a sodium chloride crystal.

Measurement of thermoelectric potential was made in sodium chloride exactly the same way as for potassium chloride. As usual an anomalous potential was found to exist in this material even in the absence of a temperature gradient. Allnatt and Chadwick(2) contended that this galvanic voltage between Pt. electrodes attached to the faces of the specimen could be connected partly with the mechanical state of the crystal and partly with the interface effect. But Christy et al(21) assumed that this potential was due to moisture contamination which could then be eliminated by annealing the specimen over a long period of time. However after annealing the specimen at 950 K for about 12 hours, six thermoelectric potential readings were taken for each central temperature. For brevity in presentation only two readings due to maximum temperature differences are shown in Table(5.5). It should be mentioned that taking two extreme points of ΔT does not cause any loss of accuracy in thermoelectric power measurement as $\Delta V - \Delta T$ is a linear line passing almost through the origin. This is shown in figure(5.8).

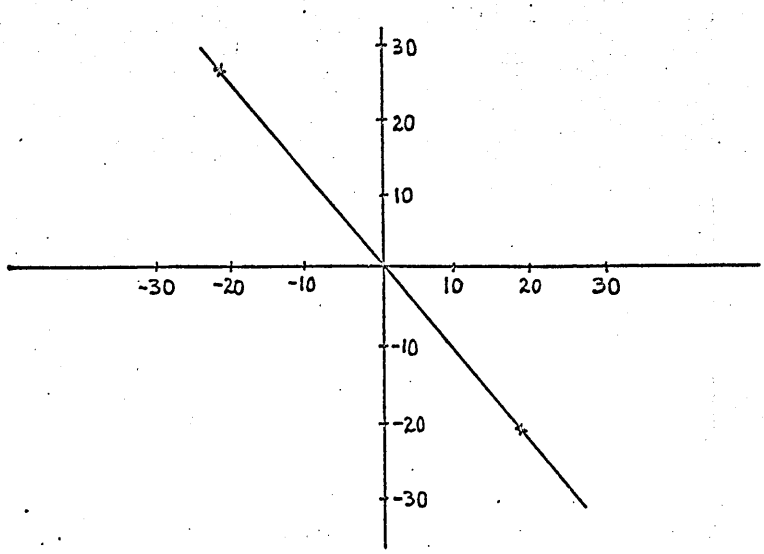

Figure 5.8. Variation of thermoelectric potential with temperature difference between faces in sodium chloride at 875 K.

Table 5.5. Thermoelectric power of pure NaCl with Pt. electrodes.

Central temperature, T/K	Temperature difference, ΔT/K	Potential differnce, ΔV/mV	Mean thermopower, θ K/mV
796.0	-20.0 +19.0	+19.80 -17.75	-0.96±.03
827.0	-20.0 +18.8	+20.40 -18.61	-1.01±.01
847.5	-20.0 +20.0	+22.90 -22.00	-1.12±.02
875.0	-21.0 +19.5	+25.20 -22.25	-1.17±.03
907.5	-20.5 +19.5	+24.93 -22.82	-1.19±.03
945.0	-19.0 +20.0	+25.27 -25.75	-1.31±.02

The thermoelectric power, θ mVK^{-1} is plotted in figure(5.9) as a function of$(10^3/T)K^{-1}$. A linear least squares fit of θ against $10^3/T$ gives the following equation,

$$\theta = (-(3.13 \pm 0.21) + (1.73 \pm 0.17) \times 10^3/T \quad mVK^{-1} \quad \cdots\cdots \quad (5.13)$$

As before, $Te\theta$ is also plotted against T in figure(5.10). The least squares fit gives the equation,

$$Te\theta = (1.74 \pm 0.17) - (3.14 \pm 0.19) \times 10^{-3} \times T \text{ meV} \quad \cdots\cdots \quad (5.14)$$

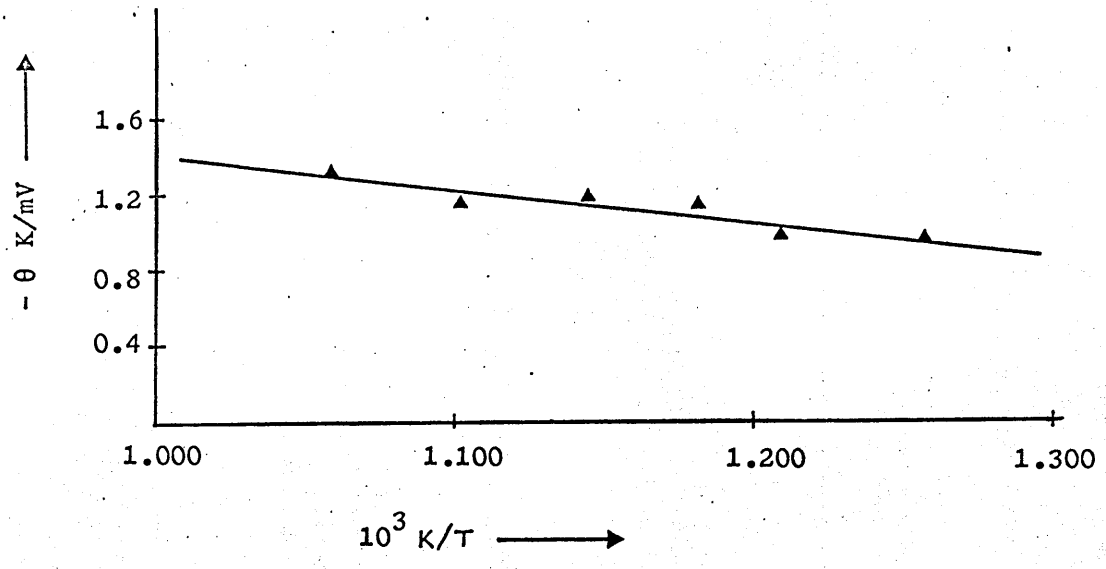

Figure 5.9. Temperature dependence of θ in NaCl.

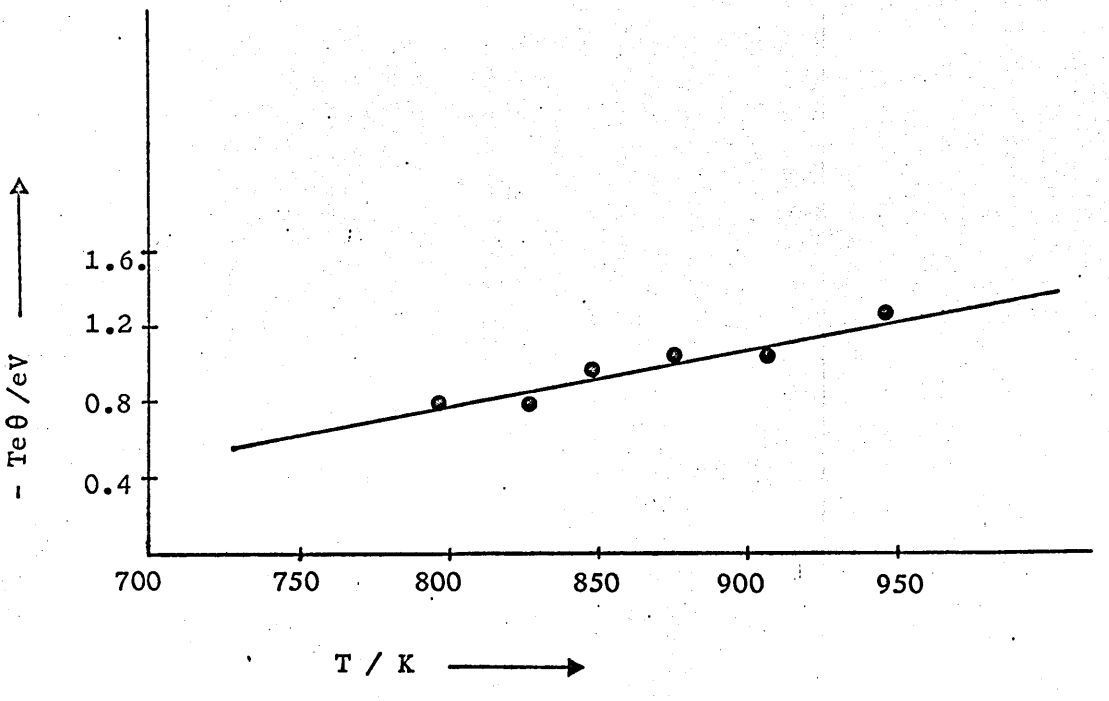

Figure 5.10. Temperature variation of Teθ in NaCl.

5.2.2. Variation of resistance with temperature in sodium chloride.

The conductance of an alkali halide crystal as a function of temperature had been very widely studied by a number of workers. For purposes of comparison and estimation of parameters like enthalpies of migration and formation of a defect, conductance of a pure NaCl specimen was also measured as a function of temperature. Figure(5.11) shows the plot of the conductance data. The data here were analysed by the graphical method to obtain rough estimates of transport parameters. From the graph the following values were obtained,

$$E_m = 0.47 \text{ eV} \quad \cdots\cdots\cdots\cdots\cdots\cdots\cdots\cdots (5.15)$$

$$\text{and } E_f = 2.20 \text{ eV} \quad \cdots\cdots\cdots\cdots\cdots\cdots (5.16)$$

As discussed in section (2.3), a true analysis of $\ln(\sigma T)$ vs $1/T$ should be done by a non-linear least-squares minimisation technique in the manner done by Beaumont and Jacobs(11). However the values above gave only a general confirmation of the technique in use. It was also intended to show that the temperature range of the experiment was safely above the 'knee' temperature of the specimen.

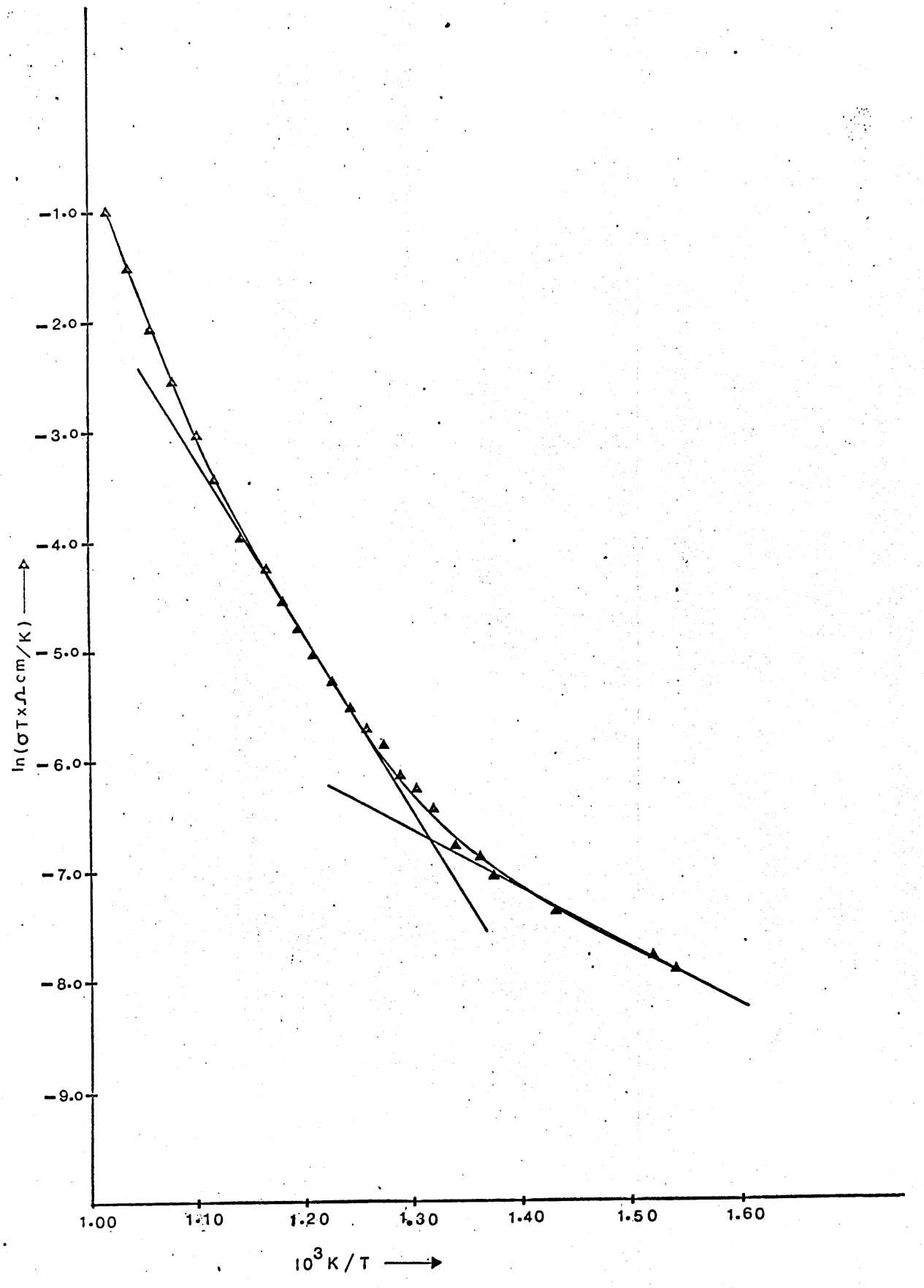

Figure 5.11. Conductivity in sodium chloride as a function of temperature.

5.2.3. Calculation of heat of transport in sodium chloride.

Heats of transport in pure sodium chloride were calculated in the same way as for potassium chloride. The drive signal frequency was 40 Hz as before. For computation the values of D_0= 3.2 cm^2/sec and E_D=1.78 eV were taken from Downing and Friauf(26) and E_f= 2.30 eV was taken from Kirk and Pratt(51). From the above references, E_m was found to be 0.63 eV. So mean free path, λ becomes,

$$\lambda = \left(3.2 \exp\left(- \frac{.63}{8.62 \times 10^{-5} \times T} \right) \times \tau \right)^{\frac{1}{2}} \quad \cdots\cdots\cdots\cdots \quad (5.17)$$

The only difference between the experimental studies of sodium chloride and potassium chloride is that in NaCl six gradients of temperature were taken at each central temperature instead of only two as in KCl. Table(5.6) shows the tabulation of data obtained on sodium chloride. It has been analysed in the pattern already introduced in potassium chloride.

Table 5.6. Calculation of cationic heat of transport in sodium chloride crystal.

T/K	$(\Delta T)/K$	$(\Delta R)_{\Delta T}/\Omega$	$(\Delta R)_{E,\Delta T}/\Omega$	$(M_A(E,\Delta T) - M_A(E,O)) \times 10^2$	$(M_B(E,\Delta T) - M_B(E,O)) \times 10^2$	$\tau \times 10^3$/sec	Mean $\tau \times 10^3$/sec	Mean $\lambda/\mu M$	Mean Q^*/eV
	-20.0	2064	435	+2.20	-2.70	4.89			
	-16.4	1542	395	+1.80	-2.30	5.09			
796.0	-10.0	674	236	+1.10	-1.40	5.07	4.87±.24	12.64±.28	.756±.024
	+ 8.0	421	210	-0.90	+1.10	4.87			
	+15.6	1247	311	-1.70	+2.10	4.92			
	+19.0	1727	367	-2.10	+2.30	4.36			
	-20.0	1227	240	+2.50	-2.50	3.98			
	-15.2	848	229	+1.90	-1.90	3.98			
827.0	- 8.8	357	174	+1.10	-1.10	3.98	3.98±.10	12.72±.03	.742±.03
	+ 8.6	312	145	-1.02	+1.00	3.96			
	+15.6	736	194	-1.80	+1.90	3.99			
	+18.8	1093	227	-2.30	+2.30	3.98			

Table 5.6. - contd -

T/K	(ΔT)/K	$(\Delta R)_{\Delta T}/\Omega$	$(\Delta R)_{E,\Delta T}/\Omega$	$(M_A(E,\Delta T) - M_A(E,0)) \times 10^2$	$(M_B(E,\Delta T) - M_B(E,0)) \times 10^2$	$\tau \times 10^3$/sec	Mean $\tau \times 10^3$/sec	Mean $\lambda/\mu M$	Mean Q^*/eV
847.5	-20.0	697	154	+3.10	-2.40	3.08	3.20±.17	13.55±.99	.754±.018
	-15.2	432	119	+2.40	-1.90	3.15			
	- 8.4	139	71	+1.30	-1.00	3.06			
	+ 7.2	139	77	-1.00	+0.90	3.58			
	+13.6	376	111	-2.00	+1.60	3.18			
	+20.0	725	154	-3.00	+2.40	3.18			
875.0	-21.0	457	97	+3.64	-2.30	2.51	2.47±.12	13.63±.30	.789±.03
	-15.8	277	75	+2.70	-1.70	2.51			
	- 8.8	103	63	+1.50	-1.00	2.65			
	+ 7.5	81	43	-1.40	+0.80	2.27			
	+13.6	221	69	-2.50	+1.50	2.38			
	+19.5	417	85	-3.50	+2.20	2.50			

Table 5.6. - contd -

T/K	(ΔT)/K	$(\Delta R)_{\Delta T}/\Omega$	$(\Delta R)_{E,\Delta T}/\Omega$	$(M_A(E,\Delta T) - M_A(E,0)) \times 10^2$	$(M_B(E,\Delta T) - M_B(E,0)) \times 10^2$	$\tau \times 10^3$/sec	Mean $\tau \times 10^3$/sec	Mean $\lambda/\mu M$	Mean Q^*/eV
907.5	-20.5	200	37	+4.90	-2.20	1.79	1.75±.078	13.32±.28	.773±.018
	-14.5	115	29	+3.50	-1.60	1.81			
	- 9.8	69	25	+2.40	-1.10	1.82			
	+ 8.5	49	21	-2.00	+0.80	1.59			
	+16.0	134	27	-3.90	+1.70	1.73			
	+19.5	190	36	-4.70	+2.10	1.78			
945.0	-19.8	89	14	+6.00	-1.90	1.26	1.37±.06	13.83±.32	.790±.022
	-12.0	32	9	+3.70	-1.20	1.29			
	- 7.8	18	7	+2.40	-1.00	1.65			
	+ 8.0	18	7	-2.40	+0.80	1.32			
	+15.6	54	10	-4.60	+1.60	1.38			
	+20.0	79	13	-6.00	+2.00	1.33			

5.2.4. Temperature dependence of heat of transport in sodium chloride.

In order to investigate dependence of heat of transport on temperature in sodium chloride, the least squares minimization technique was applied. This minimization technique offers a value of Q^* which can be quantitatively written as,

$$Q^* = ((\ 51.9 \pm 9.7)\times10^{-2} + (2.8 \pm 1.0)\times10^{-4}\times T)\ \text{eV} \quad \cdots\cdots \quad (5.18)$$

This equation shows that heat of transport in sodium chloride is a function of temperature and hence confirms the belief that the heats of transport in alkali halides are in general temperature dependent. A plot of Q^* against T is also shown in figure (5.12). However the change of Q^* over the temperature range of 796.0 K to 945.0 K is .043 eV or about 6% of the mean value of $Q^*=(.77\pm.009)$.

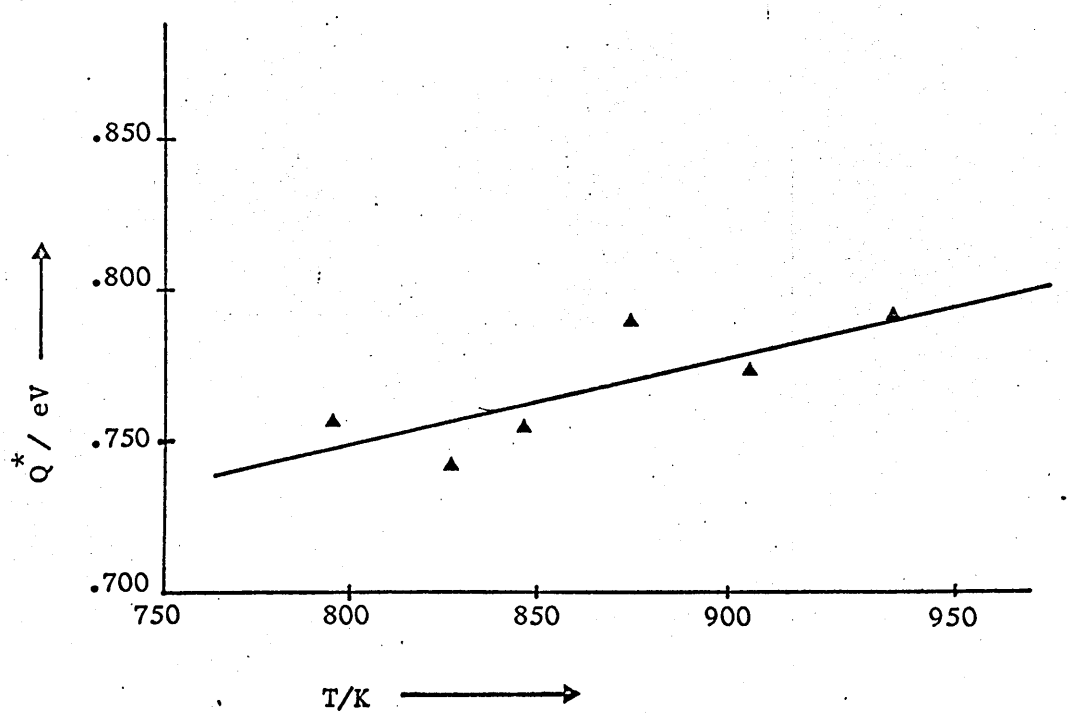

Figure 5.12. Heat of transport in NaCl as a function of temperature.

5.2.5. Variation of vacancy life-time with temperature in sodium chloride crystal.

Table (5.6) shows that vacancy life-time in sodium chloride varies with temperature. A model of vacancy motion described by equation (5.11) can also be assumed in sodium chloride specimen. Basing on this model, the energy of migration can be calculated if $\ln\tau$ is plotted against 1/T. A least squares line fit gives the following equation,

$$\ln\tau = (6.7 \pm .31)\times 10^{3} \times \frac{1}{T} - (13.7 \pm .36) \quad \cdots\cdots \quad (5.19)$$

and so

$$\tau = 1.12 \times 10^{-6} \exp(.58/KT) \quad \cdots\cdots\cdots\cdots\cdots \quad (5.20)$$

The value of energy of migration obtained here is based on a simplified model and hence should not be taken as very accurate. But none the less it offers a value which is comparable with the value of .66 eV obtained by Allnatt and Pantelis(6).

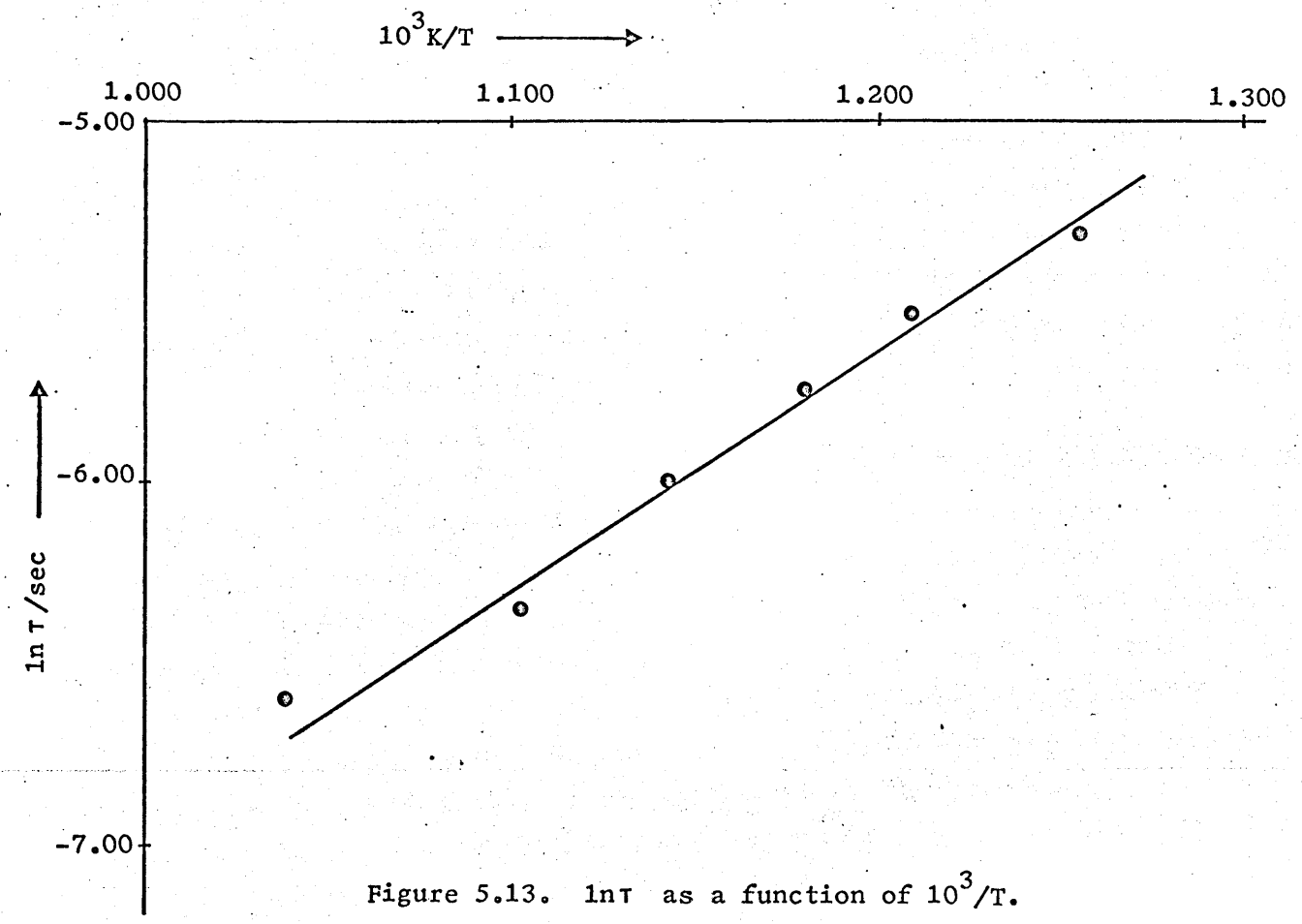

Figure 5.13. $\ln\tau$ as a function of $10^3/T$.

5.2.6. Homogeneous and heterogeneous thermoelectric powers in sodium chloride single crystals.

As before the values of Q^* and θ were taken together to calculate homogeneous and heterogeneous thermoelectric powers following equation(3.57). The values of Q^* and θ were taken from Tables (5.6) and (5.5) respectively. The variations of θ_{hom} and θ_{het} with temperature are shown in tabular form in Table (5.7) and diagrammatically in figure (5.14).

The least squares fit to these data points give the following equations,

$$\theta_{hom} = (-(1.48 \pm .09) + (6.9 \pm 1.1)x10^{-4}xT)\ mV \quad \cdots\cdots\cdots \quad (5.21)$$

$$\theta_{het} = ((2.3 \pm .2) - (29 \pm 2.4)x10^{-4}xT)\ mV \quad \cdots\cdots\cdots\cdots \quad (5.22)$$

Table (5.7) Evaluation of homogeneous and heterogeneous thermopowers in sodium chloride.

T/K	θ K/mV	Q^*/eV	θ_{hom} K/mV	θ_{het} K/mV
796.0	-0.96	.756	-0.94	-0.02
827.0	-1.01	.742	-0.90	-0.11
847.5	-1.12	.754	-0.89	-0.22
875.0	-1.17	.789	-0.90	-0.27
907.5	-1.19	.773	-0.85	-0.32
945.0	-1.31	.790	-0.83	-0.48

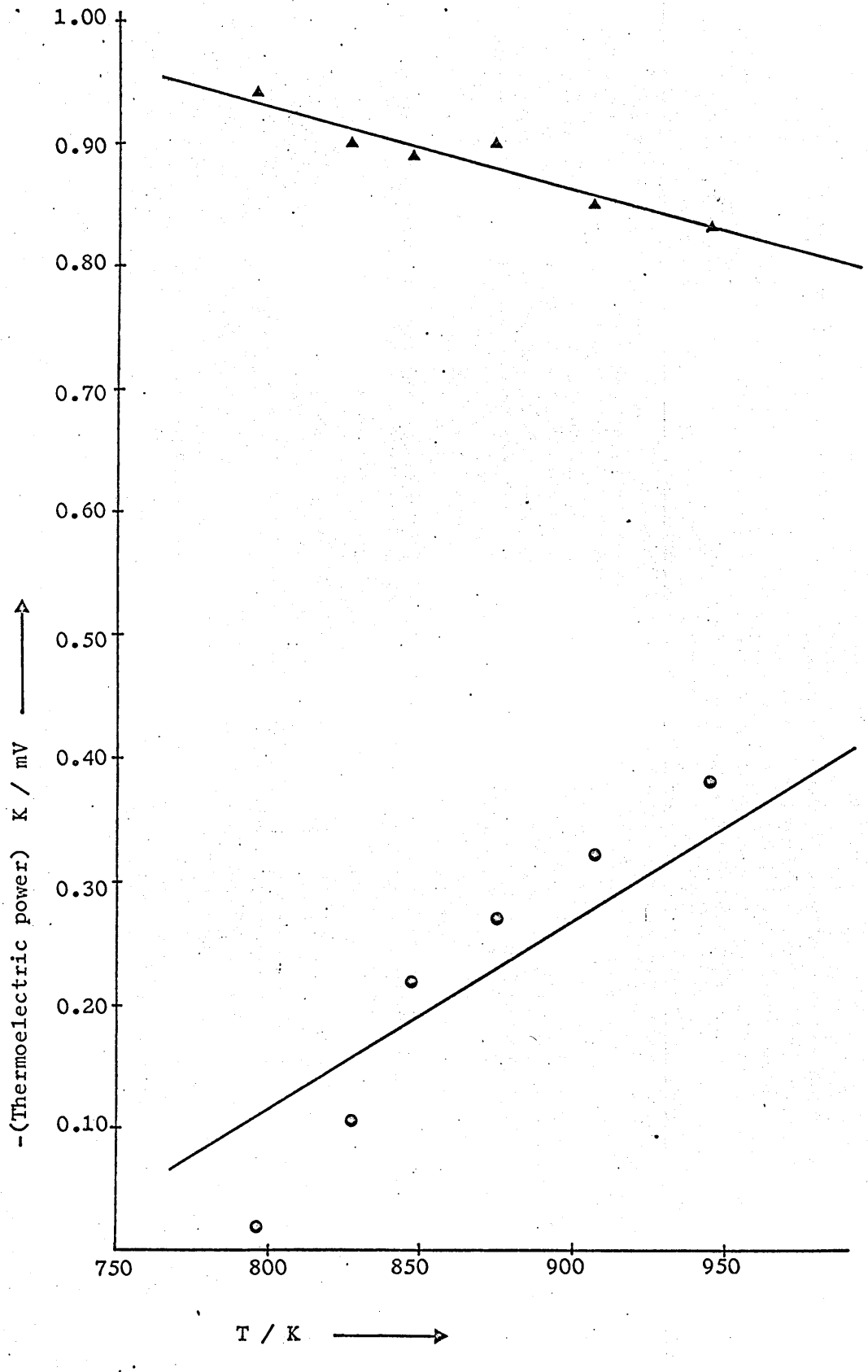

Figure 5.14. Thermoelectric powers in sodium chloride
Homogeneous component - ▲
Heterogeneous component - ⊙

5.2.7. Dislocation efficiency in sodium chloride.

The efficiency of dislocations in sodium chloride was calculated precisely the same way as in potassium chloride. The efficiency of dislocations at 796.0 K was assumed unity and relative to it, other efficiencies were calculated. Table (5.8) shows the values of relative efficiency, ε along with dislocation density, ρ.

Table 5.8. Relative efficiency of dislocations in sodium chloride.

T/K	λ/cm	ρ cm^2	ε
796.0	12.64×10^{-4}	1.88×10^{6}	1.00
827.0	12.72×10^{-4}	1.85×10^{6}	0.98
847.5	13.55×10^{-4}	1.63×10^{6}	0.87
875.0	13.63×10^{-4}	1.61×10^{6}	0.86
907.5	13.32×10^{-4}	1.69×10^{6}	0.89
945.0	13.83×10^{-4}	1.57×10^{6}	0.84

CHAPTER 6

DISCUSSION

6.1. Discussion

Of the many kinds of driving forces that can bias atomic motions in a crystalline material, thermal and electric potential gradients are the most important ones. Not only these forces are physically interesting, but also the experimental conditions in this project were such that a discussion on these forces will help to elucidate the experiment. The materials under study were strong ionic solids and consequently electronic contributions to conductivity can be neglected. It is evident from equation(3.27) that the vacancy flux in cationic sublattice is composed of three contributions which are (i) due to action of self-diffusion in homogenizing the specimen and is given by $-D_v \nabla C_v$, (ii) due to thermomigration of ions given by $D_v C_v Q^* \nabla T/KT^2$ and (iii) due to electromigration of ions which is $Z_v^* eED_v C_v/KT$. Leaving aside the homogenizing effect of diffusion, the two driving forces and menifestations of these forces will be considered. But it should be noted that as f.c.c. materials are only considered here, any complexity due to anisotropy of the non-cubic crystals are out of place.

Electromigration is the phenomenon of mass transport under the influence of an electric field or electric current(41). The electric driving force has basically two components, one is due to motion of ions in an electrostatic field and the other is due to motion and interaction of moving electrons on the ions. The second effect, known as 'wind force' effect will be discounted here as the materials under study are basically insulators. So the driving force due to an electric field is,

$$F = Z^* |e| E \qquad \cdots\cdots\cdots\cdots\cdots\cdots\cdots \quad (6.1)$$

There are conflicting points of view about Z^* by different authors. One group maintains(16) that static charge, lattice defects and shielding

impurities effectively reduces the valence, Z^* of the ion. On the other hand, another group(43) shows that the shielding on the moving ion is not operative and Z^* is effectively the valence of the moving ion. Das and Peierls(22) show that the shielding of unbound charges is generally ineffective as far as calculation of the force on the shielding is concerned. In this work also, the valence of the cation was taken undiminished when electric driving force was calculated.

The thermal driving force which gives rise to thermo--migration can be written as,

$$F = - \frac{\nabla T \, Q^*}{T} \quad \cdots\cdots\cdots\cdots\cdots\cdots \quad (6.2)$$

The parameter of prime importance, Q^* determines the strength of matter flux under fixed thermal conditions. Huntington(41) assumes that for ionic solids of above nature, there are basically two contributions to Q^*, which are,

$$Q^* = Q^*_{int} + Q^*_{ph} \quad \cdots\cdots\cdots\cdots\cdots\cdots \quad (6.3)$$

The first term is due to energy intrinsically associated with the jumping ion. The ion which is jumping over the potential barrier requires some energy to do so and this contributes positively to Q^*_{int}. Now if the vacant site adjacent to the jumping ion needs to be energetically expanded, then the contribution to Q^*_{int} is negative. However intrinsic contribution to heat of transport is positive in most cases and definitely so in alkali halides.

The other contribution to heat of transport is due to phonon scattering by defects. Sorbello(68) emphasised that in the harmonic approximation, there is no contribution to Q^* from phonon flux. However for anharmonic forces, the contribution from phonon flux based on assigning real momenta to phonons of magnitude $\hbar k$ is,

$$Q^*_{ph} = \frac{2}{3} \omega \gamma \tau k T \quad \cdots\cdots\cdots\cdots\cdots\cdots \quad (6.4)$$

where ω is of the order of Debye frequency,

τ is phonon relaxation time

and γ is Gruneisen constant.

Taking values of $\gamma = 1.63$ for NaCl and $\gamma = 1.60$ for KCl and $\omega \sim 10^{13} sec^{-1}$ from Kittel(52), Q^*_{ph} becomes approximately equal to .09eV and .08eV for NaCl and KCl respectively. Thus the effect of anharmonic forces contribute positively about 10 % to the existing values of Q^*. This will make the contending theories(7,77) that heats of transport are less than or equal to their respective energies of migration more inappropriate. However in view of imprecise knowledge about atomic forces in lattice structure, namely whether harmonic approximation is a true description or anharmonic forces should be considered, it seems superfluous at this moment to include phonon-scattering effect in alkali halide crystals.

From the present study of heats of transport in alkali halide single crystals at temperatures between 50 K and 300 K of melting points, the following important conclusions can be drawn. These are;
(i) heats of transport for cations in both materials,namely sodium chloride and potassium chloride, are higher than their respective energies of migration. This is very important in the sense that it exposes the inadequacy of simple Wirtz model and hence shows the necessity of some elaborate model, of which Schottky's one seems promising.
(ii) heats of transport are temperature dependent, that is, they increase with the increase of temperature. This is in direct conflict with earlier evaluations of this parameter by different authors(3,19,44) using thermoelectric power as the starting point, except with Christy(19) who found temperature dependence of Q^* in AgCl and AgBr. It has been mentioned in section(1.3) that the reliability of the measurement of heat of transport from thermo-power is questionable on account of uncertainty and ambiguity about heterogeneous thermopower.

(iii) the mean free path of a vacancy in both the materials increases with temperature. The explanation of this experimental evidence requires a conceptual insight into the physical process of generation and annihilation of vacancies. The vacancies are generated and annihilated in dislocation cores, vacancy pairs and impurity-vacancy complexes. As the temperature is increased, the thermal vibrations of the ions make them less efficient as vacancy traps and consequent longer distance of travel of vacancies.

(iv) if it is assumed that dislocations are mainly responsible for alteration of vacancy concentrations at non-equilibrium conditions, then it is fair to expect that mean free path of vacancies will be tied to dislocation density. An assumption of fixed dislocation density at temperatures of experimental range provides variation of effectiveness of dislocations with temperature which is presumably exponential.

In view of the above results regarding heats of transport in alkali halides, it is worth considering some of the important models. Wirtz model considers the energy acquired by a jumping ion as well as the energy required to prepare the shell ions so that jumping ion can be accommodated at the final plane. Allnatt and Chadwick(1) contend that the energy the jumping ion acquires is from atoms away from the vacancy. If the vacancy is at a temperature higher than the jumping ion, then the jumping ion receives energy at a mean temperature which is lower than the temperature of the lattice at which it resides. This has the effect of making Q^* more positive and consequently making it possibly higher than E_m. Thus the Wirtz model is not as flagrantly violated as it seems at first sight.

Schottky's model(67) which considers only the energies of the jumping ions and ignores altogether the shell ions, offers a value of heat of transport which is significantly higher than energy

of migration. The parameters W_1 and τ_1 used in equation(1.9) to find Q^*/E_m can be calculated from the following equations,

$$W_1 = (24\pi^2)^{-1/3} K\Theta a_0 / \hbar$$

$$\text{and } \tau_1 = \frac{a_o^3}{4KW_1^2}$$

where Θ is the Debye temperature

a_0 is the jump distance

K is Boltzmann constant

and τ_1 is phonon relaxation time.

From above equations, the values of W_1 and τ_1 for NaCl are $2.36\times10^3 Msec^{-1}$ and 2.05×10^{-13}sec respectively and for KCl are $2.01\times10^3 Msec^{-1}$ and 3.16×10^{-13} sec respectively. The values of Q^*/E_m can be approximated as,

$$Q^*/E_m \cong 1.5 \quad \text{for NaCl}$$

$$\text{and } Q^*/E_m \cong 2.0 \quad \text{for KCl.}$$

These values cannot be directly compared with the experimental values as contributions from shell ions were not considered in this formulation. The effect of the shell ions would be to reduce the magnitude of the above Q^*/E_m as some energy must be absorbed by these ions to make room for the diffusing ions. However this model is a step in the right direction which can eventually elucidate the mechanism of matter and energy flow in crystalline materials.

It has been mentioned that measured heats of transport in both the materials studied showed strong dependence on temperature which can be written as,

$$Q^* = (52.0 \pm 10.0) \times 10^{-2} + (3.0 \pm 1.0)\times 10^{-4} \times T, \text{ for NaCl}$$

$$Q^* = (37.0 \pm 6.0) \times 10^{-2} + (5.0 \pm 1.0) \times 10^{-4} \times T, \text{ for KCl}$$

Now taking the values of energy of migration in NaCl and KCl respectively as 0.69eV from Kirk and Pratt(51) and 0.71eV from Beaumont and Jacobs(11), the ratio of Q^*/E_m becomes,

for NaCl, Q^*/E_m = 1.09 to 1.14 at 796 K and 945 K

for KCl , Q^*/E_m = 1.06 to 1.13 at 806.5 K and 939 K

The evidence of heat of transport in excess of E_m and at the same time dependent on temperature can find an explanation from Haga(37). Haga stated that although E_m is the energy required by an atom to jump to a vacant site, diffusing atoms will have energies exceeding E_m. A simplification of the model, as carried out by John(47), offers an equation for the mean energy of an atom as,

$$\bar{E} = \frac{\int_{E_m}^{\infty} E \exp(-E/KT)\, dE}{\int_{E_m}^{\infty} \exp(-E/KT)\, dE}$$

$$= E_m + KT \cong Q^*$$

$$\text{So} \quad \frac{dQ^*}{dT} \cong K$$

The observed values of dQ^*/dT give,

for NaCl, $dQ^*/dT \cong 3.0K$

for KCl , $dQ^*/KT \cong 4.0K$

This calculation shows that heats of transport in both the materials are in excess of E_m by a factor well over KT. Thus Haga's model does not totally agree with these experimental values. But it cannot definitely be said that Haga's postulates are violated here because the discrepancy could well be less than the error introduced because of simplyfying assumptions in the above model.

6.2. Application of the technique.

The above method of experimental determination of Q^* and other related parameters can be applied to any ionic crystal which has no electronic contribution to conductivity. The pleasing aspect of this experimental study is that the parameters are evaluated from the bulk property of the specimen without making any simplifying assumptions of the crystal-electrode interface effect. In this respect the measured values of the parameters are more reliable and accurate than those from thermoelectric power measurements. Moreover this method provides an opportunity for the evaluation of cationic as well as anionic heats of transport in a material if the transport numbers of the species are known precisely.

The other important feature of this method is that it offers an estimate of homogeneous thermoelectric power from the value of heat of transport if a suitable equation connecting them can be found. At the moment homogeneous thermopower theory is quite well developed and hence θ_{hom} can very precisely be evaluated from Q^*. The only uncertainty and lack of unanimity lies regarding heterogeneous thermopower. This method provides a value of heterogeneous thermopower which could then be used to test the existing theories of heterogeneous thermoelectric power.

Appendix 1. Temperature dependence of conductivity in sodium chloride.

R/KΩ	T/K	σ cm/μυ	lnσT	10^3/T
627.20	650.2	0.558	-7.922	1.538
564.50	659.0	0.620	-7.803	1.517
389.30	699.4	0.899	-7.372	1.430
297.10	727.8	1.178	-7.062	1.374
250.40	737.2	1.398	-6.878	1.357
230.40	747.4	1.519	-6.781	1.338
169.10	758.6	2.070	-6.456	1.318
141.10	766.8	2.480	-6.265	1.304
126.80	776.8	2.759	-6.145	1.287
96.66	786.0	3.621	-5.862	1.272
84.26	796.0	4.154	-5.712	1.256
71.46	805.2	4.898	-5.536	1.242
56.74	817.0	6.169	-5.290	1.224
44.63	827.0	7.843	-5.038	1.209
35.50	837.4	9.858	-4.797	1.194
27.88	847.4	12.550	-4.543	1.180
21.18	858.0	16.523	-4.256	1.165
16.34	875.2	21.421	-3.977	1.143
9.83	895.4	35.619	-3.445	1.117
6.56	907.4	53.320	-3.028	1.102
4.11	926.4	85.250	-2.539	1.079
2.58	945.2	135.47	-2.055	1.058
1.50	963.0	232.81	-1.495	1.038
0.92	981.4	380.06	-0.986	1.019

APPENDIX 2

Heat of transport as measured in this experiment represents the total energy carried by a unit flux of matter when the temperature gradient across the specimen is effectively zero. It is a common knowledge that matter flux in materials like potassium chlorides or sodium chlorides is due to contributions both from cations and anions. The relative contributions of these two constituents are usually expressed by their respective transport numbers. The transport numbers for cations are high at relatively low temperatures and low at high temperatures. Table(2.3) which shows transport numbers as a function of temperature has to be modified in view of recent evaluations of this parameter. It should be mentioned that though there are couple of published papers from which transport numbers for potassium chloride can be deduced, there is hardly any reliable paper for evaluation of this parameter in sodium chloride. Table (A) shows the variation of transport numbers with temperature in potassium chloride. Column (a) and (b) are obtained from the transport number data whereas column (c) is evaluated from diffusion coefficients data. The present analysis of decomposition of total heat of transport into cationic and anionic contributions is restricted to potassium chloride only as transport numbers are available for this material. Of course the same analysis can be applied to sodium chloride also if reliable and accurate data for transport numbers are available.

As shown in Table(A), the transport numbers for anions over the range of experimental temperature, 800 K to 950 K, cannot be neglected. Thus an attempt is made to identify the individual

Table A. Cation transport numbers in potassium chloride specimen.

T/K	t_+^1	t_+^2	t_+^3
806.5	0.94	0.98	0.96
825.0	0.92	0.96	0.93
847.0	0.90	0.94	0.91
869.5	0.88	0.92	0.89
892.5	0.85	0.90	0.85
917.0	0.78	0.88	0.80
939.0	0.72	0.83	0.76

contributions of cations and anions to total heat of transport. So,

$$Q^* = t_+Q_+^* + t_-Q_-^* \quad \text{.....(1)}$$

where + indicates cations

- indicates anions

and t's are transport numbers.

Q^* has been found to be temperature dependent by previous analysis and so Q_+^* and Q_-^* are also assumed, for the purpose of calculation, to be temperature dependent. So equation (1) can be written as,

$$Q^* = t_+(a + bT) + t_-(c + eT)$$

so, $$\bar{Q}^* = t_+(a + b\bar{T}) + t_-(c + e\bar{T})$$

$$Q^* - \bar{Q}^* = t_+b(T - \bar{T}) + t_-e(T - \bar{T}) \quad \text{.....(2)}$$

This equation provides a means of testing whether Q_+^* or Q_-^* is temperature dependent. The unknown parameters b and e in equation(2) are solved taking values from table(5.2) and $\bar{Q}^*$=.788 eV and $\bar{T}$ =872 K. These are,

$$b = 4.73 \times 10^{-4} \text{ eV/K} \quad \text{.....(3a)}$$

$$e = 4.9 \times 10^{-4} \text{ eV/K} \quad \text{.....(3b)}$$

Comparison of equation (3a) with equation (5.10) shows that there is virtually no significant change in slope due to introduction of anion into the analysis. The values of a and c can also be found from the least squares considerations which are given as,

$$a = 36 \times 10^{-2} \text{ eV} \quad \ldots\ldots\ldots\ldots\ldots\ldots \quad (4a)$$

$$c = 48 \times 10^{-2} \text{ eV} \quad \ldots\ldots\ldots\ldots\ldots\ldots (4b)$$

Table B. Cationic and anionic heats of transport in potassium chloride.

T/K	Q^*/eV	Q_+^*/eV	Q_-^*/eV	$t_+Q_+^*$/eV	$t_-Q_-^*$/eV
806.5	.757	.741	.88	.70	.06
825.0	.766	.750	.88	.69	.07
847.0	.776	.760	.90	.68	.09
869.5	.787	.771	.91	.68	.11
892.5	.798	.782	.92	.66	.14
917.0	.810	.794	.93	.61	.20
939.0	.820	.804	.94	.57	.26

Thus taking the values of a,b,c and e the cationic and anionic heats of transport can be evaluated. Figure B shows cation and anion heats of transport as well as their products with respective transport numbers. The table shows that the temperature dependence of cationic heat of transport does not change by any significant amount due to introduction of anions in the analysis. Thus the conclusions drawn previously regarding cationic heat of transport remain valid.

The added information that can be extracted from the present analysis is the values of anionic heats of transport. It is pleasing to note that the mean value .91 eV of anionic heat of

transport agrees within the experimental error with the value of .95 eV obtained by Jacobs and Knight(4).It is also worth noting that anionic heat of transport is also slightly temperature dependent and is smaller than the evaluated energy of anion migration, 1.04 eV by Beaumont and Jacobs(5).

REFERENCES.

(1) Jacobs,P.W.M. and Maycock, J.N. Trans. Met.Soc.AIME.,1966,236,165

(2) Allnatt,A.R. and Jacobs,P.W.M. Trans.Far.Soc.,1962,58,116

(3) Jacobs,P.W.M. and Pantelis,P. Phys.Rev.B, 1971,4,3757

(4) Jacobs,P.W.M. and Knight,P.C. Trans.Far.Soc.,1970,66,1227

(5) Beaumont,J.H. and Jacobs,P.W.M. J.Chem.Phys.,1966,45,1496.

REFERENCES

(1) Allnatt, A.R. and Chadwick, A.V., Chem. Rev., 1967, 67, 681.

(2) Allnatt, A.R. and Chadwick, A.V., J.Chem.Phys.,1967,47, 2372.

(3) Allnatt, A.R. and Chadwick, A.V., Trans.Far.Soc.,1967,63,1929.

(4) Allnatt, A.R. and Jacobs, P.W.M., Proc.Roy.Soc.,1962,267A,31.

(5) Allnatt, A.R. and Jacobs, P.W.M., Proc.Roy.Soc.,1961,260A,350.

(6) Allnatt, A.R. and Pantelis, P., Sol.St.Comm.,1968,6,309.

(7) Allnatt, A.R. and Rice, S.A., J. Chem. Phys.,1960, 33, 573.

(8) Allnatt, A.R. and Sime, S.J., J. Phys. C.,1972, 5, 134.

(9) Barr, L.W. and Dawson, D.K., AERE Rep.6234, 1969, England.

(10) Barr, L.W. and Lidiard, A.B., 'Physical Chemistry- an advanced treatise', 1970,10, Chapter 3.

(11) Beaumont, J.H. and Jacobs,P.W.M., J.Chem.Phys.,1966,45, 1496.

(12) Beaumont, J.H. and Jacobs,P.W.M., J.Phys.Chem.Solids,1967,28,657.

(13) Beniere,F.,Beniere,M.and Chemla,M.,J.Phys.Chem.Solids,1970,31,1205. (In French)

(14) Boswarva, I.M. and Tan, P.L., Phys. Stat. Solidi, 1972, 50, 141.

(15) Boswarva, I.M., J. phys. C., 1972, 5, L5.

(16) Bosvieux, C. and Friedel, J., J.Phys.Chem.Solids,1962,23,123.

(17) Brown, N. and Hoodless, I.M., Sol. St. Comm., 1968, 6, 597.

(18) Chandra, S. and Rolfe, J., Can. J. Phys., 1970, 48, 412.

(19) Christy, R.W., J.Chem.Phys., 1961, 34, 1148.

(20) Christy, R.W. and Dobbs, H.S., J. Chem. Phys., 1967, 46, 722.

(21) Christy,R.W.,Hseuh,Y.W. and Mueller, R.C., J. Chem. Phys., 1963, 38, 1647.

(22) Das, A.K. and Peierls, R., J. Phys. Chem., 1973, 6,

(23) Davidge, R.W., Silverstone, C.E. and Pratt, P.L., Phil. Mag., 1959, 4, 985.

(24) Davidge, R.W. and Whitworth,R.W., Phil. Mag., 1961, 6, 217.

(25) deGroot, S.R. and Mazur, P., 'Non Equilibrium Thermodynamics', North Holland, Amsterdam.

(26) Downing, H.L. and Friauf, R.J., J.Phys.Chem.Solids, 1970,31,845.

(27) Drefus, R.W. and Nowick,A.S., J. Appl. Phys., 1962, 33, 473.

(28) Eshelby, J.D., Newey, C.W.A., Pratt, P.L. and Lidiard, A.B., Phil. Mag., 1958, 3, 75.

(29) Faux, I.D. and Lidiard, A.B., Z. Naturf., 1971, A26, 62.

(30) Fiks, V. B., Soviet Phys- Solid State,1961,3,724.

(31) Frenkel, I., Z. Phys., 1926, 35, 252.

(32) Friauf, R.J., J. Chem. Phys., 1954, 22, 1329.

(33) Fuller, R.G., Phys. Rev., 1966, 142, 524.

(34) Fuller, R.G., Reilly, M.H., Marquardt,C.L. and Wells,J.C., Phys. Rev. Letters,1968, 20, 662.

(35) Fuller,R.G. and Reilly, M.H., J.Phys.Chem.Solids, 1969, 30, 457.

(36) Greenwood, N.N., 'Ionic crystals,lattice defects and nonstoichiometry', Butterworth and Co., 1970.

(37) Haga, E., J.Phys.Soc.Japan, 1960,15, 1949.

(38) Holtan,H.,Mazur,P.and deGroot,S.R.,Physica, 1953, 19, 1109.

(39) Howard, R.E. and Lidiard, A.B., Rep. Prog. Phys., 1964, 27, 161.

(40) Howard, R.E. and Lidiard, A.B., Dis. Faraday Soc., 1957, 23, 113.

(41) Huntington,H.B., 'Low temp diff. and application to thin films',Proc.Inter.Conf.,N.Y., Aug 12 - 14, 1974.

(42) Huntington, H.B., J.Phys.Chem.Solids,1968,29, 1641.

(43) Huntington, H.B., TMS-AIME, 1969, 243, 2571.

(44) Jacobs,P.W.M. and Knight,P.C., Trans.Faraday Soc.,1970,66, 1227.

(45) Jacobs,P.W.M. and Maycock,J.N. Trans. Am. Inst. Metall. Engrs., 1966, 236, 165.

(46) Jacobs,P.W.M. and Pantelis,P., Phys. Rev. B, 1971, 4, 3757.

(47) John, R., Ph.D. Thesis, Open University, 1975.

(48) Jost, W. 'Diffusion in solids, liquids and gases', Academic Press,N.Y., 1952.

(49) Kanzaki, H., Kido,K. and Ninomiya, T., J.Appl.Phys., 1962, 33, 482.

(50) Keith,R.E. and Gilman,J.J., A.S.T.M. Symposium on basic mechanisms of fatigue, Sp.Tech.Pub.No 237, 3.

(51) Kirk, D.L. and Pratt, P.L., Proc.Brit.Cer.Society,1967,9,215.

(52) Kittel, C., 'Introduction to Solid State Physics', John Wiley and sons, 1967.

(53) Kock, E. and Wagner, C., Z. Phys. Chem., 1937, B38, 295.

(54) Kroger, F.A., 'Chemistry of Imperfect Crystals', North Holland, 1963.

(55) Laurance, N. Phys. Rev., 1960, 120, 57.

(56) Lidiard, A.B., Handbuck der Physik, 1957, 20, 246.

(57) Lidiard, A.B., 'Thermodynamics', Vol 2,IAEA,Vienna,1966.

(58) Lowe, I., D.Phil.Thesis,University of York,1973.

(59) Manning, J.R., 'Diffusion kinetics for atoms in crystals' Van Nostrand, 1968.

(60) Miliotis, Demetrois and Yoon, Duk N., J.Phys.Chem.Solids,1969,30, 1241.

(61) Nadler, C. and Rossel, J., Phys.Stat.Sol(a), 1973, 18, 711.

(62) Rahman,A.,Lowe,I. and Blackburn, D.A., Rev.Inter.Htes.Temp., 1975,12,97.

(63) Rice, S.A., Phys. Rev., 1958, 112, 804.

(64) Sastry,P.V.and Srinivasan,T.M.,Phys.Rev.,1963,132, 2445.

(65) Schottky, W. and Wagner,C., Z.Phys.Chem., 1930, 11B, 163.

(66) Schottky, W., Z. Phys. Chem., 1935, 29B, 353.

(67) Schottky, G., Phys. Stat. Solidi, 1965, 8, 357.

(68) Sorbello, R.S., Phys. Rev., 1972, B6, 4757.

(69) Shapiro,I. and Kalthoff,I.M.,J.Chem.Phys., 1947,

(70) Shewmon, P.G., 'Diffusion in Solids', McGrow Hill Book Co., 1963.

(71) Shimoji,M. and Hoshino,H., J. Phys. Chem. Solids.,1967,28, 1155.

(72) Tubandt,C. and Lorenz, E., Physik Chem., 1914, 87, 513.

(73) Vaughan, W.H., Leivo, W.J. and Smoluchowski, R., Phys. Rev., 1958, 110, 652.

(74) Vineyard, G.H., J.Phys.Chem.Solids, 1957, 3,121.

(75) Wert, C.A., Phys. Rev., 1950, 79, 601.

(76) Wimmer,J.M. and Tallan,N.M., J.Appl.Phys., 1966, 37, 3728.

(77) Wirtz, K., Z. Phys., 1943, 44, 221.